PONTIFICIA UNIVERSIDAD CATÓLICA DE CHILE
ESCUELA DE INGENIERÍA

DESIGN, CONTROL AND OPTIMIZATION OF COMPLEX FENESTRATION SYSTEMS OF OFFICE BUILDINGS

DANIEL URIBE

Thesis submitted to the Office of Research and Graduate Studies
in partial fulfillment of the requirements for the degree of
Master of Science in Engineering

Advisor:
SERGIO VERA ARAYA

Santiago de Chile, May 2016

PONTIFICIA UNIVERSIDAD CATÓLICA DE CHILE
ESCUELA DE INGENIERÍA

DESIGN, CONTROL AND OPTIMIZATION OF COMPLEX FENESTRATION SYSTEMS OF OFFICE BUILDINGS

DANIEL URIBE

Members of the Committee:
SERGIO VERA ARAYA
PAZ ARROYO RIQUELME
WALDO BUSTAMANTE GÓMEZ
CHRISTIAN OBERLI GRAF

Thesis submitted to the Office of Research and Graduate Studies
in partial fulfillment of the requirements for the degree of
Master of Science in Engineering

Santiago de Chile, May 2016

”There is a teaching; there are no divisions” (Confucius Analects 15.39)

ACKNOWLEDGEMENTS

This work was funded by the research grant FONDECYT N ° 1141240 of the National Commission for Scientific and Technological Research of Chile (CONICYT). The author also gratefully acknowledge the research support provided by the Center for Sustainable Urban Development (CEDEUS) under the research grant CONICYT/FONDAP 15110020. I would like to thank the School of Engineering for patrocining assistance to 49th ASA Conference to present the second chapter of this thesis.

Apart from the supporiting entities, I wuold like to thank my advisors Dr. Sergio Vera and Dr. Waldo Bustamante, who helped and guided me all time, and gave me very important opportunities such as researcher and to attend various conferences.

I would like to thank Germán Molina, without their help, this work would have been much harder, Ana Fernández who during his exchange he helped the development of the second chapter of this thesis and Andrew McNeil who gets constant assistance during his visit to Chile and through email.

TABLE OF CONTENTS

LIST OF FIGURES

LIST OF TABLES

ABSTRACT

The building sector accounts for 40% of the total energy consumption and one-third of the green gas house emissions. Highly glazed façades are a common element use for the architects in the modern office buildings that can produce occupants' visual discomfort and high energy consumption. Complex fenestration systems (CFS) have a fundamental role in the energy performance of office buildings, controlling solar gains and transmission of visible light. The term CFS refers to non-specular solar protection systems that redirect solar radiation in complex form. CFS can provide visual and thermal comfort to occupants if properly designed, reducing the energy consumption of buildings, overheating and glare, while improving the transmission of visible light.

This thesis presents research about the design and optimization of CFS, which is divided into: (1) the influence of louvers made of aluzinc on solar heat gains, energy consumption and occupants' visual comfort; (2) a case study of the use of *mkSchedule*, an integrated lighting and thermal simulations tool to design and/or evaluate control strategies for two movable CFS in the early design stages of buildings; (3) evaluation of control strategies of CFS; and (4) a optimization of a fixed CFS under visual comfort and energy consumption criteria.

Keywords: integrated thermal and lighting simulations, daylight metrics, complex fenestration sytems, control strategies, façade optimization.

RESUMEN

El sector de edificación consume el 40% de la energía y genera un tercio de las emisiones de gases invernadero a nivel mundial. Las fachadas altamente vidriadas son un elemento común en la arquitectura moderna de los edificios de oficinas que puede producir disconfort visual en los ocupantes y alto consumo energético. Los sistemas complejos de fenestración (CFS por sus siglas en inglés) tienen un rol fundamental en el desempeño energético de edificios de oficinas, controlando las ganancias solares y la transmisión de luz visible. El término CFS se refiere a sistemas de protección solar no especulares que redirigen la radiación solar en forma compleja. Los CFS pueden proveer confort visual y térmico a los ocupantes si son diseñados correctamente, reduciendo el consumo de energía de edificios, el sobrecalentamiento y el encandilamiento, mientras mejoran la transmisión de luz visible.

Este trabajo presenta la investigación sobre el diseño y optimización de CFS, el cual se divide en: (1) la influencia de lamas hechas de aluzinc sobre las ganancias solares, consumo energético y el confort visual de los ocupantes; (2) caso de estudio del uso de *mkSchedule*, una herramienta integrada de simulaciones lumínicas y térmicas, para diseñar y/o evaluar las estrategias de control de dos CFS móviles en las etapas tempranas de diseño de edificios; (3) evaluación de algoritmos de control de CFS; y (4) optimización de un CFS fijo bajo criterios de confort visual y consumo de energía.

Palabras Claves: Simulación térmica y lumínica integrada, métricas de confort visual, sistemas complejos de fenestración, estrategias de control, optimización de fachada.

1. INTRODUCTION

1.1. Background information

The building sector accounts for 40% of the total energy consumption and one-third of the green gas house emissions (UNEP, 2009). Different architectural design strategies could be implemented to achieve high thermal and energy performance of office buildings in climates like Santiago of Chile (i.e. reduce window-to-wall ratio, windows with very low solar heat gain coefficient or SHGC, high efficient lighting with very low heat gains, etc.). Last decades, higly glazed façades are commonly implemented for the architects in the modern office buildings (Serra, Zanghirella, & Perino, 2010; Basurto, Kämpf, & Scartezzini, 2015). Curtain walls are commonly used in commercial buildings, because of the typical large glazing area of curtain walls and the relatively low thermal performance of metal and glass, the energy consumption of buildings with curtain walls is more sensitive to the weather conditions and the variation of façade design compared to buildings with opaque insulated façade (Lam, Ge, & Fazio, 2015). Most of the buildings are designed with fully glazed façades as the ones shown in Figure 1.1, following a global architectural tendency in different climates. These types of buildings are affected by excessive solar heat gains (SHG), which turns in high cooling energy consumption and visual discomfort.

Daylighting is an important factor that affect in visual comfort (Yun, Yoon, & Kim, 2014) and SHG through windows highly impact on the building energy performance and occupant's comfort. Several authors have reported the large contribution of SHG through fenestration to cooling loads in warm and cold climates (Reilly & Hawthorne, 1998; Li & Lam, 2000; Winkelmann, 2001; Kuhn, 2006; Lam et al., 2015). Thermal and visual comfort as well as the energy consumption for lighting, heating and cooling are strongly determined by optical and thermal properties of glazed façades. The impact on demands and energy consumption of air conditioning and transmitted daylight inwards have been extensively studied by scientist community (Goia, Haase, & Perino, 2013; Correia da

Figure 1.1. Building with curtain wall configuration. (a) Le Meridien Cairo, International Airport Hotel, Cairo (Egypt). (b) Hydro Palace, Manitoba (Canada). (c) Seattle Central Library, Seattle (USA). (d) CorpBanca Building, Santiago (Chile).

Silva, Leal, & Andersen, 2013; Ochoa, Aries, van Loenen, & Hensen, 2012; Wagner, Gossauer, Moosmann, Gropp, & Leonhart, 2007; Konis, 2013; Breesch & Janssens, 2010).

Exterior shading devices are effective architectural building skins to reduce SHG through glazed façades because they intercept solar radiation before it reaches the glass. Fully shaded glazing façades can reduce SHG up to 80% according to ASHRAE (2013), while Bustamante, Vera, and Prieto (2014) have reported reduction of short wave solar transmissions above 90% due to outdoor shading devices such as rollers and undulated and perforated metallic screens. Shading devices perform well to reduce SHG and to provide visual comfort for the occupants.

This thesis is focused on the effects on energy consumption and visual comfort in office spaces with outdoor fixed and movable shading devices, and also, on the design of these devices by parametric analysis and optimization processes. In the following sections a description of fixed and movable shading devices or complex fenestration systems (CFS), their effect on energy consumption and visual comfort, comfort visual metrics, energy and lighting simulation software and optimization processes in office buildings are explained.

1.1.1. Complex fenestration systems

It is a common architectural practice to incorporate exterior shading devices to control SHG. There is a large variety of exterior shading devices such as louvers (fixed and movable), venetian blinds, and perforated screens. However, most of these devices correspond to a non-specularly transmitting layer, thus they are defined as complex fenestration systems (CFS).

In the following sections a description and definitions of CFS, characterization of CFS and kinds of CFS with their effects on visual comfort and energy consumption are explained.

1.1.1.1. CFS definition

Define the CFS is not easy, previously it mentioned that CFS correspond to a non-specularly transmitting layer, as shows in Figure 1.2. The problem arises because the thermal and optical properties of CFS are commonly unknown and most of building energy simulation tools consider them in simplified ways. As consequence, this situation makes difficult to evaluate the impact of CFS on the thermal performance of buildings, especially during the early design stages.

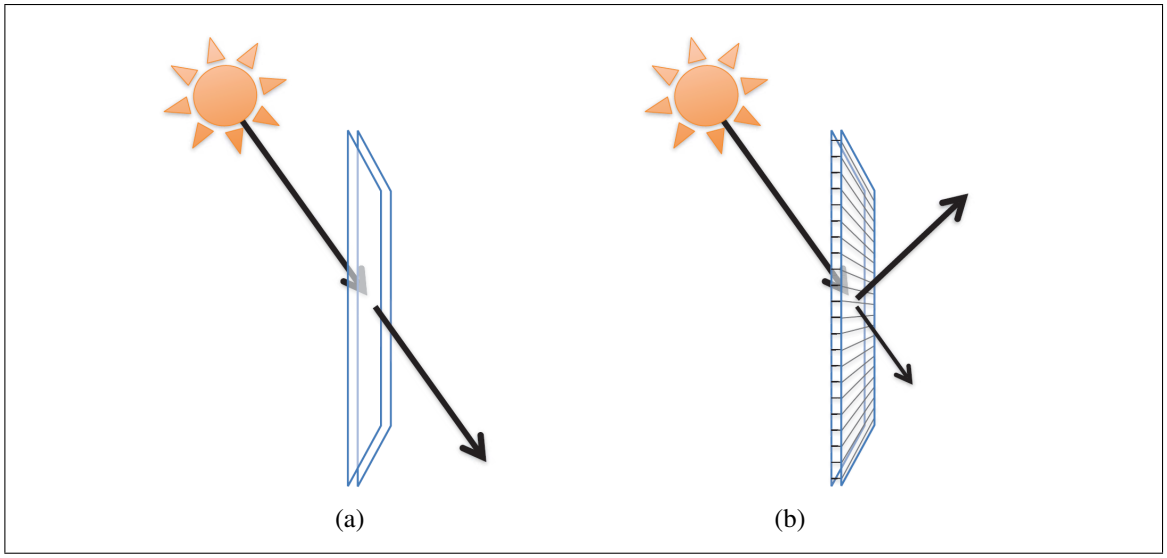

Figure 1.2. Comparison of solar ray transmission of: (a) specular material (e.g. glass). (b) a non-secular material (e.g. CFS). Adapted from (McNeil, 2015a).

From the point of view of the calculation, the definition of complex fenestration systems is not clear or formal. It defined as a complex system that the software WINDOW can not represent (McCluney, 2002), as windows that incorporate non specular layer (Laouadi & Parekh, 2007), or generally as unmanageable systems analytically because they have irregular geometries and/or highly reflective materials, or layers found somewhere between perfect specular (such as any glass) and the perfect diffusivity (as often seen fabrics). In summary, the complex façades can be seen as all those for which do not apply analytical equations Examples of CFS are those that include external protection devices such

as external blinds, horizontal or vertical undulated louvers, perforated or microperforated elements.

1.1.1.2. CFS characterization

According to McNeil (2015b), a bidirectional scattering distribution function (BSDF) describes the way that light interacts with a material including the amount and direction of reflected and transmitted light. BSDF is a combination of bidirectional transmission distribution function (BTDF) and bidirectional reflection distribution function (BRDF). A BSDF file can describe an entire fenestration system, including several layers of specular and scattering components or a BSDF file can be describe a single component of a fenestration system. In Figure 1.3 shows a illustration of BSDF and how varies the transmission distribution in respect of the incident angle of sunlight.

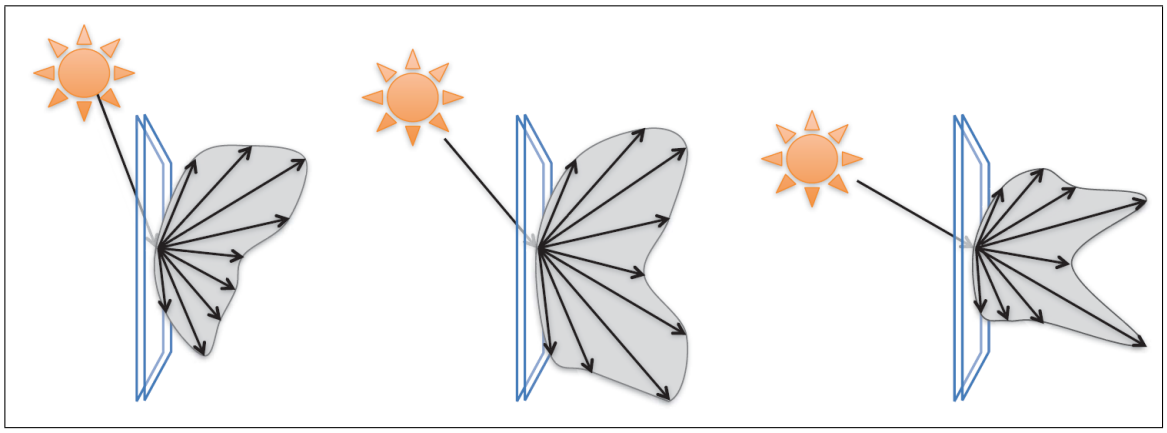

Figure 1.3. Illustraion of Bidirectional Scattering Distribution Function (BSDF) (McNeil, 2015a).

1.1.1.3. Types of fixed and movable CFS

According to Appelfeld, McNeil, and Svendsen (2012), the design criteria for windows and CFS in modern building are:

- Energy use (heating, cooling and electrical lighting)

- Thermal comfort (overheating)
- Visual comfort (daylight, glare, view to outside)

To meet these objectives, there are many kinds of outdoor CFS as it mentioned previously. Following it presents several studies that explain the effect of the different kind of CFS. It should be noted that the focus of this thesis are the outdoor CFS.

Exterior CFS has been studied by scientist community, the most commonly studies are focused on venetian blinds (Kirimtat, Koyunbaba, Chatzikonstantinou, & Sariyildiz, 2016; Yun et al., 2014; E. Shen, Hu, & Patel, 2014; Correia da Silva et al., 2013; Chan & Tzempelikos, 2013; Bueno et al., 2015) and combined systems like venetian blinds with roller shades or fabrics (H. Shen & Tzempelikos, 2012; Tzempelikos & Shen, 2013; Chan & Tzempelikos, 2015; Bueno et al., 2015). The aims of these devices are to reduce energy consumption of the buildings in terms of lighting, cooling and heating, and, improve the visual comfort of occupants related to glare control, daylighting maximization and exterior vision. Is needed collect comparable data on existing buildings with different shading devices and from various climatic areas in the world (Bellia, Marino, Minichiello, & Pedace, 2014).

Perforated screens is a tendency in modern building design (Blanco, Arriaga, Rojí, & Cuadrado, 2014; Mainini, Poli, Zinzi, & Speroni, 2014). Appelfeld et al. (2012) studied the behaviour of a micro structural perforated shading screen and compare with roller blind and venetian blind through simulations (calculate the optical properties using *genBSDF* and WINDOW 6) and experiments. They concludes that there was a strong correlation between the measurements and simulations of perforated shadings, and the screen provides similar shading effect as the venetian blinds. Mainini et al. (2014) studied different metal screens like perforated metal sheets, stamped metal sheets and metal mesh grids with 40% openness factor. They obtained angular light and solar transmittance measurement of this device through a experiment, and then, the data collected were integrated to obtain visible and solar transmittance using WINDOW 6.2. Finally, they use these information for evaluate the thermal behaviour of an office with curtain wall, but experimental

measurements are needed to apply this methodology. Stazi, Marinelli, Perna, and Munafo (2014) monitored the behaviour of real aluminium sliding perforated panels and the experimental data may be useful for other authors for the calibration of numerical models for shading devices. Blanco et al. (2014) developed a theorical model for predicting the thermal behaviour of double skin façade with glass and sheet-panels, which was, validate through experiments. This panels is able to filter the direct radiation thus significantly lowering the temperatures of the internal glass surface. This a good investigation, but they does not considerer the visual comfort and daylight performance. Blanco, Buruaga, Rojí, Cuadrado, and Pelaz (2016) studied the optimization methodology to design double skin enclosure built with metal perforated sheet panels. This CFS controlled the light and SHG changing opening areas or perforations depending on location and orientation of façade, but like the previous study, they does not considerer daylight performance.

Dynamic CFS have the potential to improve buildings' energy performance as indicated by several studies (Tzempelikos & Athienitis, 2007; H. Shen & Tzempelikos, 2012; Tzempelikos & Shen, 2013; Konstantoglou & Tsangrassoulis, 2016). According to Correia da Silva et al. (2013), office buildings occupants will activate or deactivate the shadings based on three different types of criteria:

- Quantity of daylight (illuminance) that falls on the workplane.
- Visual discomfort related to glare, accounted indirectly by window luminances, transmitted solar radiation or directly by daylight glare indexes.
- Direct solar radiation, which can create both thermal and visual discomfort.

According to literature, criteria for control of movable shading devices in office buildings are presented below. Chan and Tzempelikos (2013) evaluated venetian blinds with slat's surface with two specularity values (0 and 0.8) and combination of these, in Philadelphia (USA) for south and west orientations. They used three strategies, cut off-angle, "blocking" control (set blinds perpendicular to profile angle when a second reflection is possible and redirect transmitted light when cut-off angle redirection is not effective)

and glare control (rotate blinds when DGP index $> 35\%$). They conclude that a combination of glare strategies would yield the best results depending on climate, window properties and orientation. Yun et al. (2014) evaluated venetian blinds in Incheon (South Korea) for the south, west and east orientations. They used fixed blinds and one case with dynamic blinds controlled by glare. They found that dynamic shading control with the dimmed lights was the best case for the east and the west façade, while, the case of $0\,^{\circ}$ slat angle represents the smallest energy consumption for the south facçade. Konstantzos, Tzempelikos, and Chan (2015) evaluate controlled roller shades in office space in in West Lafayette (Indiana, USA) for south façade orientation. Three controls were evaluated, fully closed shades, work plane protection (prevents direct sunlight from falling on the work plane) and advanced control (prevent high workplane illuminances $>$ 2000 lux at all times and maximize daylight provision under cloudy sky conditions). The advanced shading control is able to protect from glare for most of the time. Vera et al. (2016) evaluated exterior venetian blinds in San Francisco (USA) for south façade orientation. Control strategies are based on outdoor dry-bulb temperature and irradiance over the window. Liu, Wittchen, and Heiselberg (2015) evaluated intelligent glazed façade through glare and cut-off angle (during occupied hours blinds cut the direct solar radiation, and during unoccupied hours, the blind is controlled by temperature), in Buddinge (Denmark) for the four cardinal orientations. Bueno et al. (2015) evaluate two systems, Winglamella (highly reflective Aluminium material) perforated and non-perforated, and Warema venetian blinds with double clear glazing in Villafranca di Verona (Italy), for the south, west and east orientations. They used two controls, cut-off angle and retro ($60\,^{\circ}$), similar to cut-off angle. Winglamella system is a device composed of two separately mechanically controlled partitions (perforated in upper part, and non-perforated in lower part). This system is particularly suitable for east and west façade orientations. De Michele, Oberegger, and Baglivo (2015) evaluate venetian blinds in a shopping mall located in Genoa (Italy) for west façade orientation. Use two controls, one depend of internal air temperature and incident solar radiation on faąde, and the second depend of illuminance level on workplace.

Dynamic CFS are not always the best from an economic point of view (installation and maintenance can be more expensive than fixed CFS) (Nielsen, Svendsen, & Jensen, 2011). Thus, it is required the evaluation of different control strategies in real time to obtain the best option of movable CFS in terms of visual comfort and energy performance (Bastien & Athienitis, 2012). Development in the shading strategies, materials used and comfort parameters inside the buildings should profoundly be coped with (Kirimtat et al., 2016).

1.1.2. Visual comfort metrics

There are two types of visual comfort metrics, those related to illuminance level at workplane (e.g. daylight autonomy and useful daylight illuminance), and those related with the illuminance level at eye observer (glare indices). Comfort metrics related with illuminance level at workplane are described below, follow by metrics associates to glare indices.

1.1.2.1. Metrics for illuminance level at the workplane

Daylight Factor (DF) was developed in the early 20th century in United Kingdom. DF is a ratio that represents the amount of illuminance available indoors relative to the illumination present outdoors at the same time under overcast skies, expressed in percent. The higher the DF, the more natural light is available in the room (*Daylighting Pattern Guide*, n.d.). Practitioners encounter guidelines and recommendations for target DF values that they know are likely to result in over-glazed buildings with excessive solar gain and/or heat loss (Mardaljevic, Heschong, & Lee, 2009).

Daylight Autonomy (DA) is a climate-based metric that represents how often in the year a specified illuminance is achieved (C. Reinhart & Mardaljevic, 2006). It is a major innovation since it considers geographic location specific weather information on an annual basis. It also relates power to electric lighting energy savings if the user defined threshold is set based upon electric lighting criteria. The user is free to set the threshold above which DA is calculated (*Daylighting Pattern Guide*, n.d.)

Useful Daylight Illuminance (UDI) is defined as the annual occurrence of illuminances across the work plane that are within a range considered useful by occupants. The UDI range is further subdivided into two ranges called UDI-supplementary and UDI-autonomous. UDI-supplementary gives the occurrence of daylight illuminances in the range of 100-500 lux. For these levels of illuminance, additional artificial lighting may be needed to supplement the daylight for common tasks such as reading. UDI-autonomous gives the occurrence of daylight illuminances in the range of 500-2500 lux, where additional artificial lighting will most likely not be needed (Mardaljevic et al., 2009).

Spacial Daylight Autonomy (sDA) and Annual Sunlight Exposure (ASE) were developed by Illuminating Engineering Society (IES) (IES, 2013). sDA is a metric describing annual sufficiency of ambient daylight levels in interior environments. It is defined as the percentage of an analysis area that meets a minimum daylight illuminance level for a specified fraction of the operating hours per year. $\text{sDA}_{300/50\%}$ is recommended as the preferred metric for analysis of daylight sufficiency. $\text{sDA}_{300/50\%}$ is reported as the percent of analysis points across the analysis area that meet or exceed 300 lux for at least 50% of the analysis period (e.g. from 8AM to 6PM, 10 hours per day). This metric and performance criteria was conducted between the N37° and N48° latitudes in North America. IES recommends two criteria to qualify the acceptability of performance:

- Preferred Daylight Sufficiency: $\text{sDA}_{300/50\%}$ must meet or exceed 75% of the analysis area
- Nominally Accepted Daylight Sufficiency: $\text{sDA}_{300/50\%}$ must meet or exceed 55% of the analysis area.

ASE is a metric that describes the potential for visual discomfort in interior work environments (IES, 2013). It is defined as the percent of an analysis area that exceeds a specified direct sunlight illuminance level more than a specified number of hours per year. $\text{ASE}_{1000/250h}$ is recommended for analysis of the potential visual discomfort. $\text{ASE}_{1000/250h}$ is reported as the percent of analysis points across the analysis area that meet or exceed

1000 lux for 250 hours per year of the analysis period. IES recommends three criteria to qualify the acceptability of visual comfort by ASE:

- Unsatisfactory: ASE is more than 10%.
- Nominally acceptable: ASE is less than 7%.
- Acceptable: ASE is less than 3%.

Values recommended for sDA and ASE are not necessarily correct when applied to larger areas, such as an entire building floor or total building area. The supporting research did not include enough variety of sun penetration patterns by various orientations, space types, shading device types or climates zones to fully understand how occupants' preferences vary by these factors. More information is needed from field studies to better understand the range of tolerance for sunlight penetration into workspaces, as well as which mitigation efforts are likely to be more successful, or unsuccessful to improve occupant comfort (IES, 2013).

1.1.2.2. Metrics for glare

Glare indices have been used to evaluate visual comfort in the luminous environment. There is a multitude of glare indices, but there only two glare indices intended for use in daylit environments. The first, the daylight glare index (DGI) was developed by Hopkinson (1972) and Hopkinson and Collins (1963) using large-area electric light glare sources and updated by Chauvel, Collins, Dogniaux, and Longmore (1982) in a setting with daylight but without sunlight or reflected sunlight. The second, daylight glare probability (DGP), was developed by Wienold and Christoffersen (2006) as an attempt to overcome the limitation of the DGI. The DGP tries to define "the probability that a person is disturbed instead of the glare magnitude" (Van Den Wymelenberg & Inanici, 2014). They found that the DGP outperformed the DGI, but this must be qualified in several ways. The basic equation for the DGP includes vertical illuminance at the eye (E_v) as a primary input in addition to the common glare equation variables (Van Den Wymelenberg

& Inanici, 2014). A simplified DGP (DGPs) was developed by Wienold (2007) and validated by Wienold (2009). DGPs based on the E_v only, and can be applied only if no direct sun or specular reflection of it hits the eye of the observer.

Van Den Wymelenberg and Inanici (2014) performed an experiment where they evaluated different visual comfort metrics based on illuminance and luminance levels with 93 participant-days in two days, one day in summer and one day in fall. It was found that DGP, does not appear to be sensitive or robust enough for being used as stand-alone design criteria for daylighting visual comfort and in some cases might underpredict glare sensation. Mardaljevic, Andersen, Roy, and Christoffersen (2012) demonstrated that there is the potential to compute measures of daylight glare probability using indirect means, such as using the DGPs and luminance renderings on a per time-step basis. Also, the relation between DGPs for the 95th percentile and two UDI metrics seems sufficiently robust to warrant further development of this approach. According to Bellia et al. (2014), daylight should be studied using more reliable indices such as DA and UDI, while also evaluating glare risk. According to Konstantzos et al. (2015) for cases without the sun in the field of view, DGP and workplane illuminance are not well correlated, except for very low openness factors or perfectly diffuse materials. For cases without the sun in the field of view, DGP and vertical illuminance are well correlated, even when sunlight falls on interior surfaces (when shades are partially opened). This allows DGPs to be used for all instances except when sunlight directly hits the occupant.

1.1.3. Energy and lighting simulation software

This section introduces the energy, lighting and integrated simulation software. Energy simulation software are very often used for estimating the energy performance of a building. Lighting simulation software are used for estimating the luminance or illuminance levels on a scene. And, as CFS are related to the thermal and lighting domains of a building, the integrated software are needed for understand how affecting the CFS on visual comfort and energy consumption of a space.

1.1.3.1. Lighting simulation software

Radiance (Ward, 1994), daylighting simulation software, was created by Lawrence Berkeley National Laboratory. It is probably the best, most complete and flexible software for lighting simulations (Ochoa, Aries, & Hensen, 2012). Most of the researchers, including architects and engineers, use Radiance both to estimate accurate illumination levels and to design spaces via artificial and natural lighting technologies. In order to make simulations, the software presents interfaces for modelling space geometry, luminaire data and material characteristics (Kirimtat et al., 2016) and allows implementation of daylight coefficient (Tregenza & Waters, 1983) or three and five phases methods (Saxena, Ward, Perry, Heschong, & Higa, 2010; McNeil, 2013; Konstantoglou, Jonsson, & Lee, 2009; McNeil & Lee, 2013; Bourgeois, Reinhart, & Ward, 2008).

DAYSIM (C. F. Reinhart, 2013) is a Radiance-based daylighting analysis software that models the annual amount of daylight in and around buildings. DAYSIM allows users to model dynamic façades systems ranging from standard venetian blinds to state-of-the-art light redirecting elements, switchable glazings and their combinations. Users may further specify complex electric lighting systems and controls including manual light switches, occupancy sensors and photocell controlled dimmed luminaires. Simulation outputs range from climate-based daylighting metrics such as daylight autonomy and useful daylight illuminance to annual glare and electric lighting energy use. DAYSIM also generates hourly schedules for occupancy, electric lighting loads and shading device status which can be directly coupled with thermal simulation engines such as EnergyPlus, eQuest and TRNSYS (C. F. Reinhart, 2013).

1.1.3.2. Energy simulation software

EnergyPlus is a building energy simulation software, development by the U.S. Department of Energy (DOE) Building Technologies Office (BTO) and managed by National Renewable Energy Laboratory (NREL) (*EnergyPlus*, n.d.). IEnergyPlus will calculate the heating and cooling loads necessary to maintain thermal control setpoints, conditions

throughout an secondary HVAC system and coil loads, and the energy consumption of primary plant equipment as well as many other simulation details that are necessary to verify that the simulation is performing as the actual building would. This software has some key capabilities for instance; infinite solutions can built into instantly, it can manipulate daylight, create thermal comfort models, heat and mass transfer can be integrated, and different window layouts can be computed (Kirimtat et al., 2016).

TRNSYS is a flexible graphically based software used to simulate the behaviour of transient systems. While the vast majority of simulations are focused on assessing the performance of thermal and electrical energy systems, TRNSYS can equally well be used to model other dynamic systems such as traffic flow, or biological processes (*TRNSYS*, n.d.).

1.1.3.3. Integrated lighting and energy simulation software

OpenStudio (Guglielmetti, Macumber, & Long, 2011) couples Radiance with EnergyPlus. This program is currently in development, but allows use of daylight coefficients and three phases method. Also, allows determine glare due to daylight through simplified method (Wienold, 2009), it do not consider individual sources of glare, generating considerable errors in assessing direct views of the windows. Other limit is in the usage of BSDF data that are only contained in the OpenStudio's database. In addition, dynamic shading control is not supported (De Michele et al., 2015).

Fener (Bueno et al., 2015) ia a tool developed at the Fraunhofer institute, that performs energy and daylight simulations for advanced analysis of CFS in a single space. Model uses the three phases method and the BSDF data to evaluate indoor illuminance measured by virtual sensors arranged on a sensors grid and solar irradiance absorbed by indoor surfaces. The solar gains are used to evaluate the heat balance of the building. Fener can not perform multi-zone energy simulations.

mkSchedule (Vera et al., 2016; Molina, 2014) is a tool that provides integrated simulations for CFS using three phases method integrating Radiance and EnergyPlus. Control algorithms is kept out of the main program and it can be defined through a Lua script. The control is flexible and can be based on weather file information or on the output of daylighting simulations.

1.1.4. Optimization methods in building simulation

Herein "Building optimization" refers to a method that uses algorithms to find the optimal combination of simulation parameters for architectural design. The goal of the optimization process is to find the optimum for the lowest total energy cost and meets the criteria of visual comfort using a much shorter simulation time that the approach of comparing each possible combination of parameters. Discrete parameters are typically used for façade design problems because continuous parameters are almost non-existent in façade design. Examples of discrete parameters are window dimension, construction material, insulation thickness, glazing types (SHGC, U-value), etc. Continuous parameters methods do not use fixed numbers for the parameter setting for building shape or dimensions such as window-to-wall ratio, building orientation, or compactness. Optimization methods using discrete parameters are more suitable to solve building façade design problems (Shan, 2014). The major obstacles in solving building optimization problems by simulation based methods involve the complex natures of building simulation outputs, the expensive computational cost, the scale of the problems, multi-objective design problems, and uncertainty of many factors during the optimization, including design variables, environmental variables, model and constraint uncertainty among others (Nguyen, Reiter, & Rigo, 2014). Successful optimization requires a nuanced understanding of the relationships between model parametrization, optimization algorithm, and performance metrics (McNeil & Lee, 2012).

EnergyPlus and TRNSYS are the mostly-used building simulation programs in optimization studies, and the mostly used optimization engines seems to be GenOpt and

Matlab optimization toolboxes (Nguyen et al., 2014). There are several optimization algorithms such as: genetic algorithms (GA), particle swarm optimization (PSO), Hooke-Jeeves algorithms (HJ), simplex algorithms, coordinate search algorithms, hybrid algorithms, among others. The stochastic population-based algorithms (GAs, PSO, hybrid algorithms, evolutionary algorithms) have been the most frequently used methods in building performance optimization (Nguyen et al., 2014). Wetter and Wright (2003) compared the performance of a HJ algorithm and a GA in optimizing building energy consumption. Their results indicated that the GA outperformed the HJ algorithm and the latter have been attracted in a local minimum. Wetter and Wright (2004) found that the GA consistently got close to the best minimum and the Hybrid algorithm PSO-HJ achieved the overall best cost reductions. Kämpf, Wetter, and Robinson (2010) compared the performance of two metaheuristics algorithms, Covariance Matrix Adaptation Evolution Strategy Algorithm (CMA-ES/HDE) and PSO-HJ algorithm. They found that CMA-ES/HDE performed better than the PSO-HJ in solving the benchmark functions with 10 dimensions or less. However, if the number of dimensions is larger than 10, the PSO-HJ performed better.

Nowadays, there are many architects, engineers and scientist working on optimization of buildings components (Blanco et al., 2016). Tsangrassoulis, Bourdakis, Geros, and Santamouris (2006) used a GA to design a slat-type shading system with one design parameter (angle of each slat segment). They demonstrated how GAs can be applied to the design of a shading system. McNeil and Lee (2012) developed an optimization process using GenOpt combined with Radiance simulation capabilities to search for optimal shapes of microprisms for a specific CFS model. The optimization process considered glare and lighting energy in the objective function to maximize lighting energy savings and minimize glare, tolerate 0.5% increase in glare frequency for a 1% decrease in fractional lighting energy use. Particle swarm algorithms was used. Has developed a film geometry with superior performance to what is commercially available. Rapone and Saro (2012) studied a typical curtain wall façade of an office building in order to find the configuration of selected parameters (percentage of glazed surface, depth of the louvers and spacing of the louvers) that minimizes the total carbon emissions arising from building

operation in four climates and the four cardinal orientations. They do not consider visual comfort evaluation. Simulation were based on PSO algorithm (using GenOpt) coupled to a dynamic energy simulation engine (EnergyPlus). Shan (2014) propose a methodology to find the optimal solutions for the total energy demand using a GA. The variables to optimize are the dimension of window grid and the depth of shading system. He used TRNSYS for energy simulations and DAYSIM for calculating loads due to artificial lights and turn off lights if exceed 500 lux, but he do not considered visual comfort metrics to evaluate daylight performance of the shading system. Manzan (2014) used a genetic optimization to design an optimal fixed shading device. The shading device is a flat panel positioned parallel to the window and inclined by its horizontal axis. He carried out this study using ESP-r for energy simulation and DAYSIM for calculating loads due to artificial lights, and ModeFRONTER with NSGA-II algorithm for optimization. The optimization is performed modifying four parameters (shading device height, width, angle and distance from the wall) and the objective function is in terms of total energy consumption. The optimized result was compared with unshaded window and results show energy savings up to 19% and 30% for Trieste and Rome (Italy), respectively. González and Fiorito (2015) developed a simplified method to overcome daylight and energy performance using DIVA, a plug-in for Rhinoceros/Grasshopper software, and Galapagos through GAs. The optimization process was carried out parametrically controlling the shadings' geometries (shading depth, angle on horizontal plane and shading number) and they have two objective functions in terms of total energy consumption and CO_2 emissions. The optimized result was compared with conventional design techniques showing energy savings between 9.3% and 35.8% and CO_2 emissions reductions between 11.4% and 47.7%. He evaluate the daylight performance for the optimized solution, but they does not considerer the visual comfort evaluation inside the optimization process. Futrell, Ozelkan, and Brentrup (2015) used a hybrid GPS Hooke Jeeves/PSO algorithm in combination with the Epsilon Constraint Method to find Pareto efficient solutions to the daylighting and thermal optimization problem of a classroom design with only one exterior shade (without CFS). They used two objective functions, one for lighting and the other for energy consumption.

They conclude that these two objectives are not strongly conflicting. Blanco et al. (2016) studied double skin enclosure built with metal perforated sheet panels. This device controls the light and SHG changing opening areas or perforations depending on location and orientation of façade. They applied a simple optimization methodology to determinate the perforations ratio for different climatic areas in Spain, but does not considered daylight performance.

The most of the studies about optimization of CFS's geometry considerer only the energy consumption in the objective function. In two cases the objective function has the both metrics (energy consumption and visual comfort), (McNeil & Lee, 2012) and (Futrell2015). The first only considerer the lighting consumption and the second methodology are appropriate but do not have CFS. It is needed a methodology that integrate energy consumption (heating, cooling and lighting) and visual comfort to optimize the geometry of CFS in the early design stage of the office buildings to save computational time, and maximize the daylight availability and energy efficiency.

1.2. Research opportunities

CFS have a fundamental role in the energy performance and control of SHG in office buildings and provide occupant's visual comfort. Designers, engineers and architects has developed many kinds of CFS such as louvers (fixed and movable), venetian blinds, perforated screens, among other, and if are not well designed can produce visual discomfort. The interaction between building and occupants have an important effect in energy consumption, for this, it is necessary modelling and optimization in the design stage of building (Nielsen et al., 2011; Kirimtat et al., 2016). It is necessary provide information to them to design correctly these devices, choosing the right CFS for the weather conditions and the building characteristics (window-to-wall ratio, façade orientation, etc.).

According to literature reviewed, the studies are focused on the following topics/opportunities:

(1) Evaluate the behaviour of CFS in terms of thermal performance, control of SHG, energy consumption and visual comfort.
(2) Evaluate different control strategies of movable CFS in terms of energy consumption and visual comfort.
(3) Optimize the geometry of fixed and movable CFS in terms of energy consumption and visual comfort.
(4) Design and optimization of complete building façades.
(5) Determine the right visual comfort metrics.

It is needed integrating all topics in a only methodology that allows to give all the information necessary for designers. *mkSchedule* have the potential in their methodology that use a time-efficient simulations to incorporate the first four topics.

In this thesis, opportunities (1) and (2) are worked, while work about opportunity (3) considerer only fixed CFS.

1.3. Objectives

The general objective of this research is to advance in the design and optimization of complex fenestration systems through a tool that integrate lighting and thermal/energy simulations and an optimization software, considering variables that influence the energy performance of the offices buildings.

Specific objectives are the following:

(1) Evaluate the performance of undulated and perforated exterior louvers in terms of SHG, energy consumption and visual comfort in a given climate.
(2) Demonstrate how the performance of movable CFS can be defined during the building design to property evaluate CFS of early design stage of office space.
(3) Evaluate four CFSs control strategies in an office space for different climates and façade orientations.

(4) Optimize the geometry of a fixed undulated and perforated exterior CFS in terms of energy consumption and visual comfort.

1.4. Hypothesis

The hypothesis for this research are the following:

(1) Using Groundhog®, *mkSchedule* Radiance and EnergyPlus allow to determinate the behavior of fixed and movable CFS in terms of SHG, energy consumption and visual comfort in several climates.
(2) *mkSchedule* and GenOpt allow to optimize CFS to reduce building energy consumption and proper visual comfort.

1.5. Methodology

This study is based on modelling and performing simulation with the following software: Groundhog®, *mkSchedule*, Radiance, EnergyPlus and GenOpt.

1.6. Thesis structure

Besides this introduction, the thesis is composed of other four chapters, each one of them being an auto-contained potential journal article with their own abstract, introduction, methodology, results and conclusions. Those chapters correspond to:

(1) Influence of four outdoor complex fenestration systems made of aluminum-zinc on solar heat gains, energy consumption and visual comfort of an office building space: evaluate the influence of four outdoor CFS in terms of their capability to control SHG and reduce the total energy consumption in a office space located in Santiago of Chile. Part of this paper was presented in the 49th ASA Conference and obtained the Best Presentation Award.

(2) Integrated thermal and lighting performance simulations for minimizing energy consumption of office buildings with complex fenestration systems: a case study that explains how *mkSchedule* allows integrating thermal and lighting performance simulations to determine the best control strategy based on incident irradiance for minimizing energy consumption of an office space with two movable complex fenestration systems, undulated and perforated horizontal louvers and venetian blinds.

(3) Impact of different control strategies of dynamic complex fenestration systems and luminaires in visual comfort and energy consumption of office buildings: a study of the impact of four different control strategies of complex fenestration systems based on incident irradiance, vertical eye illuminance, cut-off angle and blocking light control, on visual comfort and energy consumption.

(4) Optimization of a fixed outdoor complex fenestration system for achieving visual comfort and energy performance criteria: an optimization methodology for a fixed fenestration system (undulated and perforated horizontal louvers). Using *mkSchedule* and GenOpt to determine the optimum parameters (slope angle, percentage of perforations and slats' spacing) in term of energy consumption and visual comfort.

Chapters 2, 3 and 4 search to prove hypothesis 1 and accomplish specific objectives 1, 2 and 3, chapter 5 proving hypothesis 2 and accomplish specific objective 4.

1.7. Results

This section present a synthesis of the main results of this research work.

In chapter 2, four CFS made of aluminum-zinc alloy was evaluated in terms of control of SHG and reduce total energy consumption. All CFS are very effective building skins to achieve these objectives. However, visual comfort is only achieved by CFS 3 which has 20% perforations and 120 mm spacing between louvers. CFS 3 allows having a $sDA_{300/50\%}$ and $ASE_{4000/400h}$ of 100% and 11% as well as providing proper outdoor visibility. This evidences importance of evaluating all performance aspects of CFS to establish

the ones that can achieve the expected performance. In terms of total energy consumption, energy savings of all cases with CFS are between 29% and 34% in comparison with the window without CFS. CFS 3 causes the lowest energy consumption. Coincidently, this CFS is the only one that also meet visual comfort criteria.

In chapter 3, in order to define the best control strategy based on incident irradiance on the window, for each kind of CFS was obtained the optimum maximum irradiance level. For the venetian blinds, the optimum maximum irradiance for the control strategy are 450 W/m^2, 530 W/m^2, 570 W/m^2 and 610 W/m^2 for Santiago, Miami, Boulder and Montreal respectively, and for the louvers, the optimum maximum are 320 W/m^2, 290 W/m^2, 320 W/m^2 and 350 W/m^2 for Santiago, Miami, Boulder and Montreal respectively. Furthermore, a correct study of control strategy can be an important variable in the design stage to reduce energy consumption.

In chapter 4, four control strategies for a CFS was evaluated, each one based on incident irradiance level, vertical eye illuminance, cut-off angle and blockling control. In terms of energy consumption and visual comfort, the most effective control strategy is S1 (incident irradiance level) for all cases with south/north façade orientation, and for west façade orientation in all cases the best strategy is S4 (blocking control), except in Miami, where S1 is the best strategy. Energy savings are around 10%.

In chapter 5, the optimized solution was found to be a slope of 25 °, 15% of perforation and 100 mm spacing for Montreal and a slope of 50 °, 15% of perforation and 120 mm spacing for Santiago of Chile. Double clear glazing in both cities have high values for $sDA_{300/50\%}$ and $ASE_{2000/400h}$, that is discomfort for occupants, and the optimized solution meets the both criteria of visual comfort for the two cities, maximizing daylighting and preventing visual discomfort. This results was validated by a parametric analysis where the difference in respect of exact solution in terms of energy consumption is between 0.94 and 1.62%.

In summary, the results shows that using Groundhog®, Radiance and EnergyPlus, it is possible determinate the behavior of fixed and movable CFS in terms of SHG, energy consumption and visual comfort of occupants, given a certain climate; and, using *mkSchedule* and GenOpt, it is possible optimize a fixed CFS to reduce building energy consumption and proper visual comfort.

1.8. Conclusions

In chapter 2 conclude that, all evaluated CFS cause a large reduction of SHG in comparison with an unshaded double clear glazing, whereas significant differences were found among the SHG of CFS due to different percentage of perforations and spacing. Increasing the louver spacing causes higher solar heat transmission through the fenestration system than that for perforations. However, it is rather than notorious that a low percentage of perforations (20%) also increases the SHG significantly in comparison with the CFS without perforations.

In chapters 3 and 4 conclude that external movable CFS may significantly control daylighting. Results show that when a CFS is are not properly designed visual discomfort may occur, furthermore, a correct study of performance of movable CFS can be an important variable in the design stage to reduce energy consumption. Also, it has been observed that *mkSchedule* is an effective tool to be used in early design stages of architectural design to design and/or determinate the best control strategy of CFS based on visual comfort parameters and energy performance of a building.

In chapter 5, the methodology of combination of parametric design of CFS with hybrid meta-heuristic algorithm and pattern search algorithm to determine the best set of CFS's parameters, allow to determine optimized solutions to buildings performance in terms of energy consumption and visual comfort. Optimized solutions maximize the daylight availability and energy efficiency, validated through a parametric analysis.

In summary, it conclude that outdoor CFS may significantly control daylighting and SHG, and *mkSchedule* is an effective tool to be used in early design stages of architectural design. The methodology can be using to design a fixed CFS, or to design and/or determine the best control strategy of a movable CFS.

1.9. Future work

This work can be divide in two parts: lighting/energy analysis of CFS control strategies and optimization processes.

About the lighting/energy analysis through *mkSchedule*, the future work should advance in the following line: it is needed a empirically validation of the methodology using a laboratory measurements. Agreeing with Konstantoglou and Tsangrassoulis (2016), it should be studied the performance of more strategies and combinations of these, it is needed to improve the visual comfort metrics, add metric as glare indices and UDI, and additionally it should be studied the behaviour with several zones/rooms to design a complete façade.

About the optimization process, future work can expand set of optimization criteria, combining energy-related indicator with other visual comfort metrics, such glare discomfort problems, include movable external shading devices, and calculate parametrically the BSDF during optimization progress without the need to use WINDOW software to generate a BSDF's database. Finally, it is needed apply sensitivity analysis to determine the effect of each variable on the optimization problem.

2. INFLUENCE OF OUTDOOR COMPLEX FENESTRATION SYSTEMS MADE OF ALUMINUM-ZINC ON SOLAR HEAT GAINS, ENERGY CONSUMPTION AND VISUAL COMFORT OF AN OFFICE BUILDING SPACE

2.1. Abstract

Semiarid regions, such as Central Chile, are characterized by high solar radiation and temperature. In this climate, current architecture of fully glazed façade office buildings might cause high cooling energy consumption due to high solar heat gains (SHG), even in winter periods. In Chile's Central region, the implementation of outdoor complex fenestration systems (CFS) is a common practice. However, the impact of CFS on the building thermal performance is usually unknown. The main objective of this paper is to evaluate the impact of four outdoor CFS of aluminum-zinc in terms of their capability to control SHG through a window oriented northwest, energy consumption and occupant's visual comfort of an office space located in Santiago of Chile. An integrated thermal-lighting analysis tool is used to evaluate the performance of these CFS. The CFS evaluated are undulated horizontal louvers spaced 120 or 240 mm with 0 or 20% of perforations. The main results show that the CFS evaluated significantly reduce SHG over the whole-year compared with SHG through an unshaded clear double glazing window; perforations and spacing of louvers increase SHG substantially in comparison with the CFS without transparency, but they allow outdoor visibility; and the CFS 3, with slats spaced 120 mm and 20% perforations, provides a good balance between the control of SHG and outdoor visibility, and also, have the lowest energy consumption and it is the only CFS that meets the visual comfort criteria.

2.2. Introduction

The building sector accounts for 40% of the total energy consumption and one-third of the green gas house emissions (UNEP, 2009). In Chile, a developing country, the building sector consumes 28.8% of the total energy consumption (MinEnergía, 2013). Chile's

Central region, where Santiago is located (S33 $^\circ$ 22'; W70 $^\circ$ 46'), is a cooling dominated climate, thus office buildings usually presents high cooling energy consumption due to high internal and solar heat gains (SHG) even in winter-time. The SHG are significant due to the climate characteristics of Santiago of Chile and the current architecture tendency of fully glazed buildings' façades. Santiago's climate is characterized by maximum temperatures ranging from 20 to 35 $^\circ$C between October and April, while the maximum global horizontal solar radiation is between 500 and 1000 W/m^2 (ASHRAE, 2013). This climatic condition exposes office building to large heat gains due to solar radiation and heat conduction.

Different architectural design strategies could be implemented to achieve proper building performance in terms of energy consumption and occupant's visual comfort. Some of this strategies are reducing window-to-wall ratio (WWR), using windows with very low solar heat gain coefficient (SHGC), implementing high efficient lighting with very low heat gains, among others. However, most of the buildings are designed and constructed with fully glazed façades as the Titanium Tower, the second tallest building in Chile, shown in Figure 2.1, which follows a worldwide architectural tendency. In Santiago's climate, these types of buildings are affected by excessive SHG, which turns in high cooling energy consumption and visual discomfort. For instance, it is observed in Figure 2.1 that internal rollers of the north oriented façade are down in the Titanium Tower. This fact should be the user's response to high SHG or excessive daylighting. The glazing installed on this building has a low SHGC, thus the fact of observing rollers down evidences that the control of SHG in this climate can not be fulfilled by the glazing system only.

Solar heat gains through windows highly impact on the building energy performance and occupant's comfort. Several authors have reported the large contribution of SHG through fenestration to cooling loads in warm climates (Reilly & Hawthorne, 1998; Li & Lam, 2000; Winkelmann, 2001; Kuhn, 2006). Exterior shading devices are effective architectural building skins to reduce SHG through glazed façades because they intercept solar radiation before it reaches the glass. Fully shaded glazing façades can reduce SHG

Figure 2.1. Titanium Tower, a 60-story building located in Santiago of Chile.

up to 80% according to ASHRAE (2013), while Bustamante et al. (2014) have reported reduction of short wave solar transmissions above 90% due to outdoor shading devices such as rollers and curved and perforated metallic screens.

In Santiago of Chile, it is a common architectural practice to incorporate exterior shading devices to control SHG. There is a large variety of exterior shading devices such as louvers (fixed and movable), venetian blinds, and perforated screens. However, most of these devices correspond to a non-specularly transmitting layer, thus they can be defined as complex fenestration systems or CFS (Laouadi & Parekh, 2007). This means that unlike perfect specular materials, such as many glasses, which transmit the solar ray with the same angle of incidence (see Figure 2.2a), CFS transmit the solar rays in different directions as shown in Figure 2.2b.

Most commonly studied exterior CFS corresponds to venetian blinds alone (Kirimtat et al., 2016; E. Shen et al., 2014; Correia da Silva et al., 2013; Chan & Tzempelikos, 2013; Bueno et al., 2015; Yi, Srinivasan, & Braham, 2015) and combined systems like venetian blinds with roller shades or fabrics (Bueno et al., 2015; H. Shen & Tzempelikos,

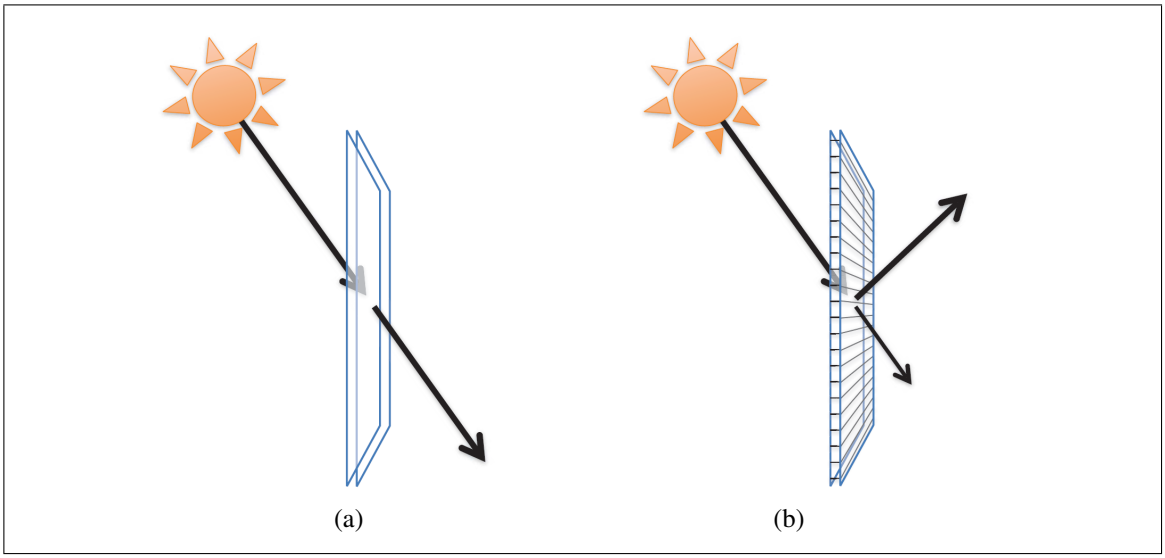

Figure 2.2. Comparison of solar ray transmission of: (a) specular material (e.g. glass). (b) a non-secular material (e.g. CFS). Adapted from (McNeil, 2015a).

2012; Tzempelikos & Shen, 2013; Chan & Tzempelikos, 2015). The purpose of these devices is to reduce energy consumption of the buildings in terms of lighting, cooling and heating, and, improve the visual comfort of occupants related to glare control, daylighting maximization and exterior vision. Bellia et al. (2014) shows an overview of building shading systems, and they pointed out the need of studying different CFS on different climatic conditions worldwide.

The use of perforated screens as shading devices is a tendency in modern building design (Blanco et al., 2014; Mainini et al., 2014). Appelfeld et al. (2012) studied the daylighting transmission of a micro structural perforated shading screen and compared its performance with rollers and venetian blinds. They concluded that the perforated screen provides similar shading effect as the venetian blinds. Mainini et al. (2014) studied different metal screens like perforated metal sheets, stamped metal sheets and metal mesh grids with 40% openness factor. They obtained angular light and solar transmittance measurement of these devices via experimental work, and then, the data collected were integrated

to obtain visible and solar transmittance using WINDOW 6.2. Finally, they use this information for evaluating the thermal behavior of an office with curtain wall. Blanco et al. (2014) developed a theoretical model for predicting the thermal behavior of double skin façades with glass and sheet-panels, which was validate through experiments. The evaluated panel was able to filter the direct radiation thus significantly lowering the temperatures of the internal glass surface. These studies on perforated screens have focused on either lighting transmission or thermal behavior of the screen but lack of the influence of these perforated screens on the building energy consumption and occupant's visual comfort. On the contrary, Stazi et al. (2014) monitored the behavior of aluminum sliding perforated panels and the experimental data was used for calibrating the numerical models for shading devices. Then, they evaluated the impact of these screens on the energy consumption and visual comfort in a located in a Mediterranean climate of Italy.

Common shading devices used in Chilean buildings corresponds to curved louvers made of aluminum-zinc alloy which can be unperforated or having different perforation percentages. The problem arises because the thermal and optical properties of these CFS are commonly unknown and most of building energy simulation tools consider them in simplified ways. As consequence, this situation makes difficult to evaluate the impact of CFS on the building performance in terms of energy consumption and occupant's visual comfort, especially during the early design stages.

For this reason, the aim of this paper is to evaluate the influence of two outdoor CFS made of aluminum-zinc alloy in terms of their capability to control SHG through fenestration system and their influence on the building energy consumption and occupant's visual comfort of an office located in Santiago of Chile, a semiarid climate.

2.3. Research methodology

2.3.1. Description of the CFS evaluated and office space

This paper evaluates, via energy and lighting simulations, the influence of two outdoor CFS composed by curved louvers, which are installed horizontally for shading a double clear glazing window. The evaluated louvers correspond to a commercial product named Celoscreen of HunterDouglas Company Chile. The material of the two evaluated CFS are identical and corresponds to aluminum-zinc alloy (55% aluminum, 43.4% zinc and 1.6% silicon). The louver thickness is 0.5 mm. The surface material is considered a reflective metal (95% of solar and visible reflectance) with 0% of specularity. The two studied CFS are louvers with the same shape and geometry by one is unperforated (Figure 2.3a) while the other has 20% perforations (Figure 2.3b). Two spacing were tested for each CFS, 120 mm and 240 mm, thus four different combination of fenestration systems were considered as shown in Figure 2.4. As can be seen, the slope of the louvers is 60 for all cases. Additionally, a double clear glazing system (without CFS) was also evaluated for comparison purposes. Table 2.1 shows the SHGC and visible transmittance (T_{vis}) of each case, while all cases have the same U-value.

(a) CFS unperforated

(b) CFS with 20% perforations

Figure 2.3. Pictures of two evaluated CFS.

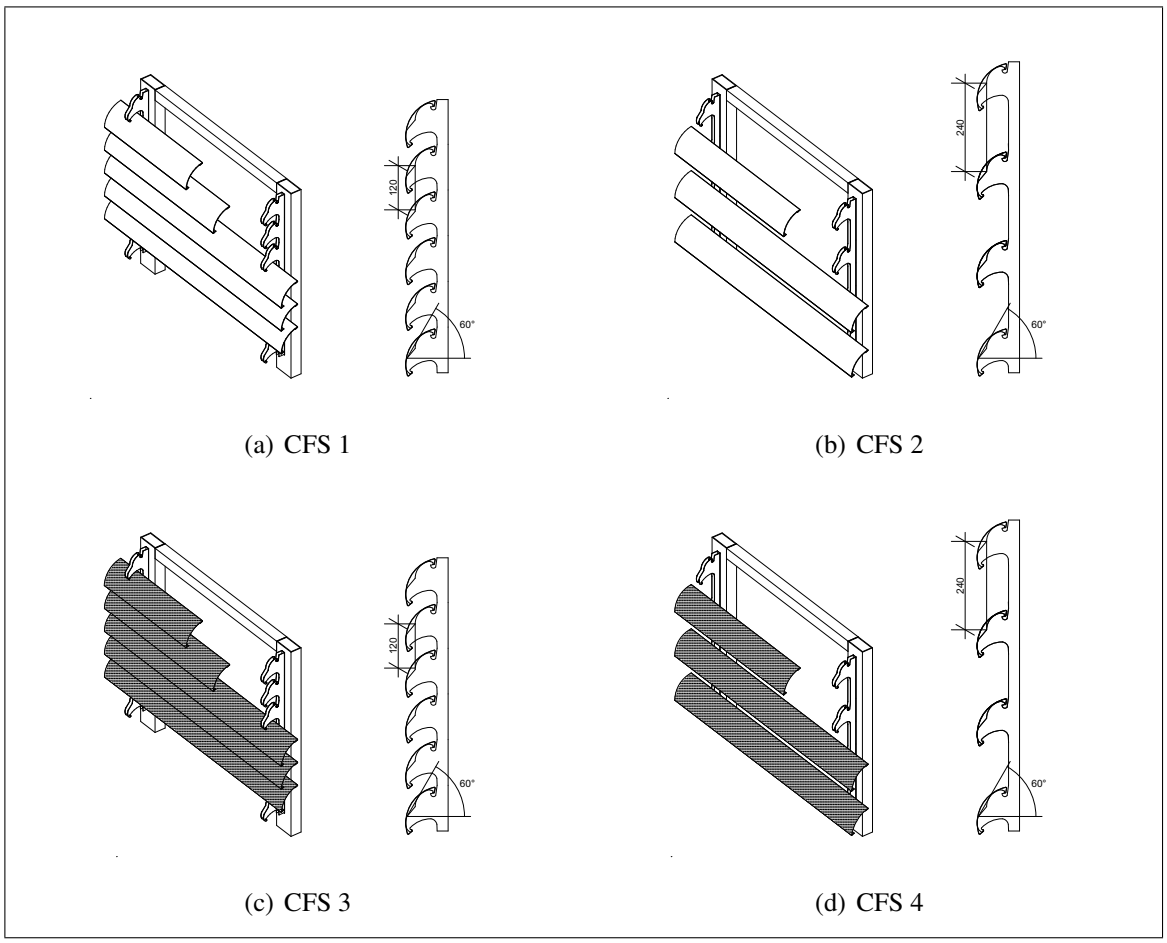

(a) CFS 1 (b) CFS 2

(c) CFS 3 (d) CFS 4

Figure 2.4. Schematic arrangement of the evaluated cases with CFS. Adapted from (HunterDouglas, 2013).

The office space considered in this study is shown in Figure 2.5 which simulates a perimeter office with the glazing façade oriented northwest. This orientation was chosen because it is the most challenging due to high incident solar radiation occurs for most of the day-time on this building façades.

Table 2.1. CFS evaluated.

CFS	Description	SHGC	T_{vis}	U-value ($Wm^{-1}K^{-1}$)
CFS 1	Undulated slats/louvers installed with slats spacing of 120 mm and slope of 60 °	0.10	0.06	2.70
CFS 2	Undulated slats/louvers installed with slats spacing of 240 mm and slope of 60 °	0.28	0.22	2.70
CFS 3	Same as CFS 1 but with 20% of perforations	0.18	0.13	2.70
CFS 4	Same as CFS 2 but with 20% of perforations	0.33	0.27	2.70
DCG	Clear double glazing window without CFS	0.83	0.83	2.70

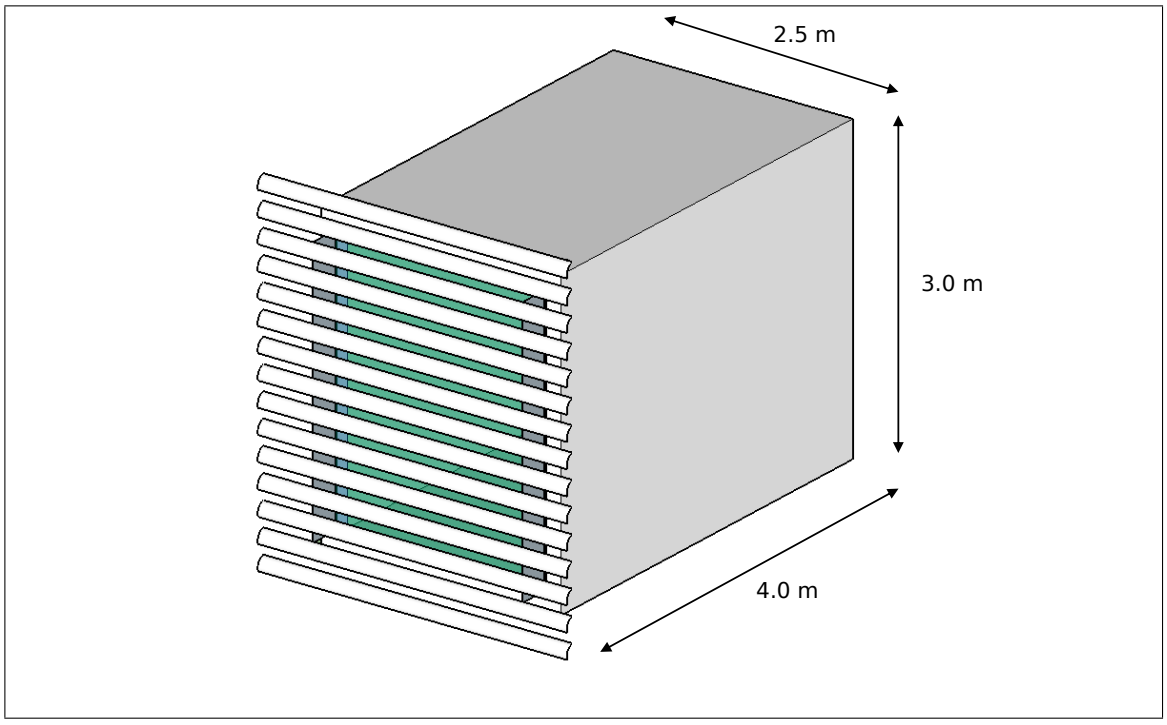

Figure 2.5. Model of the office space with CFS in SketchUp.

For the simulations, it was considered the following parameters: walls, ceiling and floor were adiabatic; surface reflectances of floor, ceiling and walls of 20%, 70% and 50%, respectively; HVAC system consisted of an electric heat pump with COP equal to 3.0 for heating and cooling; the heating and cooling thermostat setpoints were 20 °C and 24 °C, respectively; the internal heat gains for people, lights and equipment were 6.7 W/m^2, 13.85 W/m^2 and 15 W/m^2, respectively; artificial lighting devices were dimmed to take advantage of daylighting and reduce energy consumption; the illuminance level setpoint that control dimmed luminaries is 500 lux at the workplane, which was at 0.8 m; finally, the operation hours of the office were considered from 08:00 to 18:00 hrs.

2.3.2. Simulation process

The evaluation of the CFS described above was performed using an integrated thermal and lighting analysis tool that efficiently integrates SketchUp, Groundhog® (Molina, Vera, & Bustamante, 2014) (a SketchUp plugin), *mkschedule*, Radiance and EnergyPlus. Figure 2.6 show the process flow for the simulations. A synthesis of the simulation process is presented in this paper, but more details can be found in (Molina, 2014; Molina, Vera, & W., 2014; Vera et al., 2016). The CFS and the building model are created in SketchUp. Groundhog allows properly exporting the CFS to Radiance's *genBSDF* (Molina, Bustamante, Rao, Fazio, & Vera, 2015) for calculating the bidirectional scattering distribution function (BSDF) of each CFS, which describes its bidirectional optical properties.

The BSDF is needed for each CFS to properly take into account how solar radiation is transmitted through the CFS. *genBSDF*, which has been validated by McNeil, Jonsson, Appelfeld, Ward, and Lee (2013) and Molina et al. (2015), is a Radiance's program that allow obtaining the BSDF of each CFS by performing ray-tracing simulations in Radiance. Then, the BSDF of each CFS obtained with *genBSDF* needs to be assembled to the optical properties of the double clear glazing by means of WINDOW 7.3 (LBNL, 2014), thus the BSDF of the whole fenestration system (CFS + double clear glazing) is generated. EnergyPlus can read, as input, the BSDF of the whole fenestration system, thus the thermal

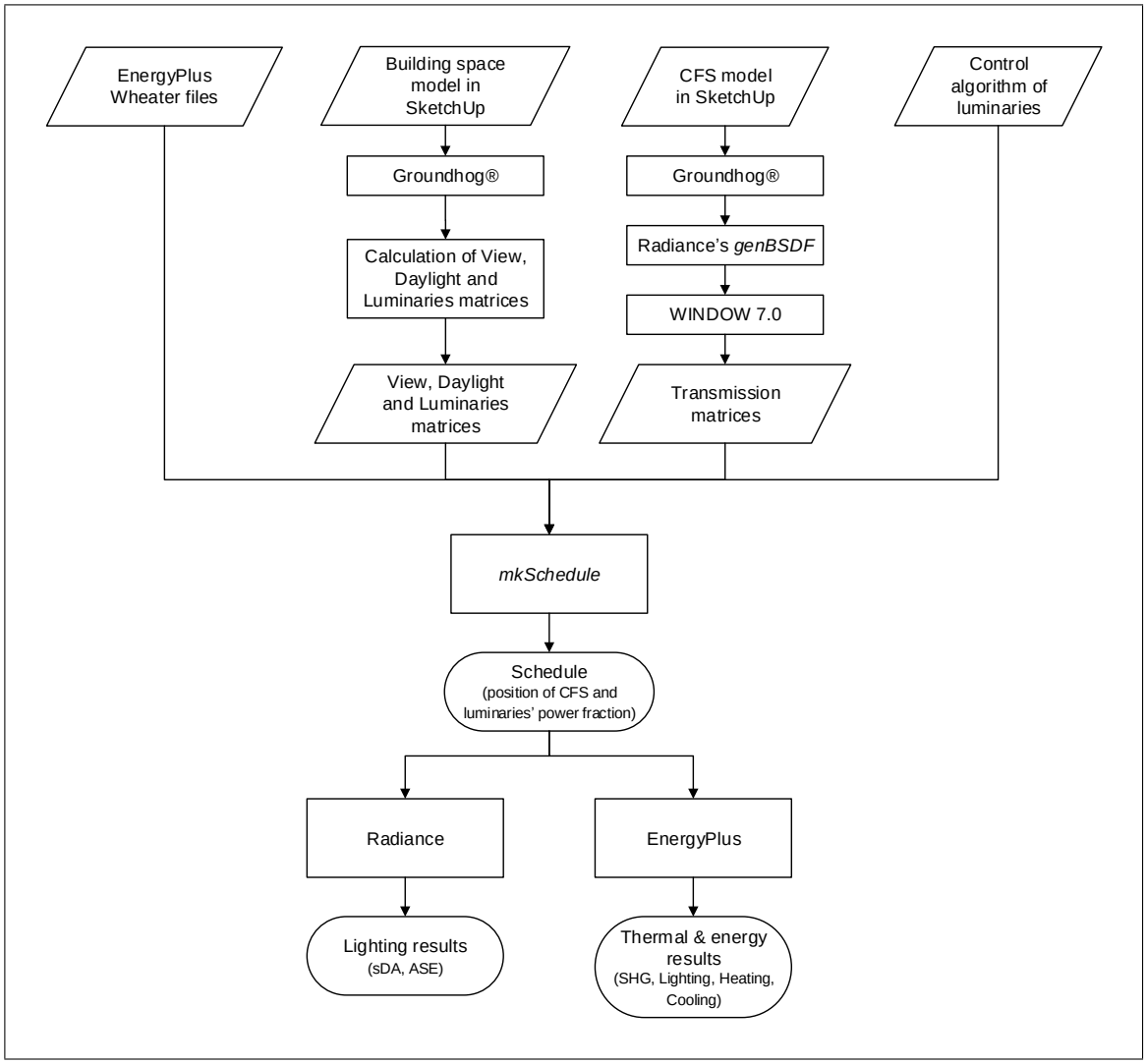

Figure 2.6. Flow chart of simulation process.

and energy simulations take into account more precisely the optical properties of each CFS.

Also, SketchUp and the Groundhog plugin are used to create the building model with properties that are recognized by Radiance to perform lighting simulations. From the lighting simulation, the Radiance's program called *mkschedule* (Vera et al., 2016), generates an annual schedule for the position of CFS and lighting power intensity. *mkschedule* was designed for simulating movable CFS and controlled lighting. Despite this study considered

fixed CFS, the luminaries were dimmed, thus *mkschedule* is needed to provide the power fraction of luminaries to EnergyPlus and Radiance for energy and lighting simulations, respectively.

Using this integrated thermal and lighting simulation tool, EnergyPlus outcomes are the hourly SHG through each fenestration system and the annual energy consumption for heating, cooling and lighting; while Radiance outcomes are the hourly illuminance levels at each sensor of the workplane, which allows obtaining the metrics to assess visual comfort across the office space.

2.3.3. Metrics for the assessment of CFS

Three different aspect are used in this paper to evaluate the effectiveness of the studied CFS, SHG through the whole fenestration system, energy consumption of the office space and occupant's visual comfort. SHG reflects the thermal impact of the CFS and allow to evaluate how effective are the studied CFS to control SHG, which affect the heating and cooling energy consumption. Since the CFS affects the daylighting transmission, they also influence the lighting energy consumption, which also affects the cooling and heating energy consumption. Finally, two metrics, based on the illuminance level at the workplane, are used to evaluate the impact of CFS on visual comfort, spatial daylight autonomy (sDA) and annual sunlight exposure (ASE), which thresholds are set according to recommendation of Illuminating Engineering Society standard (IES, 2013). $\mathrm{sDA}_{300/50\%}$ is reported as the percentage of analyzed points across the analysis area that meet or exceed 300 lux for at least 50% of the analysis period (from 8 AM to 6 PM, 10 hours per day, weekdays). $\mathrm{ASE}_{4000/400h}$ is the percentage of analyzed points across the analysis area that meet or exceed this 4000 lux value for 400 hours per year of the analysis period. sDA must meet or exceed 75% of the analysis area and ASE is considered acceptable in this study when is less than 20%.

2.4. Results and analysis

2.4.1. Solar heat gains

Table 2.2 shows the temporal maps of annual SHG for the four cases of CFS and the double clear glazing window without CFS. These temporal maps show the SHG during the whole year. The x-axis corresponds to the day of the year while the y-axis is the hour of the day. Dark-blue zones show the periods of the year with no solar radiation. It should be noted that the scale of SHG was limited to 133 W/m^2, which is the maximum SHG found for the cases with CFS. However, the clear double glazing window presents SHG up to 542 W/m^2.

Figure 2.7 shows accumulative curves of the percentage of time when SHG are lower than the value shown in x-axis. This information allows better comparison of the CFS performance with the performance of the unshaded double clear glazing window and among the evaluated CFS. For a certain SHG and CFS, the y-axis provides the percentage of time of the whole year, excluding the periods with no solar radiation, when SHG are lower than the value of the x-axis.

Table 2.2 and Figure 2.7 clearly shows the significant reduction of SHG caused by the evaluated CFS in comparison with the clear double glass window. While the peak SHG among the evaluated CFS is 133 W/m^2, the window without CFS allows very high SHG during large portion of the year that rise to 542 W/m^2. Comparing the results of SHG among the CFS assessed, it is observed that the most effective CFS for controlling SHG is CFS 1 due to it fully covers the window and has no perforations.

Furthermore, these results allow analyzing the effect of perforations (0% or 20%) and spacing (120 mm or 240 mm). First, the increase in spacing between louvers can be seen comparing the SHG of the pairs CFS 1 with CFS 2 and CFS 3 with CFS 4 in Table 2.2 and Figure 2.7. As expected, larger spacing causes higher SHG, and the increment of SHG is similar for slats with 0% (CFS 1 versus CFS 2) or 20% (CFS 3 versus CFS 4)

Table 2.2. Temporal maps of annual solar heat gains of different CFS and clear double glazing.

CFS	Solar heat gains (SHG)	Maximum SHG
CFS 1	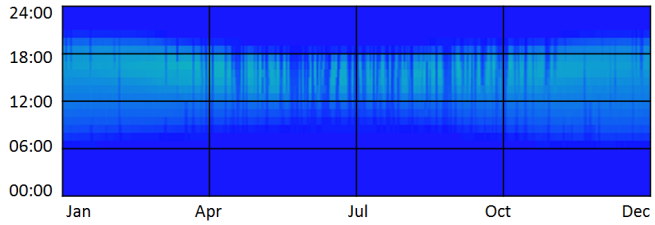	30 W/m^2
CFS 2	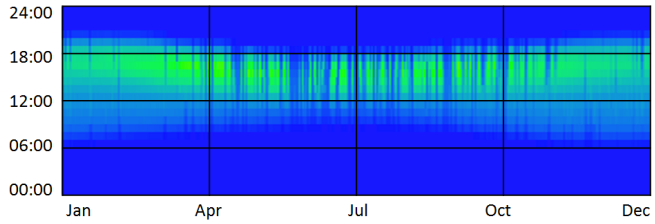	101 W/m^2
CFS 3	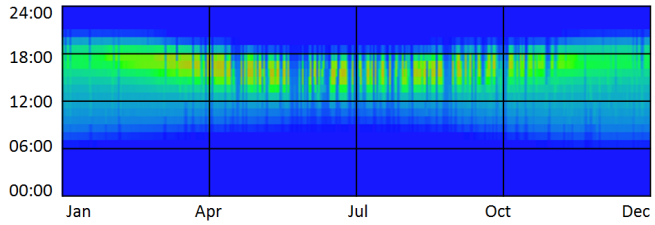	71 W/m^2
CFS 4	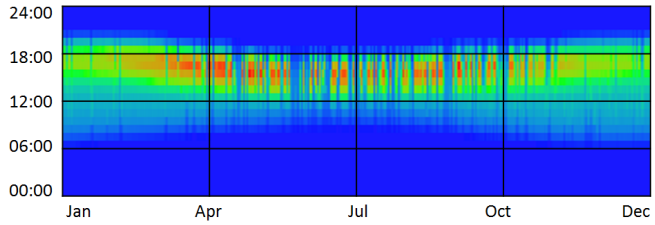	133 W/m^2
CDG	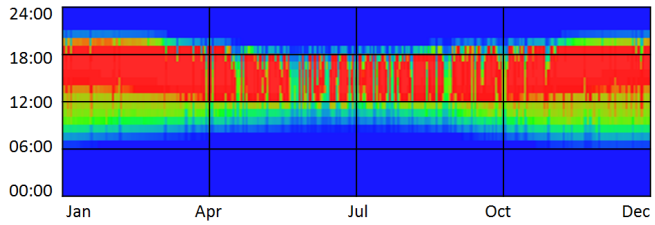	542 W/m^2
Legend		

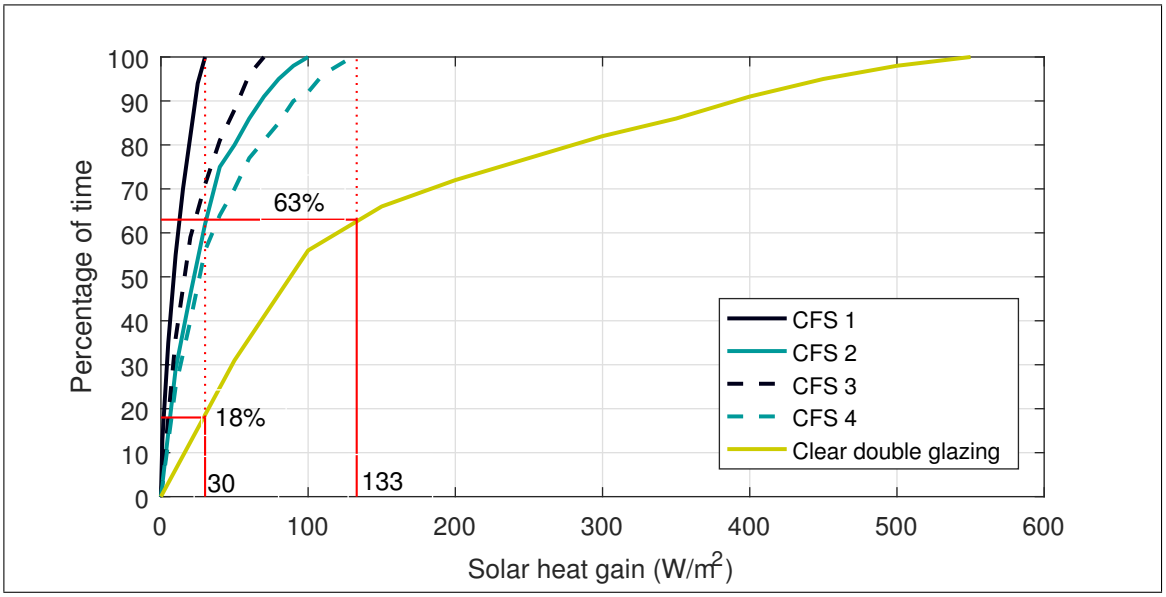

Figure 2.7. Accumulative curves of SHG of different CFS and clear double glazing.

perforations. Table 2.2 shows that the larger spacing mostly increases SHG during winter time, which makes sense because the sun altitude is lower causing higher irradiance on the northwest fenestration system after midday. Second, the effect of perforations can be analyzed comparing the resulting SHG of CFS 3 with CFS 1 and CFS 4 with CFS 2. In both cases, SHG are higher for CFS with perforations. Figure 2.7 shows that the increment of SHG is 36.7% comparing CFS 3 with CFS 1 and 31.7% comparing CFS 4 with CFS 2. Notoriously, these results evidences that a low percentage of perforations (20%) increases the SHG significantly in comparison with the CFS without perforations. Finally, these results also allow analyzing the relative impact of 20% perforations versus doubling the louvers spacing with 0% perforations. Figure 2.7 shows that the SHG of CFS 3 are much lower than that for the CFS 2. It means that larger spacing between slats allows much larger SHG than increasing the perforation to 20%, only.

2.4.2. Visual comfort

Tables 2.3 and 2.4 present the temporal maps of annual illuminance in Lightsolve format, and the $sDA_{300/50\%}$ and $ASE_{4000/400h}$ values, respectively, for the four cases of CFS and the double clear glazing window without CFS. The temporal maps show the percentage of sensors in the workplane area which meets the illuminance level, in this case between 300 lux and 4000 lux. Like in the SHG temporal maps, dark-blue zones show the periods of the year with no solar radiation, and green zone show high percentage of workplane area that meets the desired illuminance range. Overall, windows with CFS show illuminance level within the range for most of the year, expect CFS 4 that shows higher illuminance between April and October after 2 PM. On the contrary, most of the workplane presents illuminance above 4000 lux most of the year after midday for double clear glazing, which significantly diminishes visual comfort.

Table 2.4. $sDA_{300/50\%}$ and $ASE_{4000/400h}$ values for each CFS and DCG.

CFS	$sDA_{300/50\%}$	$ASE_{4000/400h}$
CFS 1	71%	0%
CFS 2	100%	29%
CFS 3	100%	11%
CFS 4	100%	43%
DCG	100%	100%

Based on illuminance level results, $sDA_{300/50\%}$ and $ASE_{4000/400h}$, are obtained and shown in Table 2.4. The lack of perforation and lower spacing reduces daylight transmission to the indoor space, thus CFS 1 shows a $sDA_{300/50\%}$ below 75%, which means that illuminance level is not suitable for visual comfort. Moreover, CFS 2 and 4 exceed the $ASE_{4000/400h}$ which evidences that the larger spacing between louvers causes excessive daylighting.

Table 2.3. Temporal maps of annual illuminance in Lightsolve format, values within 300 lux-4000 lux.

CFS	Illuminance level (lightsolve format)
CFS 1	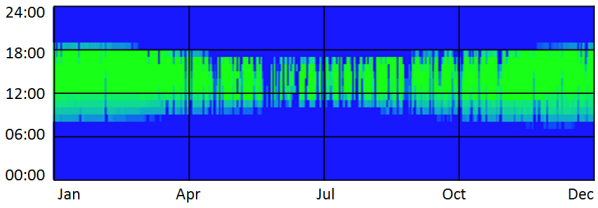
CFS 2	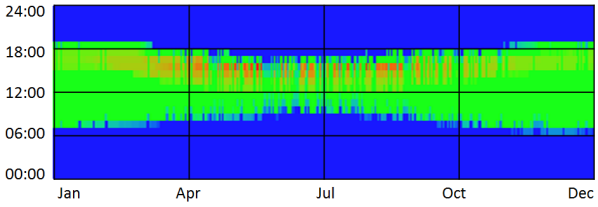
CFS 3	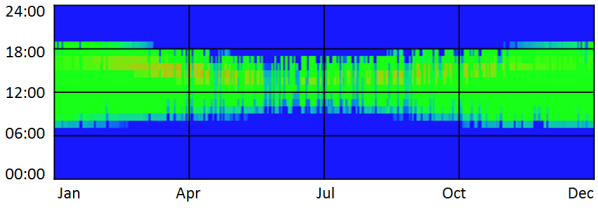
CFS 4	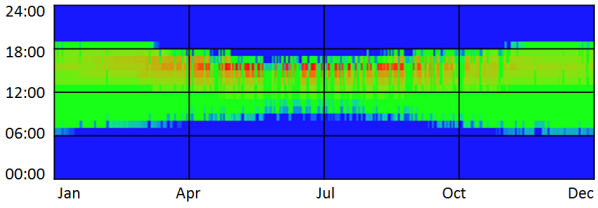
CDG	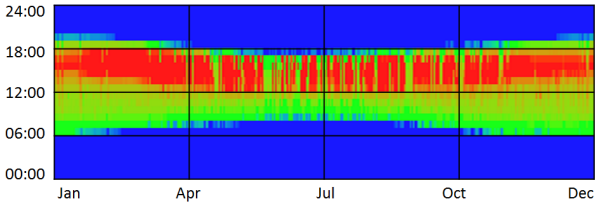
Legend	

Figure 2.8 shows the illuminance level in the workplane for January 21th, a representative day of summer, at 2 PM to analyze the illuminance distribution and determinate zones where values of $ASE_{4000/400h}$ are higher. CFS 1 does not present excessive illuminance. Otherwise, it shows too low illuminance far from the window, which causes a $sDA_{300/50\%}$ lower than 75%. On the other hand, CFS 2 and CFS 3 have a slightly high illuminance level in the zone between the window and 1 m far from the window, but the illuminance is acceptable after this zone. Similarly, CFS 4 present excessive illuminance between the window and 1.5 m far from the window, which is caused by its higher transparency due to a combination of larger spacing and percentage of perforations.

Figure 2.9 shows the outdoor visibility at 2 PM of the CFS evaluated. The images were obtained from inside of an experimental module using a fisheye lens in a summer clear sky day. Since outdoor visibility is important for human comfort, it is necessary to reduce SHG in balance with providing proper outdoor visibility. Although this paper presents this very simplistic approach to sense the outdoor visibility provided by each CFS, it can provide useful qualitative information about the impact of the different CFS on visibility. This images evidences that perforations and larger spacing between louvers allow significant improvements of outdoor visibility in comparison with CFS 1, whose louvers causes no transparency and window is fully covered. However, unshaded regions of the window due to perforations and larger slats' spacing increase the SHG. In consequence, a trade-off between reducing the SHG and allowing outdoor visibility is a key factor for the overall performance of CFS. CFS 3 seems to be the only CFS arrangement that allow low SHG and significant outdoor visibility. As shown in Figure 2.9, the outdoor visibility of CFS 3 is as good as of CFS 2 and 4 even though it has no spacing between slats and only has 20% of perforations. This means that controlling SHG but allowing outdoor visibility is better provided by perforations rather than increasing the spacing between louvers.

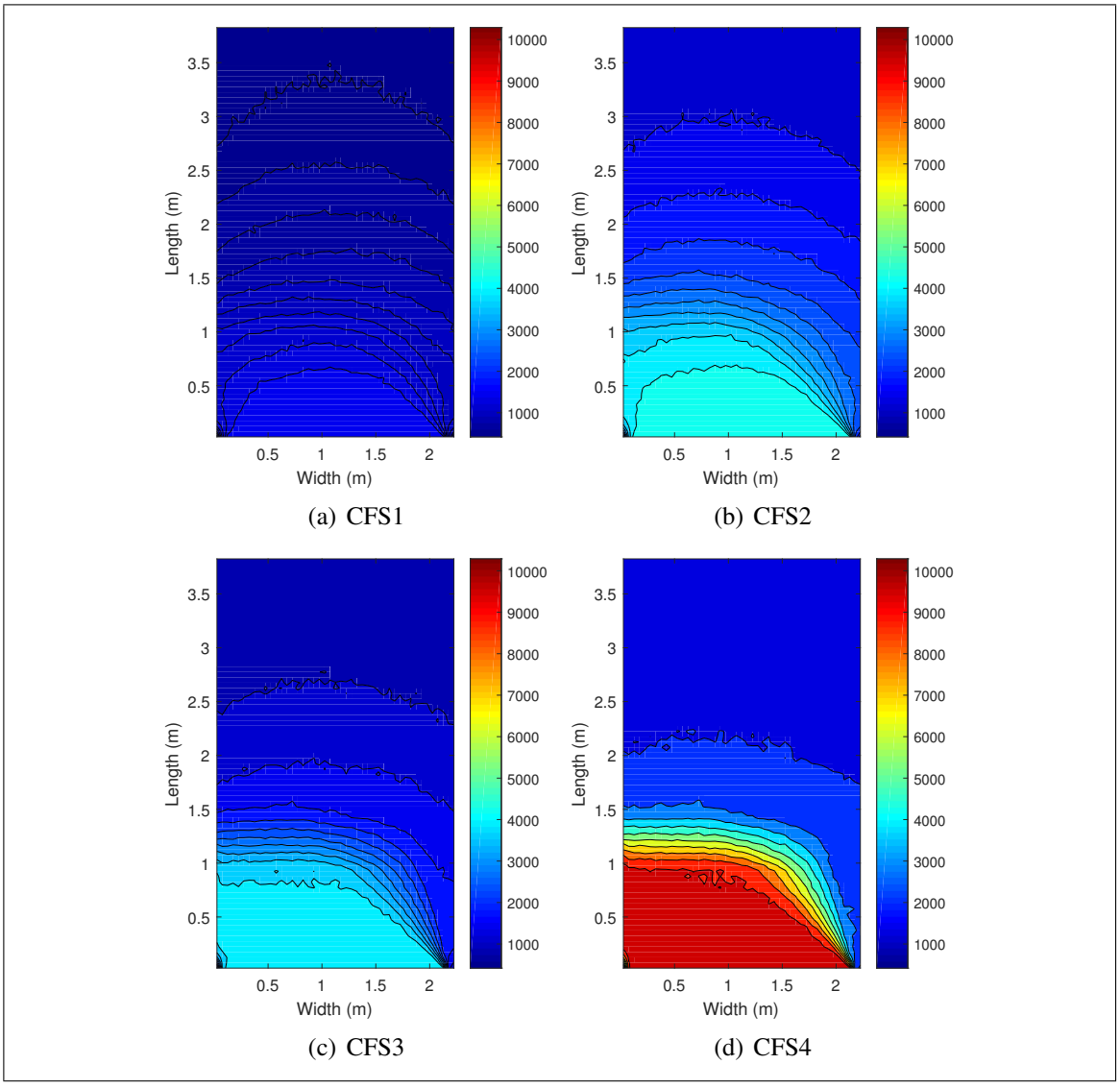

Figure 2.8. Illuminance level (lux) at workplane for different CFS, January 21th at 2 PM.

Finally, according to previous results of visual comfort, CFS 3 is the only option that meets the criteria of IES, with $\text{sDA}_{300/50\%}$ of 100% and $\text{ASE}_{4000/400h}$ of 11%, visual discomfort zone is located in the first meter from the window which is not usually occupied for seating people in offices, and provides acceptable outdoor visibility.

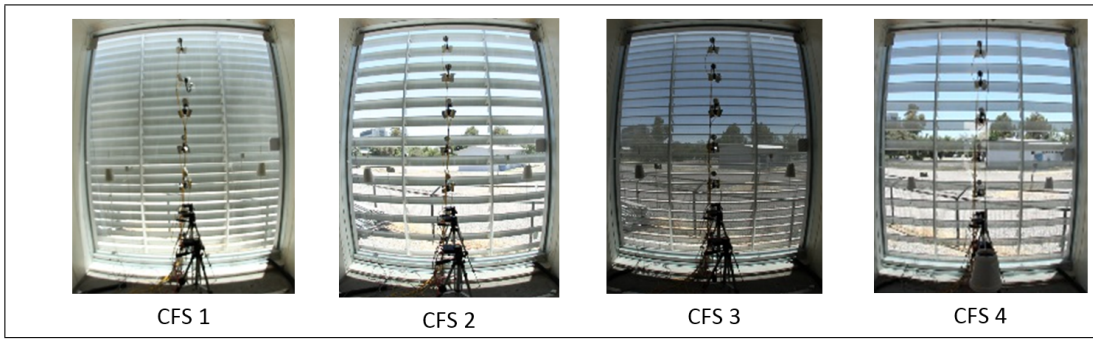

Figure 2.9. Outdoor visibility of the different CFS at 2 PM of fenestration façade oriented northwest.

2.4.3. Energy consumption

Figure 2.10 and Table 2.5 shows the lighting, heating and cooling energy consumption measured for each CFS and the double clear glazing as well as the energy saving of the cases with CFS in comparison with the case of the window without CFS. It can be seen a similar total energy consumption among the cases with CFS, while the energy savings are between 29 and 34%. CFS 3 presents the lower total energy consumption because CFS3 provides a good balance in controlling SHG to significantly reduce cooling energy consumption but allowing enough daylighting to avoid excessively increasing the lighting energy consumption. In contrast CFS 1 presents the higher energy consumption due to very high lighting energy consumption because of the lack of transmitted daylighting to the indoor space.

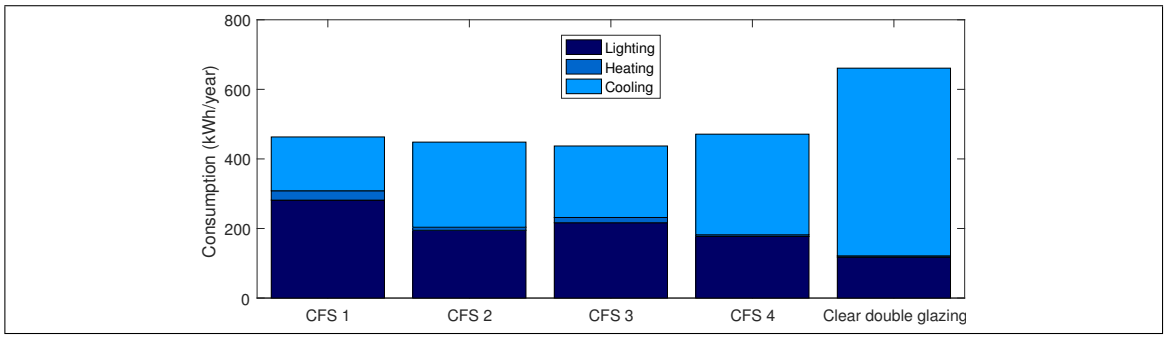

Figure 2.10. Measured energy consumption for lighting, heating and cooling (kWh/year) for different CFS.

Table 2.5. Comparison between exact solution (ES) and optimized solution (OS) performance of visual comfort and energy consumption.

CFS	Energy consumption				Energy savings	
	Lighting	Heating	Cooling	Total	(kWh/year)	%
CFS 1	282	27	155	463	198	30
CFS 2	195	9	245	448	213	32
CFS 3	217	15	206	437	224	34
CFS 4	177	5	289	471	190	29
DCG	118	4	540	661	0	0

2.5. Conclusions

This paper evaluated the effectiveness of outdoor CFS made of aluminum-zinc alloy to control SHG, reduce total energy consumption and provides occupant's visual comfort in an office space located in Santiago of Chile, which is characterized by a semiarid climate with high temperatures and solar radiation for 7 months of the year. The CFS evaluated correspond to non-specularly curved louvers with 0% or 20% perforations and louver's spacing of 120 or 240 mm. The effectiveness of CFS was evaluated among themselves as well as in comparison with the results for an unshaded clear double glazing.

Simulations were performed using a simulation tool developed for integrated thermal and lighting analysis. This tool integrates SketchUp, Groundhog® (a SketchUp plugin), Radiance and EnergyPlus. The main conclusions that can be drawn from this study are:

- The evaluated CFS made of aluminum-zinc alloy are very effective building skins to control SHG and reduce total energy consumption. However, visual comfort is only achieved by CFS 3 which has 20% perforations and 120 mm spacing between louvers. CFS 3 allows having a $\mathrm{sDA}_{300/50\%}$ and $\mathrm{ASE}_{4000/400h}$

of 100% and 11% as well as providing proper outdoor visibility. This evidences importance of evaluating all performance aspects of CFS to establish the ones that can achieve the expected performance.

- All evaluated CFS cause a large reduction of SHG in comparison with an unshaded double clear glazing, whereas significant differences were found among the SHG of CFS due to different percentage of perforations and spacing. Increasing the louver spacing causes higher solar heat transmission through the fenestration system than that for perforations. However, it is rather than notorious that a low percentage of perforations (20%) also increases the SHG significantly in comparison with the CFS without perforations.
- In terms of total energy consumption, energy savings of all cases with CFS are between 29% and 34% in comparison with the window without CFS. CFS 3 causes the lowest energy consumption. Coincidently, this CFS is the only one that also meet visual comfort criteria.

This paper evidences the importance of louvers spacing and perforations on the building energy performance and occupant's visual comfort of outdoor CFS made of aluminum-zinc alloy. Further studies are needed to optimize the design of CFS in terms of louvers spacing and percentage of perforations to obtain a balanced performance in terms of office energy consumption and occupant's visual comfort.

3. INTEGRATED THERMAL AND LIGHTING PERFORMANCE SIMULATIONS FOR MINIMIZING ENERGY CONSUMPTION OF OFFICE BUILDINGS WITH COMPLEX FENESTRATION SYSTEMS

3.1. Abstract

Office buildings are highly affected by solar heat gains through fenestrations. External shading devices allow lowering these solar heat gains which might significantly influence the building performance in terms of improving energy efficiency and visual comfort. When using automated control system in order to simultaneously evaluate and regulate solar heat gains and indoor illuminance, the energy consumption for regulating visual and thermal comfort may be adjustable to the minimum. This paper aims to determinate the optimum irradiance level for a control strategy of two different external complex fenestration systems (CFS) in four cities, Montreal, Santiago of Chile, Boulder and Miami. The shadings of the CFS are: 1.- a set of exterior curved opaque and perforated louvers and 2.- a set of venetian blinds controlled by the incident irradiance. The simulated space correspond to 4.0 m x 6.5 m x 2.8 m room, with interior dimming luminaires. Groundhog®, an extension for Sketchup -that allows exporting the models to Radiance- and *mkSchedule*, a tool that integrates EnergyPlus and Radiance to facilitate the combined thermal and lighting analysis of building using control algorithms, were used for simulations. For each case, visual comfort is assessed based on spatial daylight autonomy (sDA), annual sunlight exposure (ASE) according to Illuminating Engineering Society (IES) standard, while, building energy performance is calculated in terms of energy consumption for heating, cooling and lighting. For the venetian blinds varies between 530 W/m^2 and 610 W/m^2, and for the louvers varies between 290 W/m^2 and 350 W/m^2. It has been observed that *mkSchedule* is an effective tool to be used in early design stages of architectural design to determine the best control strategy of CFS based on visual comfort parameters and energy performance of a building.

3.2. Introduction

Buildings account for about 40% of the world's annual energy consumption, which has conducted to an intensive and varied research worldwide, in order to improve their indoor comfort conditions and energy efficiency. On the other hand, for increasing buildings' thermal performance, public policies have been implemented during the last decades, especially in developed countries (Nielsen et al., 2011).

Energy consumption in a building is directly related to the occupants' activities and the requirements of artificial lighting, heating, cooling and ventilation. The lighting, heating and cooling energy consumption -which become very significant in a building-, are directly associated with the design of its envelope, particularly in office buildings. Currently, this type of buildings of cities with very different climates of the world have been using highly glazed façades, which have increased occupants' glare and building's energy consumption (Serra et al., 2010; Bustamante et al., 2014).

To increase the visual and thermal comfort of an office building, the use of external solar protection devices on glazed façades, as louver and venetian blinds, forming a complex fenestration system (CFS), which may also include internal protections such as roller blinds, have been widely used and studied (Kirimtat et al., 2016; E. Shen et al., 2014; Correia da Silva et al., 2013; Chan & Tzempelikos, 2013; Bueno et al., 2015; Yi et al., 2015; H. Shen & Tzempelikos, 2012; Chan & Tzempelikos, 2015).

Concerning external solar protection systems, these may be fixed or movable. It has been determined that due to non-appropriated design, fixes systems not necessarily offer adequate protection, allowing the incidence of direct solar radiation on work surfaces in office buildings (Bustamante et al., 2014). At the same time, these systems can not be operated by users in order to improve the indoor environmental conditions according to their requirements. Mobility allows control of the transmitted radiation through the transparent components and therefore it is possible to regulate the indoor environment according to

users' desires in the workspace (Tzempelikos & Athienitis, 2007; H. Shen & Tzempelikos, 2012; Tzempelikos & Shen, 2013; Konstantoglou & Tsangrassoulis, 2016).

Several field studies were carried out in order to evaluate the effectiveness of solar protection systems and user behaviour (Saxena et al., 2010; Correia da Silva et al., 2013). In Porto, Portugal, it was established that the use of electric lighting and shading devices were more influenced by users' dynamics than to achieve better environmental indoor conditions, such as illuminance level in the work plane or solar transmission control through the glazed area. A high variability of performances were observed in different offices and between different users (Correia da Silva et al., 2013). However, on the other hand, in a study that considered 40 Dutch offices with automatic control of external venetian blinds with manual handling options, a significant correlation between weather parameters and blind adjustments was found ("Building automation and perceived control: A field study on motorized exterior blinds in Dutch offices", 2014).

For analyzing thermal and lighting performance of indoor spaces, multiple software and design tools have been developed in recent decades. Not all of these software and tools allow the simultaneous simulation of thermal and light performance of these spaces in an accurate way (Ward, 1994; C. F. Reinhart, 2013; *EnergyPlus*, n.d.; *TRNSYS*, n.d.).

Several studies examining dynamic control systems in façades, which can regulate interior environmental conditions regarding thermal and visual comfort and even air quality, have recently carried out (Tzempelikos & Athienitis, 2007; H. Shen & Tzempelikos, 2012; Tzempelikos & Shen, 2013; Konstantoglou & Tsangrassoulis, 2016). These studies generally include complex fenestration systems, with external solar protection systems and with indoor sun shading in some cases. Given the complexity of the transfer phenomena involved in these studies, different effective design tools, calculation models and methodologies that have enabled the integration these phenomena, such as solar and light transmission through CFS, have been developed (Guglielmetti et al., 2011; Bueno et al., 2015; Vera et al., 2016). Given the importance of achieving visual and thermal comfort

with energy efficiency in office spaces, it is highly recommended to use these tools and their application to different weather conditions.

Given a certain condition of thermal comfort in an office space with two sets of CFS system (exterior movable curved opaque and perforated slats or louvers that were spaced at 120 mm with 20% of perforation, and venetian blinds), a methodology that integrates their thermal and lighting performance has been applied. The methodology consists of, integrate Groundhog® (an extension for SketchUp that allows exporting the models to Radiance), *genBSDF* (that allows obtain bidirectional properties of CFS) and *mkSchedule* (a tool that integrates EnergyPlus and Radiance to facilitate the combined thermal and lighting analysis of building using control algorithms), for performing integrated thermal and lighting analysis of spaces with controlled artificial lighting and CFS. This methodology aims to control the irradiance transmitted through the CFS into the office space, in order to minimize the heating, cooling and electrical lighting energy consumption and ensuring thermal and visual comfort. An office space located in cities with very different climatic conditions such as Montreal (Canada), Boulder and Miami (USA) and Santiago (Chile) has been considered in the present study.

3.3. Methodology

The process for the designing a control strategy based on incident irradiance for a movable CFS, consists in a parametric analysis, where the maximum incident irradiance level varies within a specified range, resulting different scenarios where the visual comfort and energy consumption of the space are evaluated. The process requires an integrated thermal and lighting analysis tool in order to evaluate the performance of these CFS in each scenario.

The tool for integrating the thermal and lighting analysis that it has been used is *mkSchedule* (Vera et al., 2016; Molina, 2014). According to Vera et al. (2016) and Molina

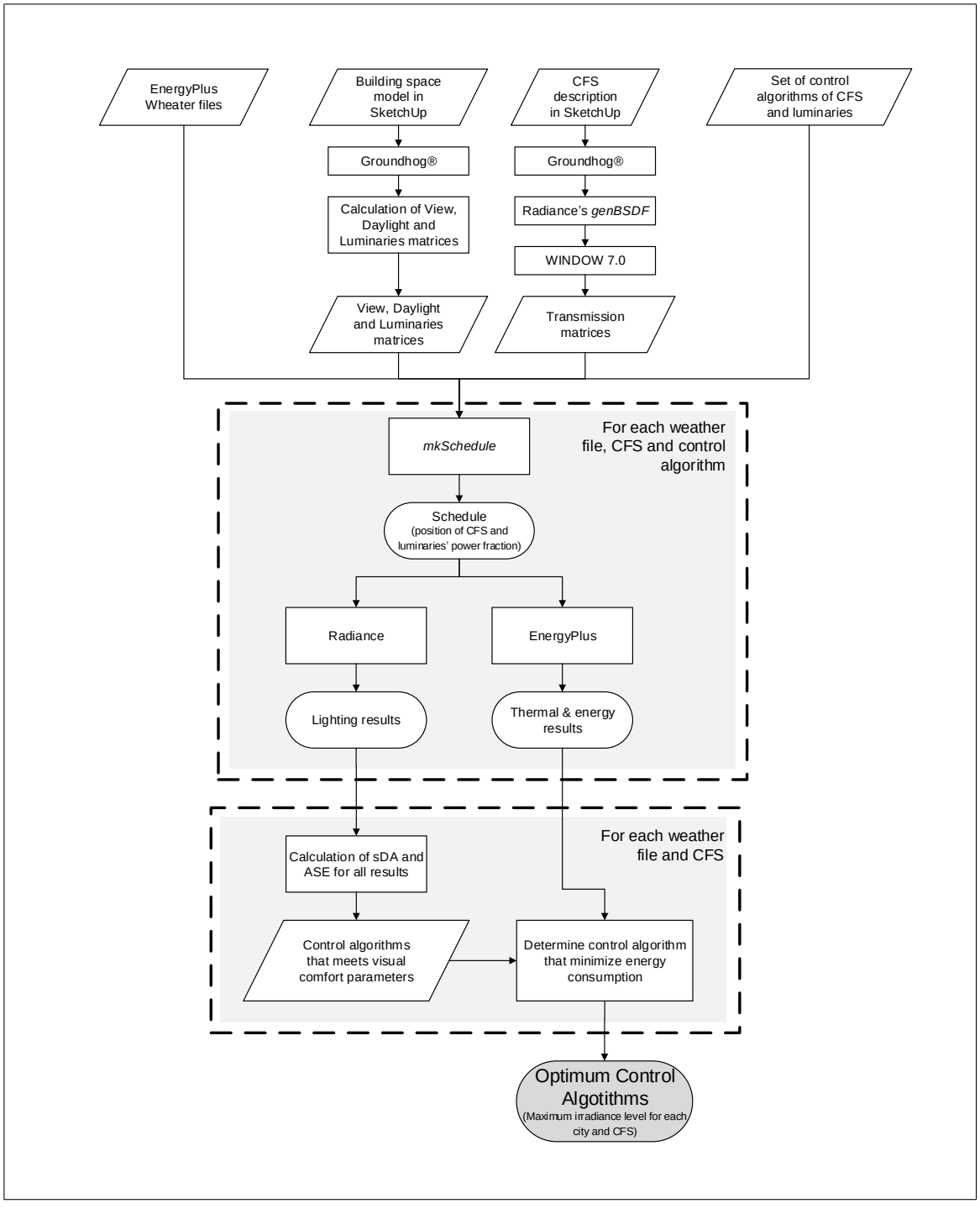

Figure 3.1. Flow chart of the methodology to determine the optimum control algorithm for each case.

(2014), the methodology used by this tool improves the one presented by (Wienold, Frontini, Herkel, & Mende, 2011).Wienold et al. methodology consisted of three steps: first, multiple lighting simulations are performed using DAYSIM (C. F. Reinhart, 2013); second, a control algorithm was applied to the results in order to choose artificial lighting power and shading position for each time step; and third, the chosen positions and luminaire power were transferred to ESP-r for carrying out energy performance simulations. The improved methodology used by *mkSchedule*, on the other hand, separates the control sensors (i.e. those whose measurements will be used control luminaires or CFS) from the workplane sensors (i.e. those that will be analyzed to quantify quality of the lighting in the space). Working with only the control sensors makes the process of creating schedules faster and more realistic (i.e. control is usually done by installing one or two photosensors on the ceiling, not many of them in the workplane). Finally, the schedules can be used for carrying out both energy performance and lighting simulations, and their results can be analyzed holistically to quantify the thermal and visual comfort, and the whole building energy consumption.

The building was designed in SketchUp, and then exported (using Groundhog®) in an appropriated format for multiphase analysis. In this case the Three-phase method (McNeil, 2013; Sexena, Ward, Perry, Heschong, & Higa, 2010) is used through *mkSchedule*. This implies exporting the building itself separately from the shading devices, which will allow assessing the bidirectional properties of the latter and change the parameter of control strategy easily (i.e. maximum incident irradiance level). Following, in Figure 3.1 shown the flow chart of the methodology applied to determinate the optimum irradiance level for the control strategy in each city and CFS.

3.3.1. Office space building

This study includes four cities with different climates: Santiago (Chile), Miami (USA), Boulder (USA) and Montreal (Canada). Montreal has a semi-continental climate, with a warm, humid summer and a very cold winter. Climate of Boulder is semi-arid with

several sunny days each year. Miami has a tropical climate with hot and humid summers and short warm winters. Santiago of Chile has a semi-arid climate characterized by high temperatures and solar irradiance for around 8 months of the year.

The space to be studied correspond to a 4.0 m x 6.5 m 2.8 m space, with two sets of dimming luminaires, and one south oriented glazed façade north hemisphere (Montreal, Boulder and Miami), and north oriented glazed façade for Santiago of Chile. The building is shown in Figure 3.2, and Table 3.1 shows the simulation layout.

Table 3.1. Simulation layout.

Parameter	Details	
Cities	Santiago (Chile)	S33.38 °, W70.78 °
	Miami (USA)	N25.82 °, W80.30 °
	Boulder (USA)	N40.02 °, W105.25 °
	Montreal (Canada)	N45.47 °, W73.75 °
Façade orientations	Noth/south[1]	
Office space	Size	4.0m(w) x 6.5m(l) x 2.8m(h)
	WWR[2]	0.53
Opaque surfaces	Exterior	λ = 1.66 $Wm^{-1}K^{-1}$
		e=15 cm
	Interior	λ = 0.025 $Wm^{-1}K^{-1}$
		e=5 cm
Window	Size	3.5m(w) x 1.7m(h)
(Double clear glass)	T_{vis}	0.83
	SHGC	0.83

Continued on next page

[1]South for north hemisphere (Montreal, Boulder and Miami), and, north for Santiago of Chile.
[2]Window-to-wall Ratio (WWR) is the measure of the percentage area determined by dividing the building's total glazed area by its exterior envelope wall area.

Parameter	Details	
	U-factor	2.70 $Wm^{-1}K^{-1}$
Surface reflectances	Floor	20%
	Ceiling	70%
	Wall	50%
HVAC system	Electric heat pump (EHP)	COP 3.0
	Heating thermostat setpoint	20 °C
	Cooling thermostat setpoint	24 °C
Ventilation + infiltration	0.7 ACH (Gowri, Winiarski, & Jarnagin, 2009)	
Internal gains	People	6.7 W/m^2
	People radiant fraction	0.3
	Lighting	13.85 W/m^2
	Light radiant fraction	0.3
	Electric equipment	15 W/m^2
Lighting level setting	Workplane at 0.8 m	500 lux
Schedule	Occupancy, lights, equipment & HVAC	08:00 - 18:00 hrs. (weekdays)

3.3.2. Complex fenestration systems

Two kinds of movable CFS were used. One of them corresponds to a set of venetian blinds that were generated using WINDOW 7.3 (LBNL, 2014), and the other corresponds to a set of horizontal curved and perforated louvers (commercial product named Celoscreen of HunterDouglas Company Chile) designed in SketchUp, and exported to into Radiance with Groundhog®. The movable CFS can be fixed in six different angles (0 °, 15 °, 30 °, 45 °, 60 ° and 75 °). The material of both shading devices are identical and corresponds to a reflective metal (95% solar and visible reflectance) with 0% of specularity.

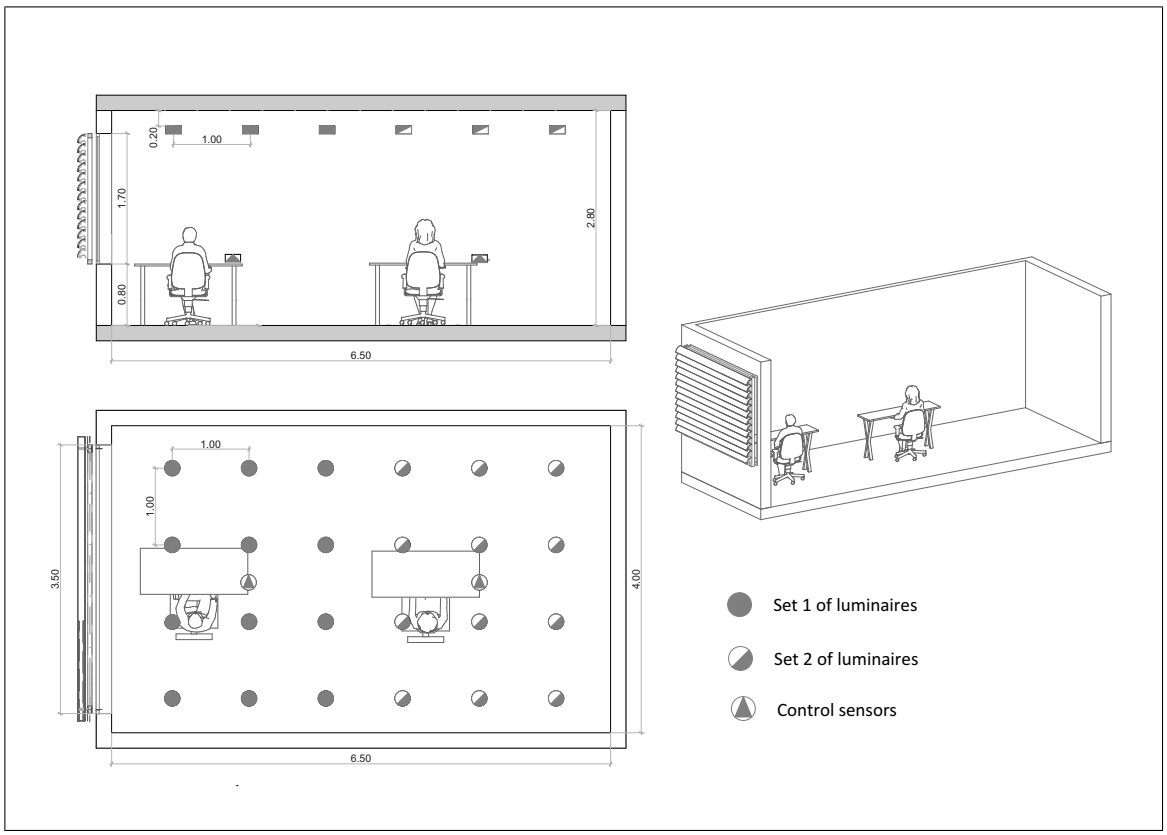

Figure 3.2. Model of the office space with louvers and interior dimensions (m), plain view and side view.

Figure 3.3 presents the dimensions of the venetian blinds.

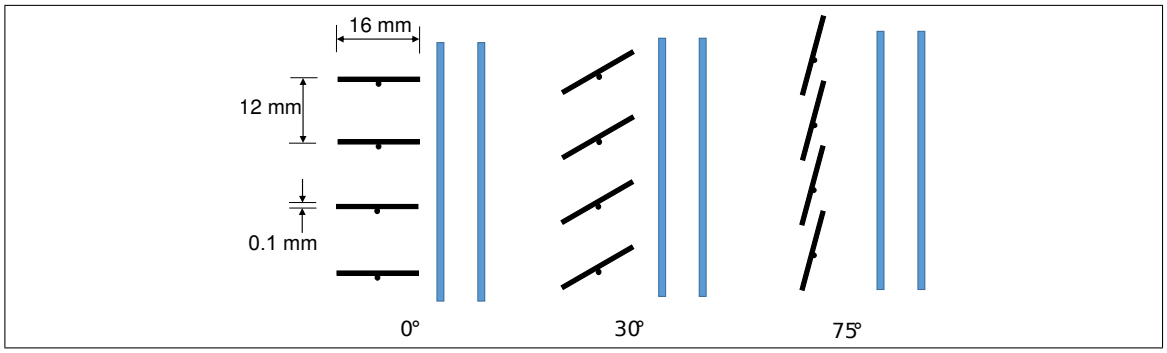

Figure 3.3. Dimensions of venetian blinds.

Figure 3.4 and 3.5 show dimensions and views of the louvers.

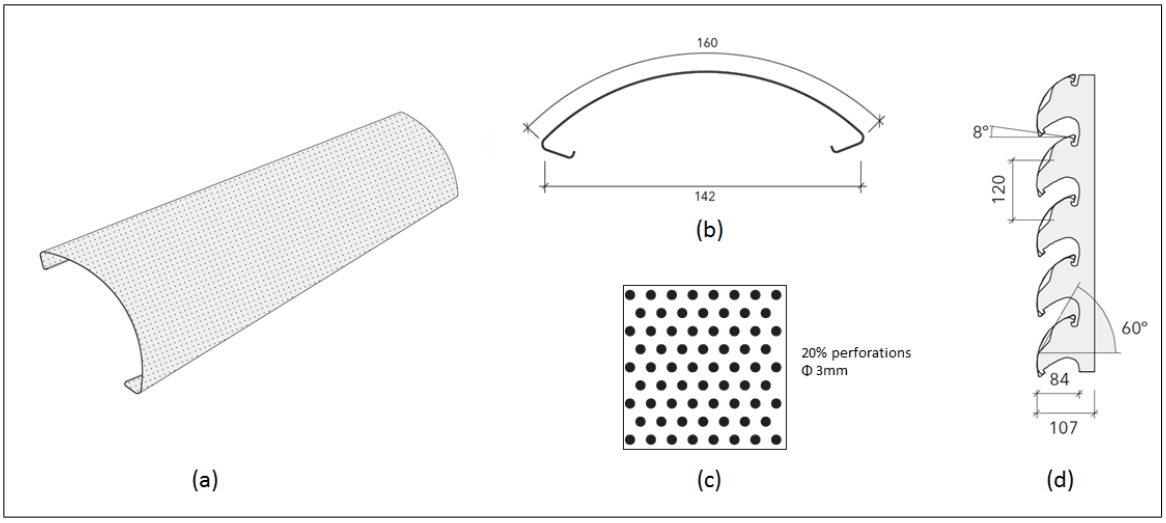

Figure 3.4. Perforated undulated louvers. (a) 3D view of louver. (b) Louver dimensions (mm). (c) Perforation dimensions (mm). (d) Installed louver dimensions (mm). Adapted from (HunterDouglas, 2013).

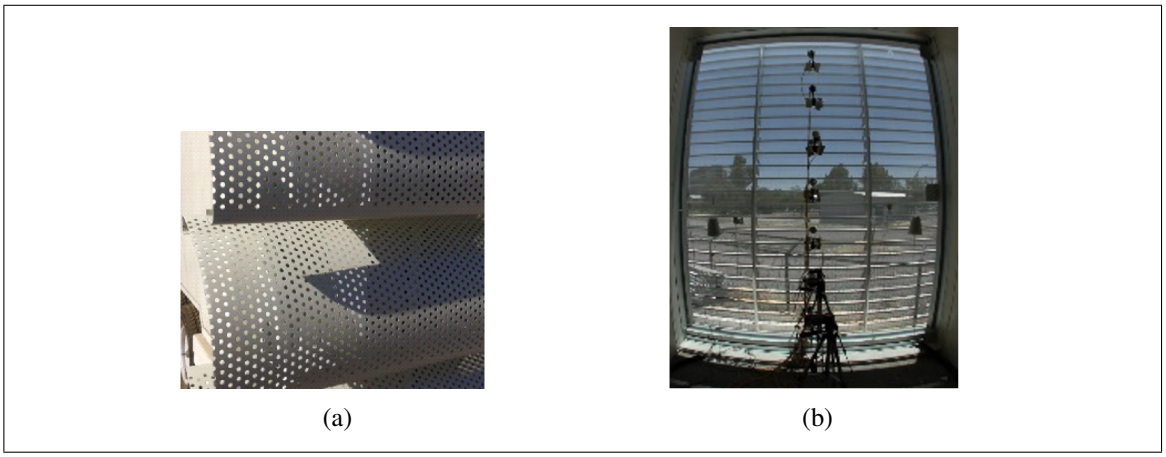

Figure 3.5. Perforated undulated louvers. (a) Perforation pattern. (b) Outdoor visibility of CFS.

There are three main options for assessing the BSDFs of complex fenestration systems, such as 1.- Laboratory measurements, 2.- Development of analytical models usually based on Radiosity, and 3.- Emulation of laboratory measurements in a virtual environment using ray-tracing techniques (Andersen & de Boer, 2006). However, since the materials of the shading devices used are specular and the shading systems to be evaluated have not been built yet, ray-tracing techniques are the only option available for this case (as often

happens at design stage). Ray-tracing techniques have been used for the assessment of bidirectional properties in various studies, (Konstantoglou et al., 2009; McNeil & Lee, 2013; Rubin, Jonsson, Kohler, & Klems, 2007). In this study, Radiance's program *genBSDF* has been used for assessing both the visible and the solar bidirectional properties for lighting (Radiance) simulations and energy performance (EnergyPlus) simulations respectively. Although Radiance is usually used within the visible ranges, Molina et al. (2015) verified that *genBSDF* is a very accurate tool for assessing solar BSDFs of CFS when materials are not spectrally selective.

On the other hand, McNeil et al. (2013) also validated *genBSDF* for the visible range. McNeil et al. explained the basis and use of the *genBSDF* tool and validated the tool by comparing results for four cases with BSDFs produced via different methods. This validation demonstrates that BSDFs created with *genBSDF* are comparable to BSDFs generated analytically using TracePro and by measurement with a scanning goniophotometer.

The BSDFs were obtained in Klems full form, which corresponds to a matrix form for performing the annual simulations. The Radiance models of the shading devices that were inputted into *genBSDF* were in standard Radiance geometry and materials format. After generating the BSDF for each shading position, they were imported to WINDOW 7.3 (LBNL, 2014) to be lately exported into an EnergyPlus readable format. Table 3.2 shows solar heat gain coefficient (SHGC), visible transmission coefficient (T_{vis}) and U-value for venetian blinds and louvers obtained with WINDOW 7.3, which are the glazing units' main characteristics.

Table 3.2. Solar heat gain coefficient (SHGC), visible transmission coefficient (T_{vis}) and U-value for shadings.

Slat angle	Venetian Blinds			Louvers		
	SHGC	T_{vis}	U-value ($Wm^{-1}K^{-1}$)	SHGC	T_{vis}	U-value ($Wm^{-1}K^{-1}$)
0°	0.84	0.84	2.70	0.43	0.31	2.70
15°	0.63	0.62	2.70	0.39	0.30	2.70
30°	0.41	0.39	2.70	0.33	0.26	2.70
45°	0.19	0.16	2.70	0.25	0.18	2.70
60°	0.11	0.08	2.70	0.18	0.13	2.70
75°	0.06	0.03	2.70	0.14	0.10	2.70

3.3.3. Control strategy

The CFS control strategy consists of three main steps: first, to position the blinds according to the solar irradiance over the facing window; second, recalculate the illuminance values on the interior (the daylighting levels of the space have been modified due to the new position of the CFS); and third, dim the luminaire power to achieve the desired illuminance on the sensors (i.e. increase the luminaire power until the setpoint is achieved).

For this case study, two sets of dimming luminaires were installed, and two control sensors were located in the space to control each of them: one in the first half of the space and the other one is centered in the second half of it (see Figure 3.2). It should be noticed that a more realistic approach could be made by placing the sensors in the ceiling, and correlating their measurements with the workplane illuminance, as is explained in (Tzempelikos, 2012). However, in this case, the sensors were located just under the central luminaire of each set pointing to the ceiling in order to simplify the process.

Figure 3.6 shows how the position of the CFS varies according to irradiance level over the facing window.

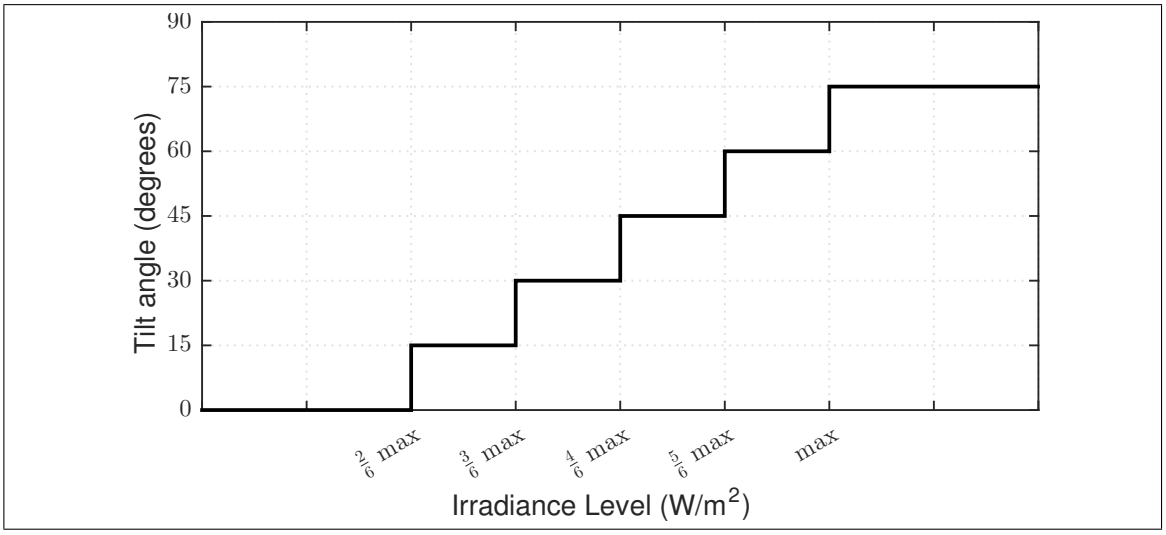

Figure 3.6. Irradiance control of CFS.

Simulation consist in a parametric analysis, varying the value of maximum irradiance level of the control algorithm between 10 W/m^2 and 1000 W/m^2 with step of 10 W/m^2. The optimum irradiance level corresponds to the one achieves the minimum energy consumption (total of heating, cooling and lighting) and meets the visual comfort parameters for each CFS in a certain city.

3.3.4. Visual comfort evaluation

Visual comfort is evaluated through the spatial daylight autonomy (sDA) and annual sunlight exposure (ASE). These metrics were developed by Illuminating Engineering Society (IES) (IES, 2013). sDA describes the annual sufficiency of ambient daylight levels in interior environments. It is defined as the percentage of an analysis area that meets a minimum daylight illuminance level for a specified fraction of the operating hours per year. ASE is a metric that describes the potential for visual discomfort in interior work environment. It is defined as the percentage of an analysis area that exceeds a specified

direct sunlight illuminance level for more than a specified number of hours per year (e.g. working hours in weekdays).

$sDA_{300/50\%}$ and $ASE_{1000/250h}$ is recommended for the analysis of daylight sufficiency and potential visual discomfort. $sDA_{300/50\%}$ is reported as the percentage of analysis points across the analysis area that meets or exceeds this 300 lux value for at least 50% of the analysis period (from 8AM to 6PM, 10 hours per day, weekdays). $ASE_{1000/250h}$ is reported as the percentage of analysis points across the analysis area that meet or exceed this 1000 lux value for 250 hours per year of the analysis period. sDA must meet or exceed 55% of the analysis area and ASE is acceptable when is less than 7%.

Since IES standard based on studies in 100 m^2 rooms, with the longest distant to the window of 12 m, ASE values may easily exceed 7%. In our case, due to smaller dimensions of the space, it has been considered an acceptable ASE value less than 20%. On the other side, 1000 lux illuminance level is too low in some cases; according to (Mardaljevic et al., 2012) 3000 lux is a recommended value for offices. IES standard say until 4000 lux can be an acceptable level and is possible exceed this value for 400 hours per year even. In this case is evaluated $ASE_{2000/400h}$ like a visual discomfort parameter. For daylight autonomy, $sDA_{300/50\%}$ >50% it has been acceptable.

3.3.5. Simulation tool

Since CFS are often installed to provide enhanced visual and thermal comfort as well as an excellent energy performance, an holistic lighting/thermal analysis of spaces with complex fenestration systems is highly relevant. Since this step is probably the most important part of the workflow, this section will be deeply explained. There are different options for carrying out holistic lighting/thermal analysis (Guglielmetti et al., 2011; Janak, 2007; Petersen & Svendsen, 2010; Tzempelikos & Athienitis, 2007). As mentioned, in our case, *mkSchedule* is being used. This tool was developed in (Vera et al., 2016; Molina, 2014) and allows easy application and modification of different control algorithms, and

implements control in only one simulation via the Three-phase method very efficiently (*mkSchedule's* methodology shown in Appendix A).

mkSchedule is a program based on Radiance's *dctimestep* and *gendaymtx* programs to implement the Three-phase method and create the Perez et al. sky (Perez, Ineichen, Seals, Michalsky, & Stewart, 1990; Perez, Seals, & Michalsky, 1993) required for the simulations, respectively. Also, *mkSchedule* use EnergyPlus weather files, that may be extracted from DAYSIM's *epw2wea* program, which reads and selects information from the weather files. This program was developed with the intention of simplifying the integration of lighting and thermal simulations using Radiance and EnergyPlus or ESP-r. *mkSchedule* receives as input all the matrices required for the Three-phase method calculations (i.e. View, Daylight and all the BSDF in matrix form in Klems basis, computed as explained in (McNeil, 2013), the contributions of the luminaires over the sensors in matrix form (i.e. standard *rcontrib* or *rtrace* Radiance's program output) and a control algorithm written in Lua scripting language. The output is a schedule file with sensor illuminance values, luminaire fraction of power (i.e. 0 is off, and 1 is on), and the shading position represented as an integer. One of the key features of *mkSchedule* is its flexibility to modify and try different control algorithms easily by performing fast calculations. This is achieved by defining the control algorithm as an argument to the main program, and by allowing the user to program it in Lua, a scripting language much simpler than the main program's C. From the control scripts, the user can use predefined functions to retrieve relevant information for making decisions and use it as triggers. For example, luminaire power and shading position can be controlled according to sun position (i.e. azimuth, zenith and altitude), exterior dry-bulb temperature, irradiance over a surface calculated according to Perez et al. (Perez et al., 1990, 1993), and as shown in (Duffie & Beckman, 1996), illuminance over a sensor, previous luminaire power and shading position, or any information that can be derived from the lighting simulation and/or the EnergyPlus weather file.

3.4. Results and analysis

3.4.1. Lighting results

The lighting simulation at each time step, implemented the Three-phase method for the window, and then summed them together along with the luminaire contribution scaled by the fraction of the total power, which was registered on the schedule based on the CFS control strategy. For this analysis, 104 sensors were placed in a horizontal workplane located 0.8 m over the floor (Neufert, 2012; IES, 2013).

A total of 800 simulations were run, 100 for each CFS and city, with the maximum irradiance level of the control strategy varies in a range between 10 W/m^2 and 1000 W/m^2. For each case, it was evaluated the $\text{sDA}_{300/50\%}$ and $\text{ASE}_{2000/400h}$, and also, it was calculated the energy consumption (lighting, heating and cooling).

Figure 3.7 shows results of $\text{sDA}_{300/50\%}$ and $\text{ASE}_{2000/400h}$. The maximum irradiance level for each control strategy is shows in x axis, and y axis shows the $\text{sDA}_{300/50\%}$ and $\text{ASE}_{2000/400h}$ for each case. It may notice that $\text{sDA}_{300/50\%}$ meets the minimum illuminance levels in most of analyzed points in all cases (over than 50%), and the $\text{ASE}_{2000/400h}$ meets the maximum percentage for low values of irradiance.

3.4.2. Energy results

The energy performance simulation was carried in EnergyPlus by defining the windows as Complex Fenestration. Both sets of luminaires and the CFS were controlled using the schedule previously generated, which was also used for performing the lighting simulation.

Figure 3.8 shows the lighting, heating and cooling energy consumption for venetian blinds and louvers respectively. It can be seen that lighting energy consumption decreases while the maximum irradiance level increases in both cases (venetian blinds and louvers). This may be explained since a higher level of irradiance implies that control strategy will

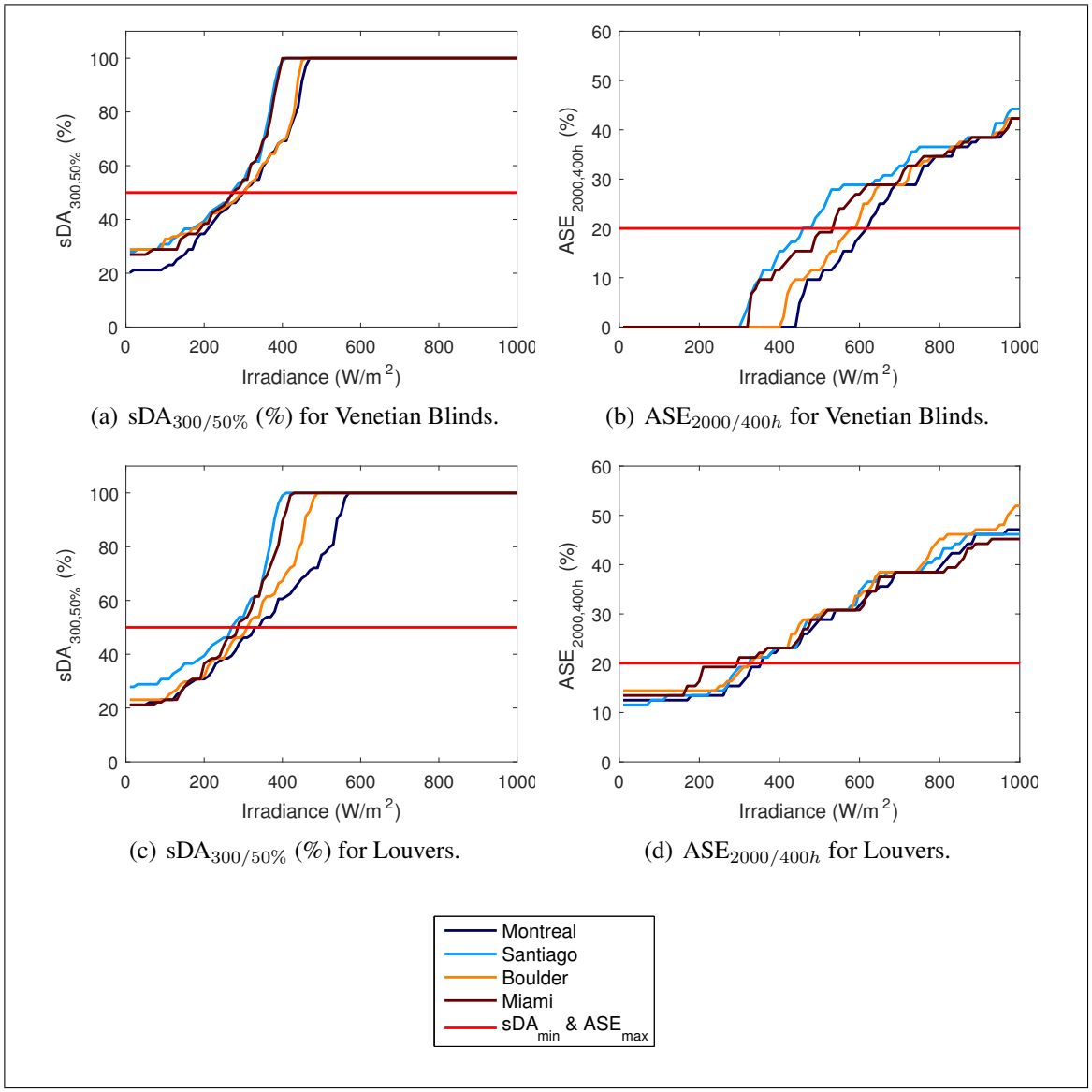

(a) $\text{sDA}_{300/50\%}$ (%) for Venetian Blinds.

(b) $\text{ASE}_{2000/400h}$ for Venetian Blinds.

(c) $\text{sDA}_{300/50\%}$ (%) for Louvers.

(d) $\text{ASE}_{2000/400h}$ for Louvers.

Figure 3.7. $\text{sDA}_{300/50\%}$ and $\text{ASE}_{2000/400h}$ for each CFS.

tend to open the external blinds, therefore, lights are not necessary to be turn on. This situation is similar on the four studied cities, which means that climate do not affect significantly the lighting energy consumption.

Regarding heating energy consumption, this is similar in both types of CFS (venetian blinds and louvers), but it varies considerably according climate. In Miami, a city with a tropical and warm climate, heating energy consumption is almost negligible. In the case

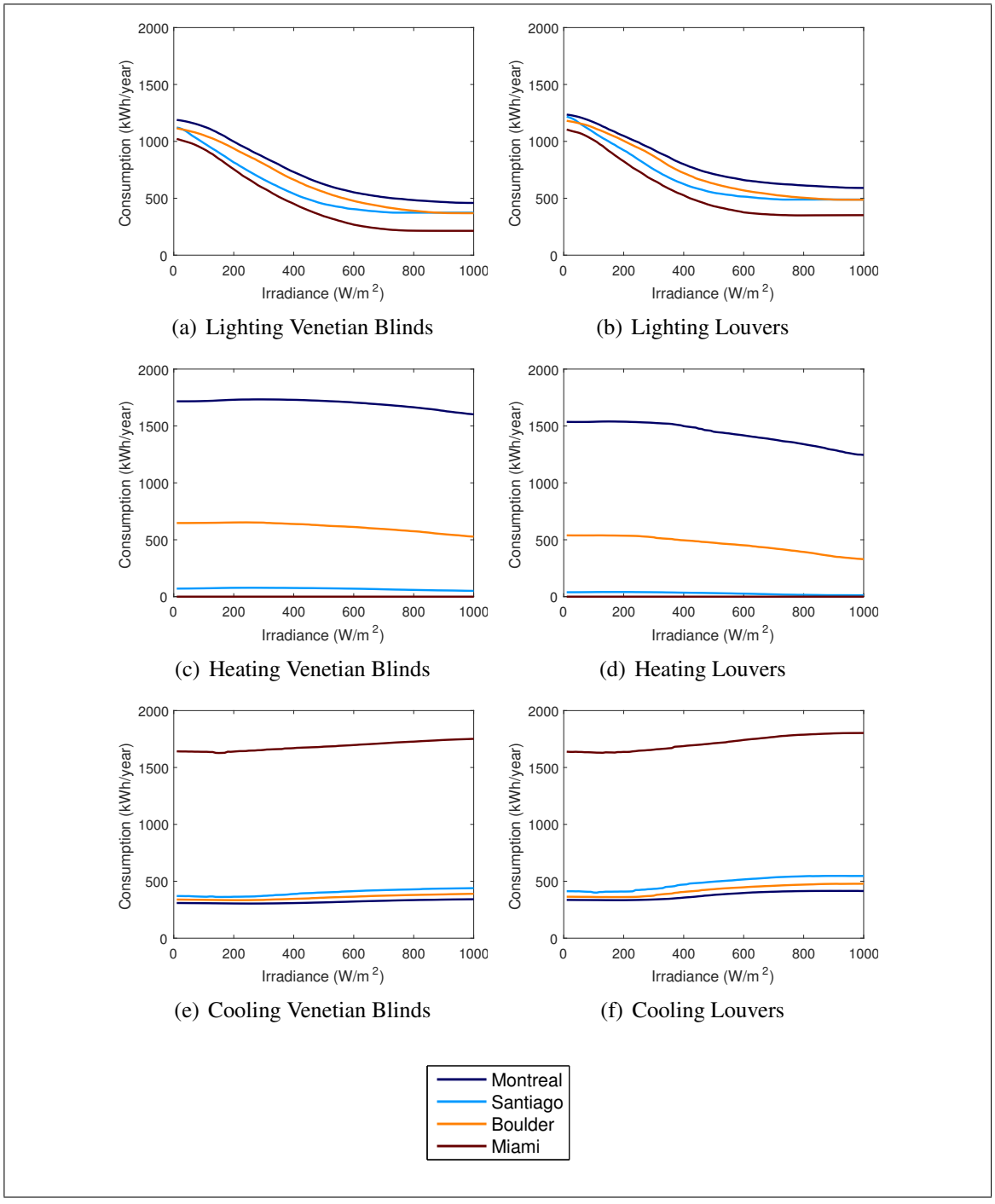

(a) Lighting Venetian Blinds (b) Lighting Louvers

(c) Heating Venetian Blinds (d) Heating Louvers

(e) Cooling Venetian Blinds (f) Cooling Louvers

Figure 3.8. Consumption of lighting, heating and cooling foreach CFS (kWh/year) respect maximum irradiance level.

of Montreal, heating is significant (1300 - 1500 kWh/year) because of its cold weather. In the case of Santiago of Chile, heating energy consumption is also close to zero. On the other hand, heating consumption do not vary significantly when increases the maximum irradiance level, this is because to the form of the strategy control, which generally it tends to have the blinds closed (over 45 °). Even so, it appears that over 400 W/m^2, heating consumption low slightly.

The behaviour of cooling is similar in both cases (venetian blinds and louvers), but varies considerably in each climate with the heating consumption in Figures 3.8c and 3.8d. Unlike heating consumption, Miami have the highest cooling consumption (around 1700 kWh/year), while Montreal, Santiago and Boulder have similar value but much lower (around 400 kWh/year). As heating, cooling do not varies significantly when the maximum irradiance level increases.

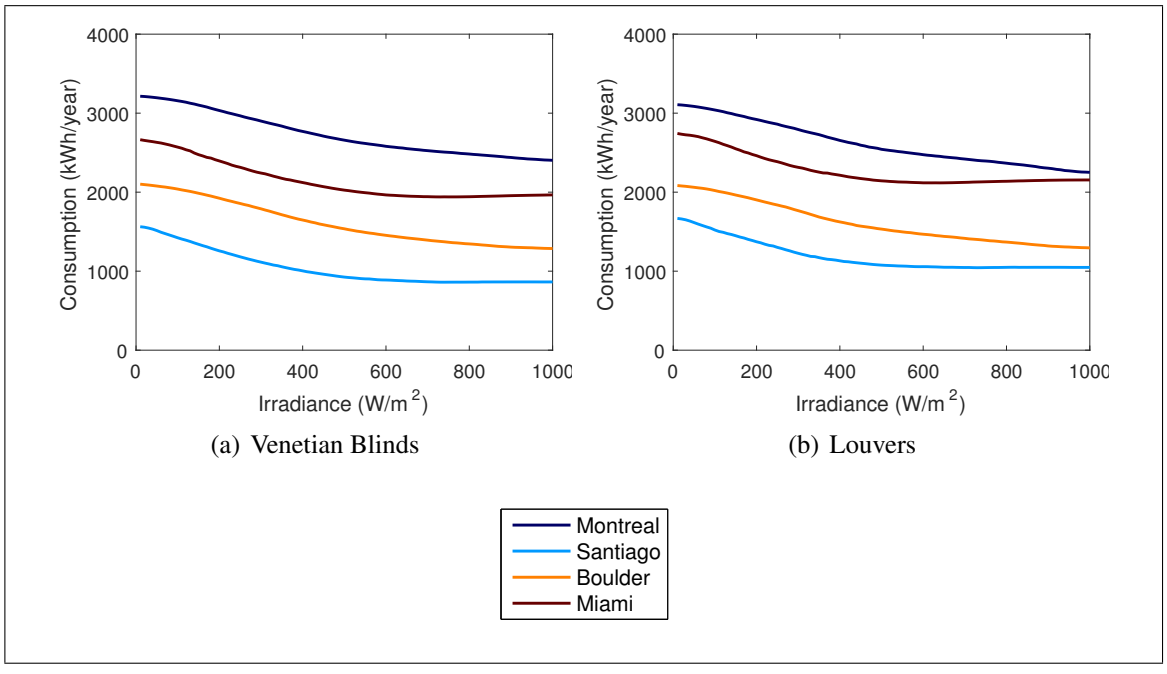

(a) Venetian Blinds (b) Louvers

Figure 3.9. Total consumption for each CFS (kWh/year).

In Figure 3.9 it can be seen the total consumption (lighting, heating and cooling) for venetian blinds and louvers. The figure shows that the behaviour while increases the maximum irradiance level is similar to lighting as shown in Figures 3.8a and 3.8b, therefore, the total consumption is mainly determined by the lighting energy consumption.

3.4.3. Optimum results

The optimum irradiance level to determine the best control strategy for each case is obtained combining the information of the total consumption showed in graphics of Figure 3.9 and the visual comfort parameters $sDA_{300/50\%}$ and $ASE_{2000/400h}$ of Figure 3.7. Figure 3.10 shows an example of this process for determine the optimum irradiance level for office space with venetian blinds at Montreal. Filled zone shows the irradiance levels that meets the visual comfort criteria. In this zone, it must select the minimum total energy consumption.

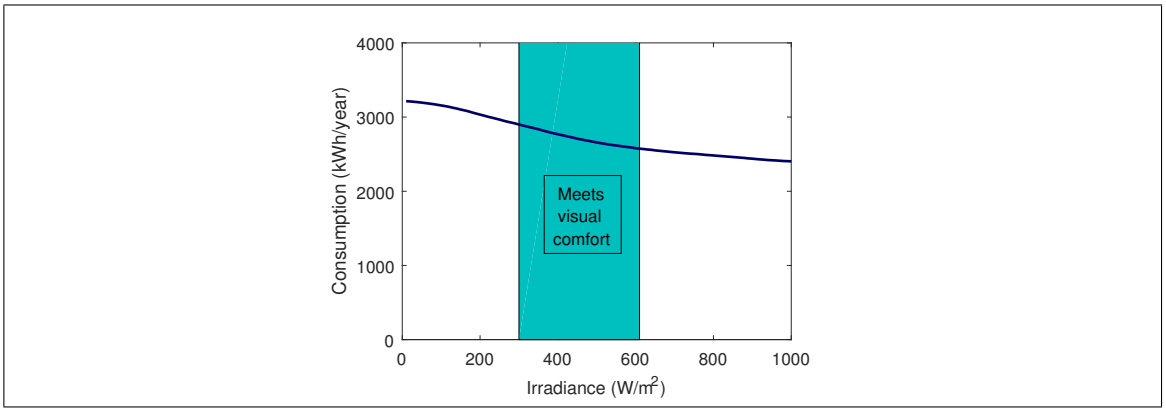

Figure 3.10. Determination of the optimum irradiance level for office space with venetian blinds at Montreal.

Furthermore, the best option is controlled by the visual comfort parameters. Following, in Table 3.3 shows the optimum values of maximum irradiance levels for the control strategy for each city and CFS, and Figure 3.11 shows the optimum consumption according EnergyPlus simulation for each city and CFS. Venetian blinds present higher irradiance levels (between 450 and 610 W/m^2) than louvers (between 290 and 350 W/m^2),

which agrees with SHGC values as shown in Table 3.2, where SHGC values of venetian blinds are higher than louvers. It may be noticed that climate do not affect significantly the optimum irradiance level, especially in case of louvers.

Table 3.3. Optimum maximum irradiance level (W/m^2) for each city and CFS.

City	Maximum irradiance level (W/m^2)	
	Venetian blinds	Louvers
Montreal	610	350
Santiago	450	320
Boulder	570	320
Miami	530	290

3.4.4. Time efficiency

The methodology that has been applied uses of *mkSchedule* needs to perform time efficient simulations due to their high number. In order to evaluate this efficiency, calculation and simulation times were measured for each case studied. These simulations were performed in a desktop computer with an AMD FX™ 8350 eight-core processor (4.00 GHz) and 16 Gb RAM. As it can be seen in Table 3.4, time to obtain the matrix for the Three-Phase Method is low (excluding the time of calculating BSDFs), which is around 01:15 minutes in each case (considering the two cases, one by each orientation). *mkSchedule* takes around of 38 seconds per case (generating the CFS and luminaires schedules), lighting simulation takes around 01:13 minutes per case, and, energy simulation takes around 01:18 minutes per case. These simulation times are for each core processor, i.e. in this study perform eight parallel simulations.

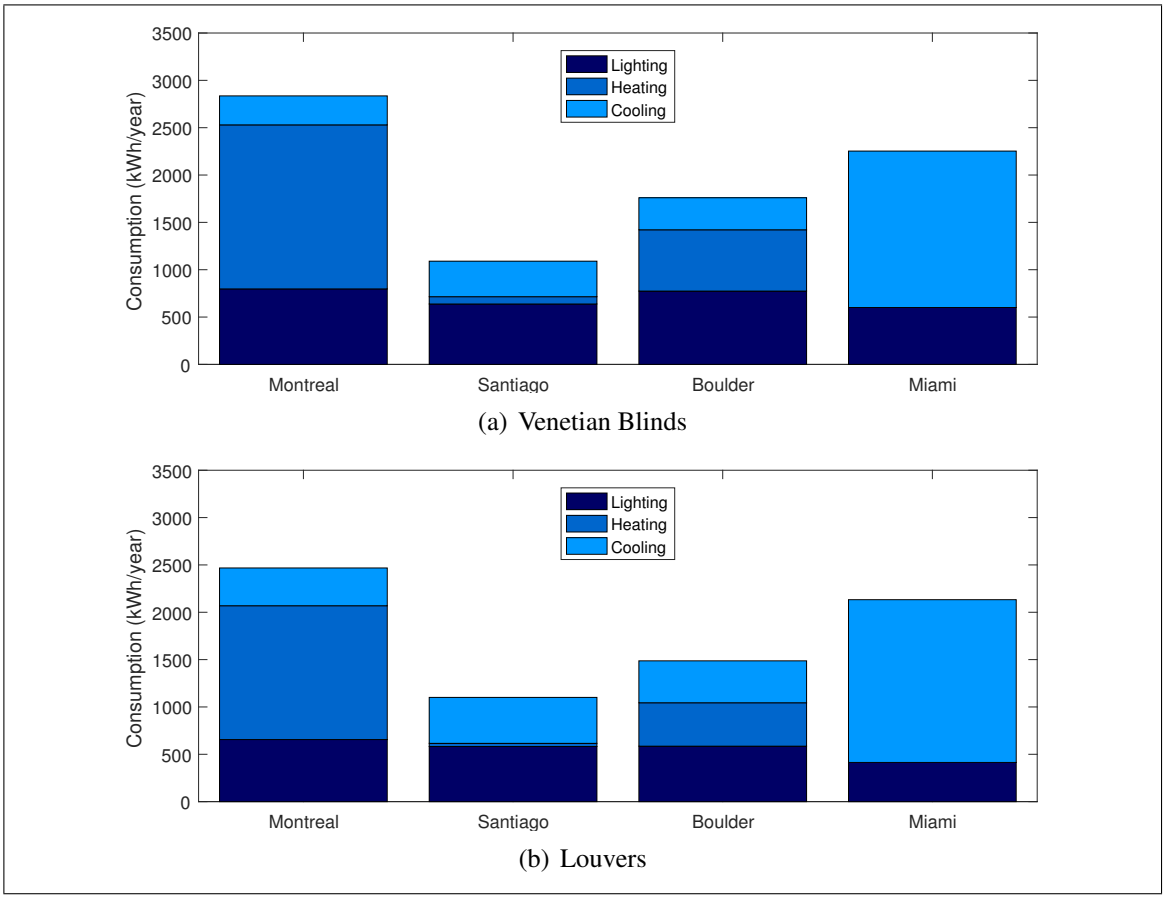

(a) Venetian Blinds

(b) Louvers

Figure 3.11. Optimum energy consumption (kWh/year) for each city and CFS.

Table 3.4. Simulation time.

Task	Time
Calculating Matrices	00:02:37 hrs
Run *mkSchedule*	01:03:11 hrs
Run Lighting Simulation	02:02:16 hrs
Run Energy Simulation	02:06:47 hrs

mkSchedule is time efficiently because just evaluating the control sensors. While increases the control sensors, more time take this task. Time of lighting simulation depends

only of the quantity of workplane sensors (i.e. dimensions of space), in this case 104 sensor were placed in the workplane. Finally, energy simulation takes relatively constant time. The total time simulation can still be more efficiently if change the limits of irradiance levels for example, being that simulation with irradiance levels over 750 W/m^2 and less than 200 W/m^2 are not necessary according to the results, and/or increases the maximum irradiance level step.

3.5. Conclusions

This paper aims to determine the optimum irradiance level for a control strategy of two external CFS (venetian blinds and louvers) in four cities (Santiago of Chile, Montreal, Boulder and Miami). In this study *mkSchedule* was used, a flexible and time-efficient tool that allows to run integrated thermal and lighting simulations using Radiance and EnergyPlus with different control strategies.

In order to define the best control strategy, based on incident irradiance on the window, a total of 800 simulations were run, 100 for each CFS and city. For each case, $\mathrm{sDA}_{300/50\%}$ and $\mathrm{ASE}_{2000/400h}$ as visual comfort standards were considered. Energy performance was calculated in terms of energy consumption for lighting, heating and cooling. The main conclusions that can be drawn from this study are:

- External movable CFS may significantly control daylighting. In terms of visual and thermal comfort, these can generate a positive or a negative effect on occupants. Results show that when a CFS is are not properly designed visual discomfort may occur.
- For defining an effective control strategy of a certain CFS, assuming certain visual comfort and energy performance standards, it has been showed that *mkSchedule* is an effective tool to be used in early stages of building design process.
- For each kind of CFS was obtained the optimum maximum irradiance level. For the venetian blinds, the optimum maximum irradiance for the control strategy

are 450 W/m^2, 530 W/m^2, 570 W/m^2 and 610 W/m^2 for Santiago, Miami, Boulder and Montreal respectively, and for the louvers, the optimum maximum are 320 W/m^2, 290 W/m^2, 320 W/m^2 and 350 W/m^2 for Santiago, Miami, Boulder and Montreal respectively. Furthermore, a correct study of control strategy can be an important variable in the design stage to reduce energy consumption.

Further studies are needed to evaluate correctly the parameters of visual comfort, and to perform a cost analysis during design stage of buildings, to determe if a movable CFS are really a good option in comparison with fixed CFS.

4. IMPACT OF DIFFERENT CONTROL STRATEGIES OF DYNAMIC COMPLEX FENESTRATION SYSTEMS AND LUMINAIRES SYSTEMS IN VISUAL COMFORT AND ENERGY CONSUMPTION OF OFFICE BUILDINGS

4.1. Abstract

Office buildings are highly affected by solar heat gains through fenestrations. External shading devices allow lowering these solar heat gains which might significantly influence the building performance in terms of improving energy efficiency and visual comfort. This paper aims to evaluate the performance of four control strategies of complex fenestration systems (CFS) based on incident irradiance level, vertical eye illuminance, cut-off angle and angle for blocking light, in four cities, Montreal (Canada), Boulder and Miami (USA) and Santiago (Chile) has been considered in the present study. The simulated space corresponds to 4.0 x 6.5 m room, with interior dimming luminaires. Groundhog®, an extension for SketchUp -that allows exporting the models to Radiance- and *mkSchedule*, a tool that integrates EnergyPlus and Radiance to facilitate the combined thermal and lighting analysis of building using control algorithms, were used for simulations. For each case, visual comfort is assessed based on spatial daylight autonomy (sDA), annual sunlight exposure (ASE) according to Illuminating Engineering Society (IES) and simplified daylighting glare probability (DGPs) standard, while, building energy performance is calculated in terms of energy consumption for heating, cooling and lighting. The most effective control strategy is incident irradiance level for all cases, that meets visual comfort and minimize energy consumption. Energy savings are between 10% and 20%, furthermore, a correct choose of control strategy can be an important variable in the design stage. It has been observed that *mkSchedule* is an effective tool to be used in early stages of building design for determine the best control strategy of a certain CFS to reduce energy consumption and provide visual comfort.

4.2. Introduction

The building sector accounts for 40% of the total energy consumption and one-third of the green gas house emissions (UNEP, 2009). Different architectural design strategies could be implemented for achieving high thermal and energy performance standards of office buildings (i.e. reduce window-to-wall ratio, incorporation of low solar heat gain coefficient (SHGC) glazing, use of efficient electrical lighting with low heat gains, use of effective solar protection systems, etc.). During the last decades it has been widespread the use of high glazed façades in office buildings (Serra et al., 2010; Basurto et al., 2015). Indeed, curtain walls with high glazed area have been used with high frequency in office buildings. Due to the low thermal performance glass and metals normally used in curtain walls, these are very sensitive to climate conditions compared with buildings with higher opaque thermal insulated walls (Lam et al., 2015). Buildings with high window to wall ratio (WWR) are affected by excessive solar heat gains (SHG), which turns in high cooling energy consumption and lack of visual comfort.

Daylighting is a relevant factor that affects visual comfort (Yun et al., 2014) and SHG through windows highly impact on the building energy performance and occupant's comfort. Several authors have reported the large contribution of high SHG through fenestration to cooling loads in warm and cold climates (Reilly & Hawthorne, 1998; Li & Lam, 2000; Winkelmann, 2001; Kuhn, 2006; Lam et al., 2015). Thermal and visual comfort as well as the energy consumption for lighting, heating and cooling are strongly determined by optical and thermal properties of glazed façades. The impact on air conditioning energy consumption and daylight transmission to indoor have been extensively studied (Goia et al., 2013; Correia da Silva et al., 2013; Ochoa, Aries, van Loenen, & Hensen, 2012; Wagner et al., 2007; Konis, 2013; Breesch & Janssens, 2010).

In order to control the solar heat gains through glazed façades, incorporation an exterior shading devices have been widely used. There is a large variety of exterior shading

fixed and movable devices such as louvers, venetian blinds, and perforated screens. However, most of these devices correspond to a non-specular transmitting layer. This layer next to the glazed surface on which it is applied corresponds to a complex fenestration systems or CFS (Laouadi & Parekh, 2007).

CFS with external solar shading systems have been widely studied. Most of these studies have been focused on venetian blinds (Kirimtat et al., 2016; E. Shen et al., 2014; Correia da Silva et al., 2013; Chan & Tzempelikos, 2013; Bueno et al., 2015; Yi et al., 2015) and combined systems like venetian blinds with roller shades or fabrics (Bueno et al., 2015; H. Shen & Tzempelikos, 2012; Tzempelikos & Shen, 2013; Chan & Tzempelikos, 2015). The aim of these devices is to reduce buildings energy consumption in terms of lighting, cooling and heating, and to improve the visual comfort of occupants related to glare control, daylighting and vision to outdoor. Bellia et al. (2014) shows an overview of building shading systems, and they pointed out the need of studying different CFS on different climatic conditions worldwide.

Dynamic CFS have the potential to improve building's energy performance as indicated by several studies (Tzempelikos & Athienitis, 2007; H. Shen & Tzempelikos, 2012; Tzempelikos & Shen, 2013; Konstantoglou & Tsangrassoulis, 2016). According to Correia da Silva et al. (2013), office buildings occupants will activate or deactivate the shadings based on three different types of criteria:

- Quantity of daylight (illuminance) that falls on the workplane.
- Visual discomfort related to glare, accounted indirectly by window luminances transmitted solar radiation or directly by daylight glare indexes.
- Direct solar radiation, which can create both thermal and visual discomfort.

Table 4.1 shows a review of the criteria for control of shading devices in office buildings.

Table 4.1. Review of the criteria for control of shading devices in office buildings.

Reference	Criteria for adjustment of shading position
(Chan & Tzempelikos, 2013)	They evaluated venetian blinds with slat's surface with two specularity values (0 and 0.8) and combination of these, in Philadelphia (USA) for south and west orientations. They used three strategies, cut off-angle, "blocking" control (set blinds perpendicular to profile angle when a second reflection is possible and redirect transmitted light when cut-off angle redirection is not effective) and glare control (rotate blinds when DGP index $> 35\%$). They conclude that a combination of glare strategies would yield the best results depending on climate, window properties and orientation.
(Tzempelikos & Shen, 2013)	They evaluated interior roller shades in Philadelphia (USA), for the four cardinal orientations. Four control strategies were evaluated, shades automatically close completely when incident beam radiation on the façade exceeds 20W/m^2, roller shades automatically close completely when transmitted illuminance exceeds 9000 lux, roller shades move automatically to a position that just prevents direct sunlight to observer workplane, and finally, the fourth control is same that third control with control in cooling mode.
(Bastien & Athienitis, 2012)	They evaluated an exterior roller shutter and an interior roller blind in a solarium of green house in Montreal (Canada), for four exterior glazed surfaces: east, west, vertical south and tilted south. Control strategies depends of solar radiation transmitted through the window (global, individual or combined solar control of exterior and interior devices).

Continued on next page

Reference	Criteria for adjustment of shading position
(E. Shen et al., 2014)	They evaluate interior and exterior venetian blinds in Baltimore (USA), London (UK) and Abu-Dhabi (United Emirates); building has four floors and windows in facing in each direction. Two integrated control strategies are evaluated based on cut-off angle and dimming luminaires.
(Yun et al., 2014)	They evaluated venetian blinds in Incheon (South Korea) for the south, west and east orientations. They used fixed blinds and one case with dynamic blinds controlled by glare. They found that dynamic shading control with the dimmed lights was the best case for the east and the west façade, while, the case of 0° slat angle represents the smallest energy consumption for the south façade.
(Konstantzos et al., 2015)	They evaluate controlled roller shades in office space in in West Lafayette (Indiana, USA) for south façade orientation. Three controls were evaluated, fully closed shades, work plane protection (prevents direct sunlight from falling on the work plane) and advanced control (prevent high workplane illuminances $>$ 2000 lux at all times and maximize daylight provision under cloudy sky conditions). The advanced shading control is able to protect from glare for most of the time.
(Chan & Tzempelikos, 2015)	They evaluated roller shades, venetian blinds and light-shelves in Miami and Chicago (USA), for south and west façade orientations. Two control strategies were evaluated, ”effective illuminance” control (workplane illuminance $<$ 2000 lux up to 1 m from the window for roller shades, and cut-off angle with light-redirect (Chan & Tzempelikos, 2013) for venetian blinds and light-shelves).
(Vera et al., 2016)	They evaluated exterior venetian blinds in San Francisco (USA) for south façade orientation. Control strategies are based on outdoor dry-bulb temperature and irradiance over the window.

Continued on next page

Reference	Criteria for adjustment of shading position
(Liu et al., 2015)	They evaluated intelligent glazed façade through glare and cut-off angle (during occupied hours blinds cut the direct solar radiation, and during unoccupied hours, the blind is controlled by temperature), in Buddinge (Denmark) for the four cardinal orientations.
(Bueno et al., 2015)	They evaluated two systems, Winglamella (highly reflective aluminum material) perforated and non-perforated, and Warema venetian blinds with double clear glazing in Villafranca di Verona (Italy), for the south, west and east orientations. They used two controls, cut-off angle and retro (60 °), similar to cut-off angle. Winglamella system is a device composed of two separately mechanically controlled partitions (perforated in upper part, and non-perforated in lower part). This system is particularly suitable for east and west façade orientations.
(De Michele et al., 2015)	They evaluated venetian blinds in a shopping mall located in Genoa (Italy) for west façade orientation. Use two controls, one depend of internal air temperature and incident solar radiation on façade, and the second depend of illuminance level on workplace.

Nevertheless, this review suggests the following:

- It is required the evaluation of different control strategies in real time to obtain the best option of movable CFS in terms of visual comfort and energy performance (Bastien & Athienitis, 2012).
- Development in the shading strategies, materials used and comfort parameters inside the buildings should profoundly be coped with (Kirimtat et al., 2016).

Given a certain condition of thermal comfort in an office space with a set of CFS system (exterior movable curved opaque and perforated slats or louvers that were spaced at

120 mm with 20% of perforation), a methodology that integrates their thermal and lighting performance has been applied. The methodology consists of, integrate Groundhog® (an extension for SketchUp that allows exporting the models to Radiance), *genBSDF* (that allows obtain bidirectional properties of CFS) and *mkSchedule* (a tool that integrates EnergyPlus and Radiance to facilitate the combined thermal and lighting analysis of building using control algorithms), for performing integrated thermal and lighting analysis of spaces with controlled artificial lighting and CFS. This paper aims to evaluate the effect of four CFS's control strategies based on incident irradiance level, vertical eye illuminance, cut-off angle and angle for blocking light, in order to evaluate the heating, cooling and electrical lighting energy consumption and ensuring thermal and visual comfort. An office space located in cities with very different climatic conditions such as Montreal (Canada), Boulder and Miami (USA) and Santiago (Chile) has been considered in the present study.

4.3. Methodology

The tool for integrating the thermal and lighting analysis that it has been used is *mkSchedule* (Vera et al., 2016; Molina, 2014). According to Vera et al. (2016) and Molina (2014), the methodology used by this tool improves the one presented by (Wienold et al., 2011). Wienold et al. methodology consisted of three steps: first, multiple lighting simulations are performed using DAYSIM (C. F. Reinhart, 2013); second, a control algorithm was applied to the results in order to choose artificial lighting power and shading position for each time step; and third, the chosen positions and luminaire power were transferred to ESP-r for carrying out energy performance simulations. The improved methodology used by *mkSchedule*, on the other hand, separates the control sensors (i.e. those whose measurements will be used control luminaires or CFS) from the workplane sensors (i.e. those that will be analyzed to quantify quality of the lighting in the space). Working with only the control sensors makes the process of creating schedules faster and more realistic (i.e. control is usually done by installing one or two photosensors on the ceiling, not many

of them in the workplane). Finally, the schedules can be used for carrying out both energy performance and lighting simulations, and their results can be analyzed holistically to quantify the thermal and visual comfort, and the whole building energy consumption.

The building was designed in SketchUp, and then exported (using Groundhog®) in an appropriated format for multiphase analysis. In this case the Three-phase method (McNeil, 2013; Sexena et al., 2010) is used through *mkSchedule*. This implies exporting the building itself separately from the shading devices, which will allow assessing the bidirectional properties of the latter and change the parameter of control strategy easily. Following, the methodology is presented in detail.

4.3.1. Office space building

The space to be studied correspond to a 4.0 m x 6.5 m 2.8 m space, with two sets of dimming luminaires, and one south oriented glazed façade north hemisphere (Montreal, Boulder and Miami), and north oriented glazed façade for Santiago of Chile. The building is shown in Figure 4.1, and Table 4.2 show the simulation layout.

Table 4.2. Simulation layout.

Parameter	Details	
Cities	Santiago (Chile)	S33.38 °,W70.78 °
	Miami (USA)	N25.82 °,W80.30 °
	Boulder (USA)	N40.02 °,W105.25 °
	Montreal (Canada)	N45.47 °,W73.75 °
Orientation	South/north[1] & west	
Office space	Size	4.0m(w) x 6.5m(l) x 2.8m(h)

Continued on next page

[1]South for north hemisphere (Montreal, Boulder and Miami), and, north for Santiago of Chile.

Parameter	Details	
	WWR[2]	0.88
Opaque surfaces	Adiabatic	
Window	Size	3.8m(w) x 2.6m(h)
(Double clear glass)	T_{vis}	0.83
	SHGC	0.83
	U-factor ($Wm^{-1}K^{-1}$)	2.70 $Wm^{-1}K^{-1}$
Surface reflectances	Floor	20%
	Ceiling	70%
	Wall	50%
HVAC system	Electric heat pump (EHP)	COP 3.0
	Heating thermostat setpoint	20 °C
	Cooling thermostat setpoint	24 °C
Ventilation + infiltration	0.7 ACH (Gowri et al., 2009)	
Internal gains	People	6.7 W/m^2
	People radiant fraction	0.3
	Lighting	13.85 W/m^2
	Light radiant fraction	0.3
	Electric equipment	15 W/m^2
Lighting level setting	Workplane at 0.8 m	500 lux
Schedules	Occupancy, lights, equipment & HVAC	08:00 - 18:00 hrs. (weekdays)

This study includes four cities with different climates: Santiago (Chile), Miami (USA), Boulder (USA) and Montreal (Canada). Montreal has a semi-continental climate, with a warm, humid summer and a very cold winter. Climate of Boulder is semi-arid with

[2]Window-to-wall Ratio (WWR) is the measure of the percentage area determined by dividing the building's total glazed area by its exterior envelope wall area.

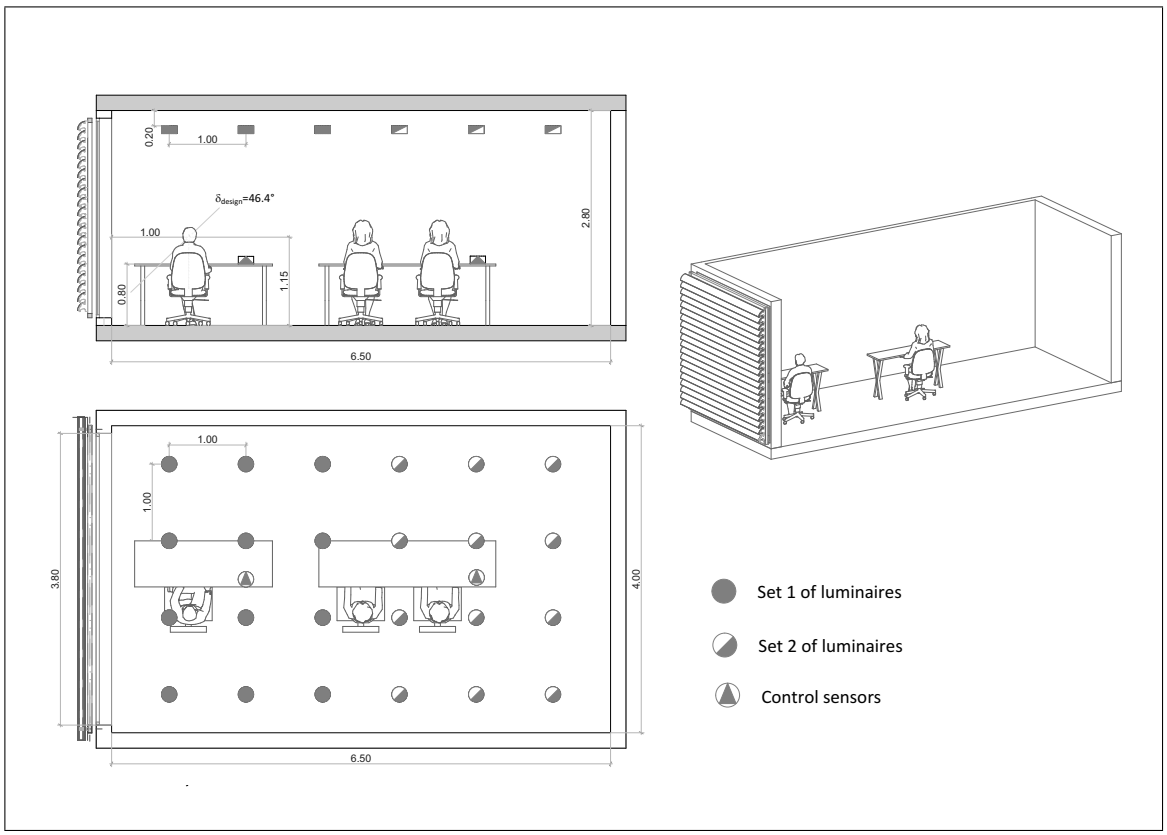

Figure 4.1. Model of the office space with louvers and interior dimensions (m), plain view and side view.

several sunny days each year. Miami has a tropical climate with hot and humid summers and short warm winters. Santiago of Chile has a semi-arid climate characterized by high temperatures and solar irradiance for around 8 months of the year.

4.3.2. Complex fenestration systems

CFS were used corresponds to a set of horizontal curved and perforated louvers (commercial product named Celoscreen of HunterDouglas Company Chile) designed in SketchUp, and exported to into Radiance with Groundhog®. The movable CFS can be fixed between -75 ° to 75 ° with step of 5 °. The material of CFS corresponds to a reflective metal (95% solar and visible reflectance) with 0% of specularity.

Figure 4.2 and 4.3 shows dimensions and views of the curved louvers.

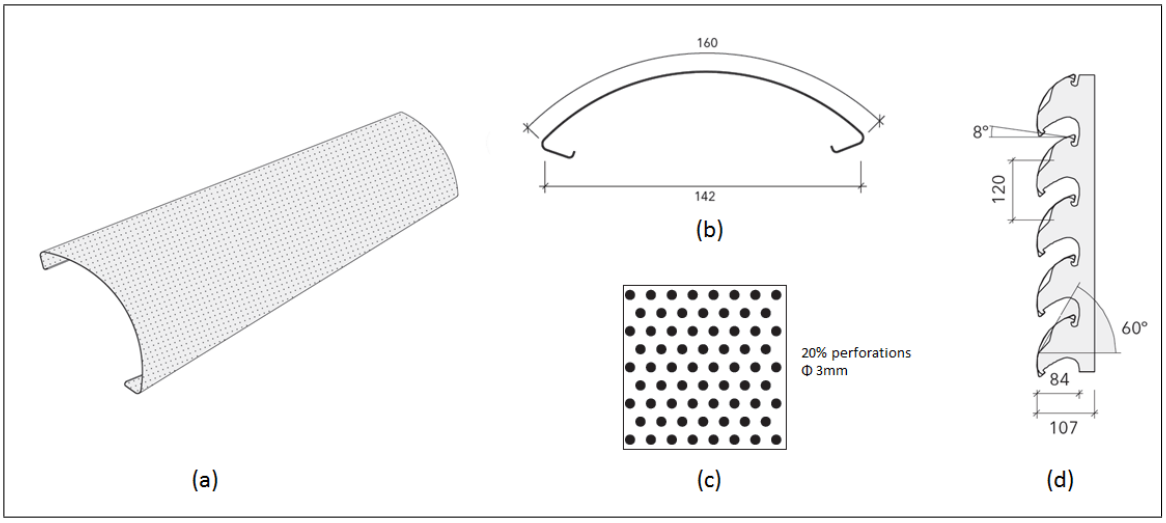

Figure 4.2. Perforated undulated louvers. (a) 3D view of louver. (b) Louver dimensions (mm). (c) Perforation dimensions (mm). (d) Installed louver dimensions (mm). Adapted from (HunterDouglas, 2013).

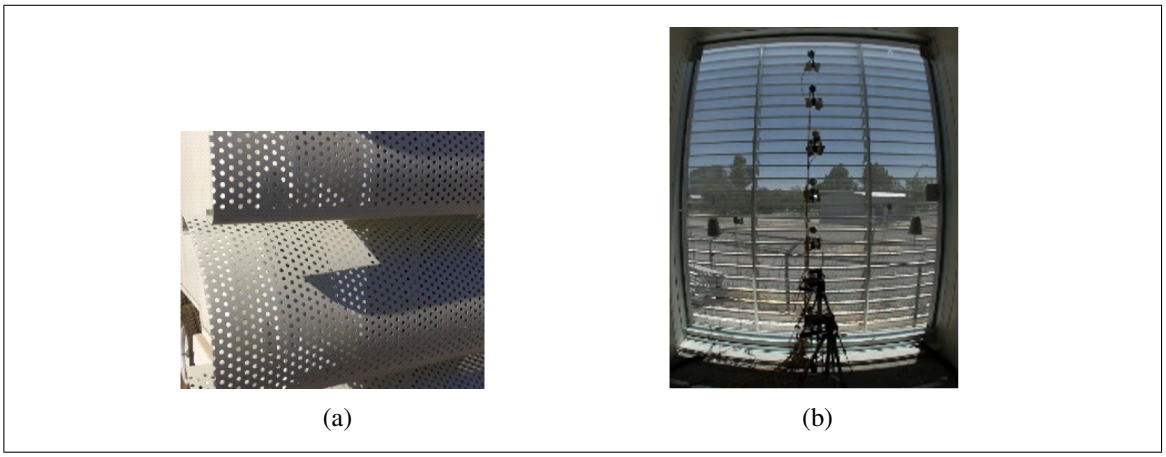

Figure 4.3. Perforated undulated louvers. (a) Perforation pattern. (b) Outdoor visibility of CFS.

There are three main options for assessing the BSDFs of complex fenestration systems, such as 1.- Laboratory measurements, 2.- Development of analytical models usually based on Radiosity, and 3.- Emulation of laboratory measurements in a virtual environment using ray-tracing techniques (Andersen & de Boer, 2006). However, since the materials of the shading devices used are specular and the shading systems to be evaluated have not been built yet, ray-tracing techniques are the only option available for this case (as often

happens at design stage). Ray-tracing techniques have been used for the assessment of bidirectional properties in various studies, (Konstantoglou et al., 2009; McNeil & Lee, 2013; Rubin et al., 2007). In this study, Radiance's program *genBSDF* has been used for assessing both the visible and the solar bidirectional properties for lighting (Radiance) simulations and energy performance (EnergyPlus) simulations respectively. Although Radiance is usually used within the visible ranges, Molina et al. (2015) verified that *genBSDF* is a very accurate tool for assessing solar BSDFs of CFS when materials are not spectrally selective.

On the other hand, McNeil et al. (2013) also validated *genBSDF* for the visible range. McNeil et al. explained the basis and use of the *genBSDF* tool and validated the tool by comparing results for four cases with BSDFs produced via different methods. This validation demonstrates that BSDFs created with *genBSDF* are comparable to BSDFs generated analytically using TracePro and by measurement with a scanning goniophotometer.

The BSDFs were obtained in Klems full form, which corresponds to a matrix form for performing the annual simulations. The Radiance models of the shading devices that were inputted into *genBSDF* were in standard Radiance geometry and materials format. After generating the BSDF for each shading position, they were imported to WINDOW 7.3 (LBNL, 2014) to be lately exported into an EnergyPlus readable format. Table 4.3 shows solar heat gain coefficient (SHGC), visible transmission coefficient (T_{vis}) and U-value obtained with WINDOW 7.3, which are the glazing units' main characteristics.

Table 4.3. Solar heat gain coefficient (SHGC), visible transmission coefficient (T_{vis}) and U-value ($Wm^{-1}K^{-1}$) for louvers.

Slat angle	SHGC	T_{vis}	U-value ($Wm^{-1}K^{-1}$)	Slat angle	SHGC	T_{vis}	U-value ($Wm^{-1}K^{-1}$)
-75 °	0.13	0.09	2.70	0 °	0.43	0.31	2.70
-70 °	0.15	0.10	2.70	5 °	0.43	0.33	2.70
-65 °	0.16	0.11	2.70	10 °	0.40	0.32	2.70
-60 °	0.17	0.11	2.70	15 °	0.39	0.30	2.70
-55 °	0.19	0.13	2.70	20 °	0.37	0.29	2.70
-50 °	0.22	0.15	2.70	25 °	0.35	0.27	2.70
-45 °	0.26	0.18	2.70	30 °	0.33	0.26	2.70
-40 °	0.29	0.20	2.70	35 °	0.30	0.22	2.70
-35 °	0.32	0.22	2.70	40 °	0.27	0.20	2.70
-30 °	0.34	0.24	2.70	45 °	0.25	0.18	2.70
-25 °	0.36	0.26	2.70	50 °	0.22	0.16	2.70
-20 °	0.38	0.28	2.70	55 °	0.20	0.14	2.70
-15 °	0.40	0.29	2.70	60 °	0.18	0.13	2.70
-10 °	0.42	0.31	2.70	65 °	0.17	0.12	2.70
-5 °	0.43	0.32	2.70	70 °	0.15	0.11	2.70
				75 °	0.14	0.10	2.70

4.3.3. Simulation tool

Since CFS are often installed to provide enhanced visual and thermal comfort as well as an excellent energy performance, an holistic lighting/thermal analysis of spaces with complex fenestration systems is highly relevant. Since this step is probably the most important part of the workflow, this section will be deeply explained. There are different options for carrying out holistic lighting/thermal analysis (Guglielmetti et al., 2011; Janak,

2007; Petersen & Svendsen, 2010; Tzempelikos & Athienitis, 2007). As mentioned, in our case, *mkSchedule* is being used. This tool was developed in (Vera et al., 2016; Molina, 2014) and allows easy application and modification of different control algorithms, and implements control in only one simulation via the Three-phase method very efficiently (*mkSchedule's* methodology shown in Appendix A).

mkSchedule is a program based on Radiance's *dctimestep* and *gendaymtx* programs to implement the Three-phase method and create the Perez et al. sky (Perez et al., 1990, 1993) required for the simulations, respectively. Also, *mkSchedule* use EnergyPlus weather files, that may be extracted from DAYSIM's *epw2wea* program, which reads and selects information from the weather files. This program was developed with the intention of simplifying the integration of lighting and thermal simulations using Radiance and EnergyPlus or ESP-r. *mkSchedule* receives as input all the matrices required for the Three-phase method calculations (i.e. View, Daylight and all the BSDF in matrix form in Klems basis, computed as explained in (McNeil, 2013), the contributions of the luminaires over the sensors in matrix form (i.e. standard *rcontrib* or *rtrace* Radiance's program output) and a control algorithm written in Lua scripting language. The output is a schedule file with sensor illuminance values, luminaire fraction of power (i.e. 0 is off, and 1 is on), and the shading position represented as an integer. One of the key features of *mkSchedule* is its flexibility to modify and try different control algorithms easily by performing fast calculations. This is achieved by defining the control algorithm as an argument to the main program, and by allowing the user to program it in Lua, a scripting language much simpler than the main program's C. From the control scripts, the user can use predefined functions to retrieve relevant information for making decisions and use it as triggers. For example, luminaire power and shading position can be controlled according to sun position (i.e. azimuth, zenith and altitude), exterior dry-bulb temperature, irradiance over a surface calculated according to Perez et al. (Perez et al., 1990, 1993), and as shown in (Duffie & Beckman, 1996), illuminance over a sensor, previous luminaire power and shading position, or any information that can be derived from the lighting simulation and/or the EnergyPlus weather file.

4.3.4. Control strategies

The CFS control strategy consists of three main steps: first, to position the blinds according to a given parameter (e.g. solar position or irradiance over a surface); second, recalculate the illuminance values on the interior (the daylighting levels of the space have been modified due to the new position of the CFS); and third, dim the luminaire power to achieve the desired illuminance on the sensors (i.e. increase more and more the luminaire power until the setpoint is achieved).

Table 4.4 shows control algorithms used in this study. Lua scripts with the control algorithms used in the simulations are presented in Appendix C.

Table 4.4. Control strategies. Definition and steps.

Case	Algorithm control method	Details
S1	Incident irradiance. max=300 W/m^2	According to Figure 4.4. Step: 15 °.
S2	Vertical eye illuminance (E_v)	E_v <2760 lux (Chan & Tzempelikos, 2015). Step: 5 °.
S3	Cut off angle	Step: 5 °.
S4	Blocking control	According to (Chan & Tzempelikos, 2013). Step: 5 °.

4.3.4.1. Luminaires control

For this case study, two sets of dimming luminaires were installed, and two control sensors were located in the space to control each of them: one in the first half of the space and the other one is centered in the second half of it (see Figure 4.1). It should be noticed that a more realistic approach could be made by placing the sensors in the ceiling, and correlating their measurements with the workplane illuminance, as is explained in

(Tzempelikos, 2012). However, in this case, the sensors were located just under the central luminaire of each set pointing to the ceiling in order to simplify the process.

4.3.4.2. Incident irradiance control

This control strategy was proposed in Chapter 3.3.4, where was obtained the optimum maximum irradiance level for each city of this study. In this case, the maximum irradiance level is 300 W/m^2. In Figure 4.4 can be seen how the position of the CFS varies according to irradiance over the facing window.

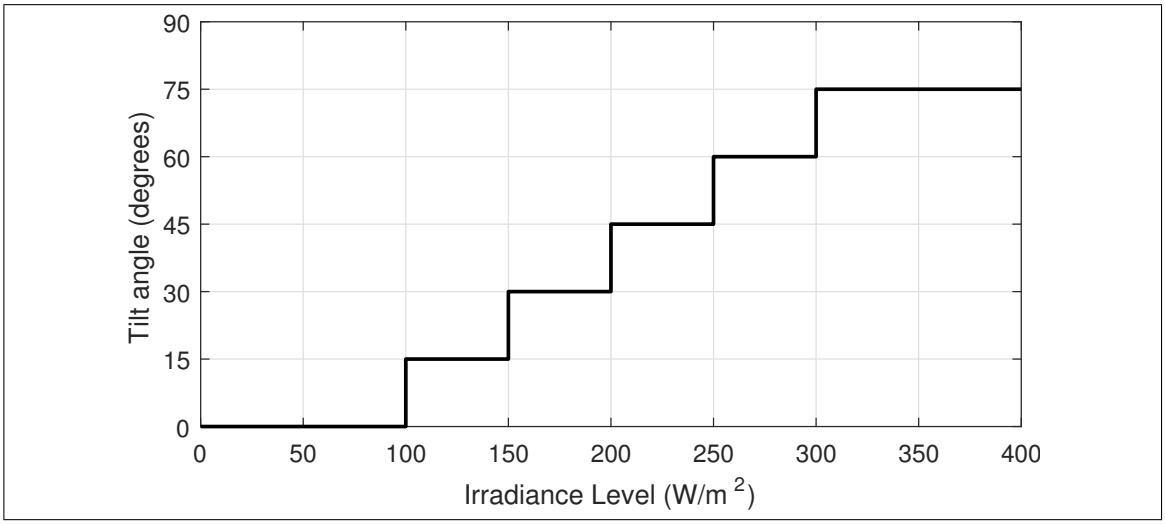

Figure 4.4. Incident irradiance control.

4.3.4.3. Vertical eye illuminance control

The CFS control strategies consists of three major steps: first, position the louvers are horizontal (opened) initially; Second, the control receives as input the illuminance level at eye of observer; third, if the illuminance measured by the sensor is below 2760 lux, shading is kept, but if the measured illuminance is still above 2760 lux (Chan & Tzempelikos, 2015), the slat angle is gradually changed from 0 ° to 75 ° in steps of 5 ° until the illuminance is below 2760 lux.

4.3.4.4. Cut-off angle control

Cut-off angle corresponds to the angle of inclination of the blinds such that no direct radiation is transmitted to the observer. Chan and Tzempelikos (2013) calculate cut-off angle as Equation (4.1).

$$\beta_1 = 90 - 2\Omega \tag{4.1}$$

where β is the slat angle and Ω is the profile angle, defined following in Equation (4.2).

$$\Omega = \arctan\left(\frac{\tan\alpha}{\cos\left(\theta_{sun} - \theta_{surf}\right)}\right) \tag{4.2}$$

where, α correspond to solar altitude and θ_{sun} y θ_{surf} correspond to azimuth of sun and surface respectively.

Liu et al. (2015) use to cut the direct solar radiation and improve the visual comfort and maximize the daylight transmittance into the room the Equation 4.3.

$$\beta_2 = \arccos\left[\frac{\frac{d}{w}\tan\alpha + \sqrt{\tan^2\alpha - \left(\frac{d}{w}\right)^2 + 1}}{\tan^2\alpha + 1}\right] \tag{4.3}$$

where β is the angle between the slat and horizontal plane, α is the solar altitude angle, d is the distance between slats, and w is the width of the slats.

Bueno et al. (2015) use cut-off angle defined by the same equation of Liu et al. (2015), but in terms of profile angle. It shows in Equation 4.4.

$$\beta_2 = \arcsin\left(\frac{d}{w}\cos\Omega\right) - \Omega \tag{4.4}$$

In Figure 4.5 can see comparison of cut-off angle defined in Equations (4.1) and (4.4) in respect of the profile angle Ω.

In this study use cut-off angle β_2 defined in Equation (4.4) because considering the dimensions of louvers and is less restrictive than Equation (4.1).

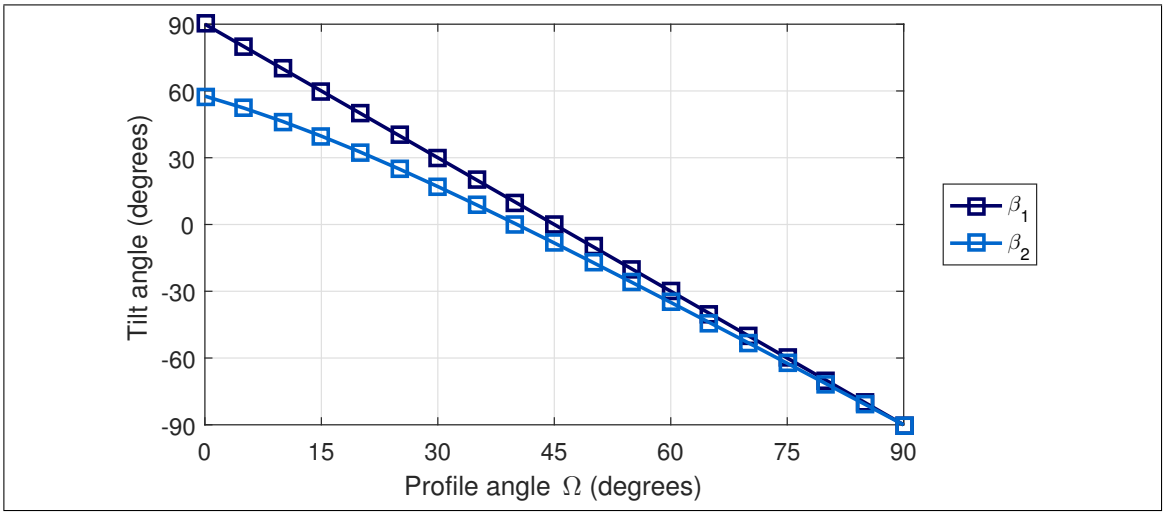

Figure 4.5. Cut-off angle β_1 defined by Chan and Tzempelikos (2013) and β_2 defined by Bueno et al. (2015) in respect of the profile angle Ω.

4.3.4.5. Blocking control

There are two problems in cut-off angle control according to Chan and Tzempelikos (2013). First is the second reflection originating from the bottom of slats, and second problem has to do the general direction of reflected rays, as this is also related to glare. These problems can see in Figure 4.6a

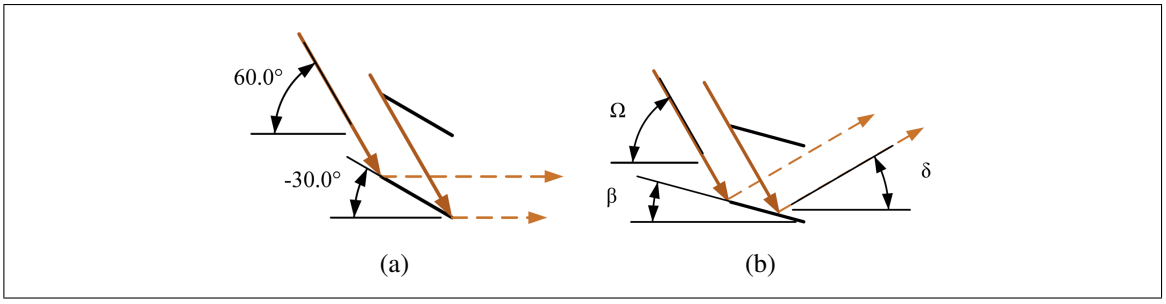

Figure 4.6. (a) Avoiding a second reflection but transmitted light direction will cause glare high profile angel/cut-off slat angle (Chan & Tzempelikos, 2013). (b) Angle definition use in equations (Chan & Tzempelikos, 2013).

Second reflection occurs when

$$[\delta < 90 | \cos\beta \tan\delta > 1 + \sin\beta]$$

where angles are defined in Figure 4.6b.

According to Chan and Tzempelikos (2013), cut-off angle dos not represent an efficient redirection ever, so that, define the tilt angle that redirects light to desired angle can be obtained by Equation (4.5),

$$\beta_{design} = \frac{(\delta_{design} - \Omega)}{2} \tag{4.5}$$

where δ_{design} is defined in Figure 4.1.

In Figure 4.7 can see how β_1, β_2 and β_{design} varies in respect of the profile angle Ω.

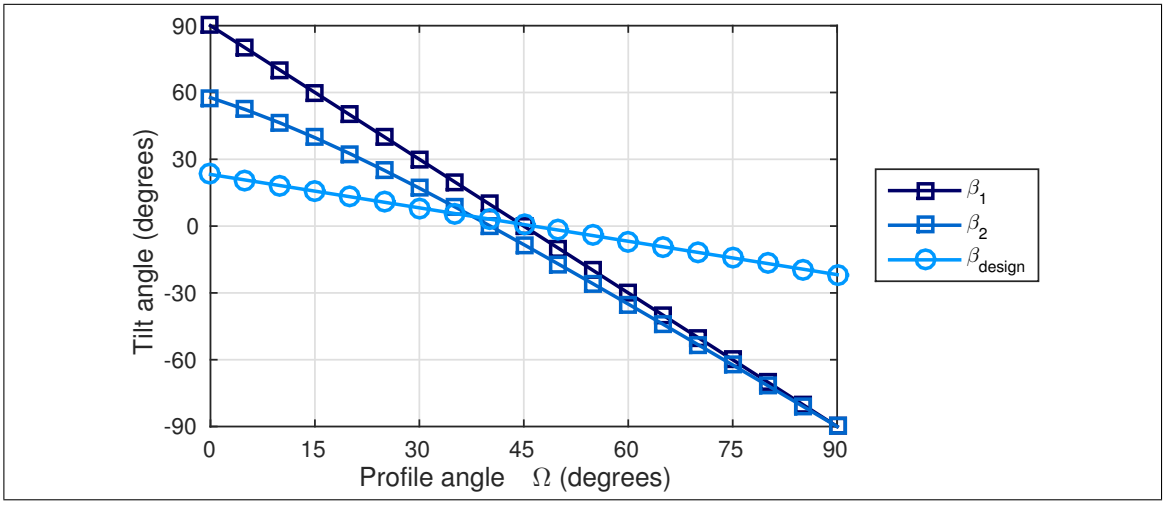

Figure 4.7. Cut-off angle (β_1 and β_2) and β_{design} in function of profile angle (Ω).

For this control strategy, used cut-off angle β_2 defined in Equation (4.4) because considering the dimensions of louvers and is less restrictive than Equation (4.1).

In Figure 4.8 presents the flowchart of blocking control for light redirection.

Cut-off control do not consider sky conditions, only works well in clear skies; and when window-to-wall ratio or the glass transmittance is high, there is a risk of glare even if direct sunlight is blocked (Chan & Tzempelikos, 2013).

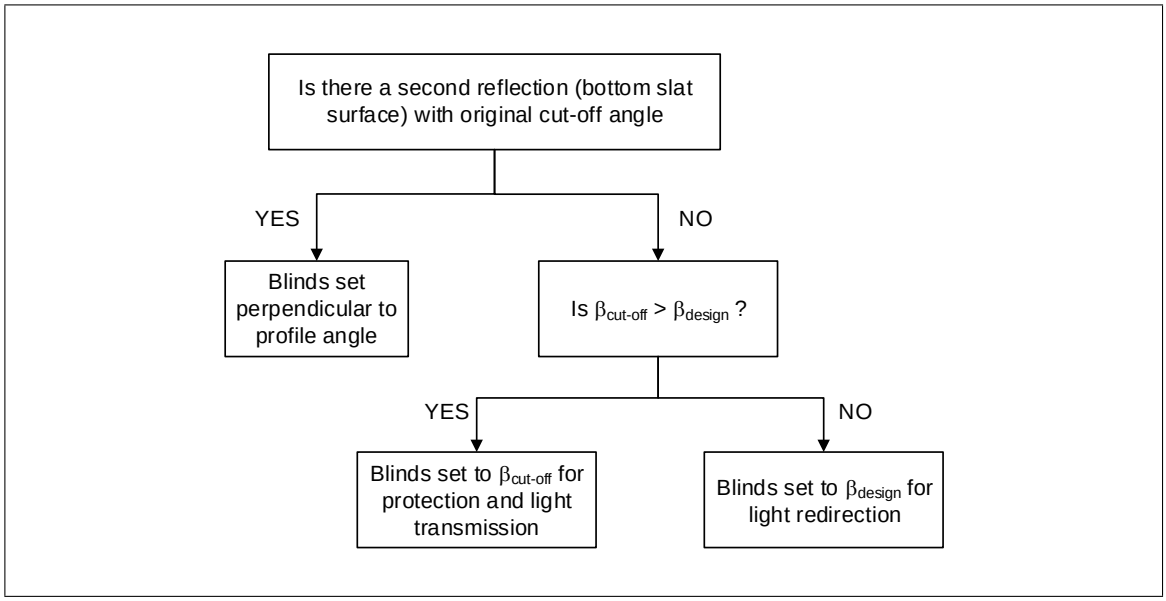

Figure 4.8. Flow chart of blocking control for light redirection. Adapted from (Chan & Tzempelikos, 2013).

4.3.5. Visual comfort evaluation

In the literature have two methods to evaluate the visual comfort of occupants: one according to workplane illuminance level and other related with the glare risk. According to Konstantzos et al. (2015) for cases without the sun in the field of view, DGP and workplane illuminance are not well correlated, except for very low openness factors or perfectly diffuse materials. For cases without the sun in the field of view, DGP and vertical illuminance are well correlated, even when sunlight falls on interior surfaces (when shades are partially open or controlled). This allows DGPs to be used for all instances except when sunlight directly hits the occupant. Furthermore, in this study it evaluates two metrics: spatial daylight autonomy (sDA) and annual sunlight exposure (ASE) for workplane illuminance and simplified daylight glare probability (DGPs) for glare risk.

4.3.5.1. Spatial daylight autonomy (sDA) and annual sunlight exposure (ASE)

Visual comfort trough workplane illuminance level is evaluated by the spatial daylight autonomy (sDA) and annual sunlight exposure (ASE). These metrics were developed by

Illuminating Engineering Society (IES) (IES, 2013). sDA describes the annual sufficiency of ambient daylight levels in interior environments. It is defined as the percentage of an analysis area that meets a minimum daylight illuminance level for a specified fraction of the operating hours per year. ASE is a metric that describes the potential for visual discomfort in interior work environment. It is defined as the percentage of an analysis area that exceeds a specified direct sunlight illuminance level for more than a specified number of hours per year (e.g. working hours in weekdays).

$sDA_{300/50\%}$ and $ASE_{1000/250h}$ is recommended for the analysis of daylight sufficiency and potential visual discomfort. $sDA_{300/50\%}$ is reported as the percentage of analysis points across the analysis area that meets or exceeds this 300 lux value for at least 50% of the analysis period (from 8AM to 6PM, 10 hours per day, weekdays). $ASE_{1000/250h}$ is reported as the percentage of analysis points across the analysis area that meet or exceed this 1000 lux value for 250 hours per year of the analysis period. sDA must meet or exceed 55% of the analysis area and ASE is acceptable when is less than 7%.

Since IES standard based on studies in 100 m^2 rooms, with the longest distant to the window of 12 m, ASE values may easily exceed 7%. In our case, due to smaller dimensions of the space, it has been considered an acceptable ASE value less than 20%. On the other side, 1000 lux illuminance level is too low in some cases; according to (Mardaljevic et al., 2012) 3000 lux is a recommended value for offices. IES standard say until 4000 lux can be an acceptable level and is possible exceed this value for 400 hours per year even. In this case is evaluated $ASE_{2000/400h}$ like a visual discomfort parameter. For daylight autonomy, $sDA_{300/50\%}$ >50% it has been acceptable.

4.3.5.2. Daylight glare probability

Glare indices have been used to evaluate visual comfort in the luminous environment. Have a multitude of glare indices, but there only two glare indices intended for use in daylit environments. The first, the daylight glare index (DGI) was developed by Hopkinson (1972) and Hopkinson and Collins (1963) using large-area electric light glare sources and

updated by Chauvel et al. (1982) in a setting with daylight but without sunlight or reflected sunlight. The second, daylight glare probability (DGP), was developed by Wienold and Christoffersen (2006) as an attempt to improve upon the DGI. The DGP tries to define "the probability that a person is disturbed instead of the glare magnitude". They found that the DGP outperformed the DGI, but this must be qualified in several ways. Following, DGP is defined in Equation (4.6):

$$DGP = 5.87 \cdot 10^{-5} E_v + 9.18 \cdot 10^{-2} \log\left(1 + \sum_i \frac{L_{s,i}^2 \omega_{s,i}}{E_v^{1.87} P_i^2}\right) + 0.16 \tag{4.6}$$

where E_v is the vertical eye illuminance (lux); L_s the luminance of source (cd/m^2); ω_s the solid angle of source; P is the position index. In (Wienold & Christoffersen, 2006), it was shown that the vertical illuminance at eye level shows a reasonable correlation to the glare perception. From this publication, a simplified DPG (called DGPs) could be derived as:

$$DGPs = 6.22 \cdot 10^{-5} \cdot E_v + 0.184 \tag{4.7}$$

This equation neglects the influence of individual glare sources. Therefore, it must be clear that the DGPs can be applied only if no direct sun or specular reflection of it hits the eye of the observer (Wienold, 2007).

According to Wienold (2009), to evaluate visual discomfort with the DGPs, the recommendation given is that the 95% of the occurrences of DGPs should be below a certain value to qualify for the comfort class. The limits of the DGPs for the 95th percentile $\left(L_{DGPs}^{95\%}\right)$ and the mean for the remaining 5 percent of the time $\left(M_{DGPs}^{5\%}\right)$ are given below in Table 4.5.

Table 4.5. Glare rating of Daylight Glare Probability (DGP) (Wienold, 2009).

Glare rating	95% DGPs limit	Mean DGPs (5%)	Class
Imperceptible	<0.35	<0.38	A
Perceptible	0.35-0.40	0.38-0.42	B
Disturbing	0.40-0.45	0.42-0.53	C
Intolerable	>0.45	>0.53	-

4.4. Results and analysis

Since this paper focuses on evaluating the behaviour of a CFS in terms of their capability to control daylighting and minimizing energy consumption under four control strategies, graphics of energy consumption and evaluation of visual comfort in respect of workplane illuminance level and glare indices are presented below for each CFS. Additionally, to test the proper operation of the CFS under each control strategy, graphics with position of the CFS are presented for characteristics days.

Figures 4.9 and 4.10 show the position of the CFS for each control strategy. Characteristic summer and winter days in Montreal (July, 20th and 21th, and January, 1st and 2nd) and south façade orientation were chosen to present this graphic. It should be noted that outside the work hours, louvers are closed (75 °) for all control strategies. For the incident irradiance control, louvers are closed when irradiance are higher than 300 W/m^2 and has intermediate positions when irradiance y lower than 300 W/m^2; the vertical eye illuminance control allows open louvers (0 °) in summer generally, but do not have the same behaviour in winter when the impact of sunlight occurs directly in the façade and increases the illuminance values at eye observer; the cut-off control in summer have higher profile angles generally (over 45 °), resulting in negative inclination angles of louvers, while in winter have lower profile angle, resulting in positive inclination angles for louvers; and, for blocking control, in respect of cut-off angle as exist higher profile angles in summer,

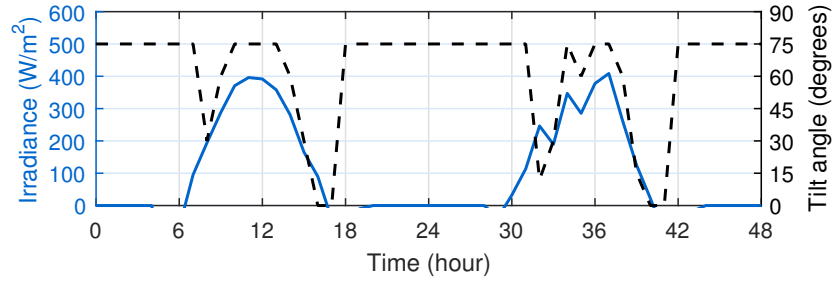

(a) Incident irradiance control

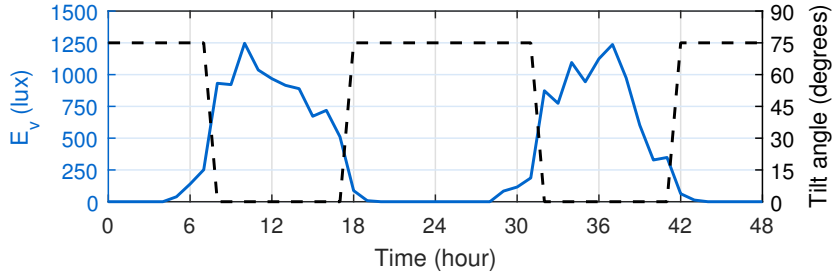

(b) Vertical eye illuminance control

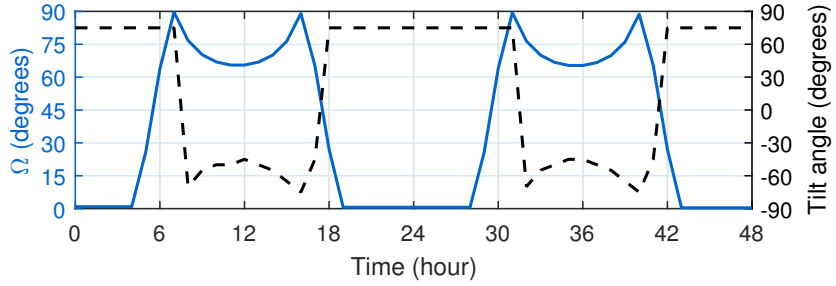

(c) Cut-off angle control

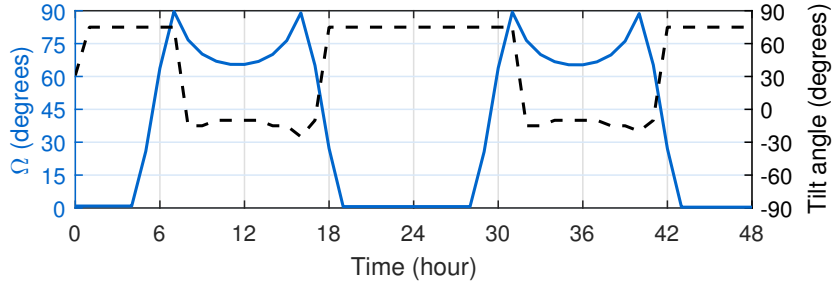

(d) Blocking control

Figure 4.9. Position of the CFS during July, 20th and 21th at Montreal and south façade orientation for each scenario.

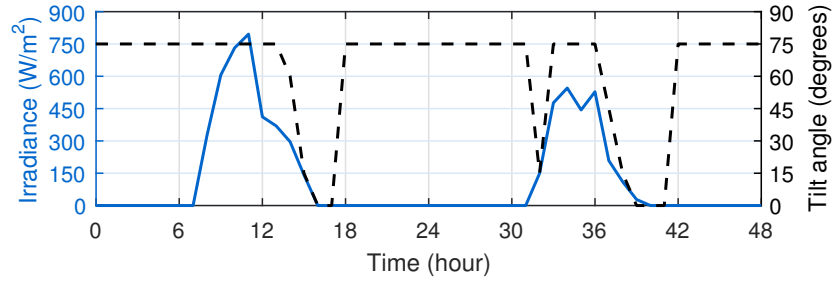

(a) Incident irradiance control

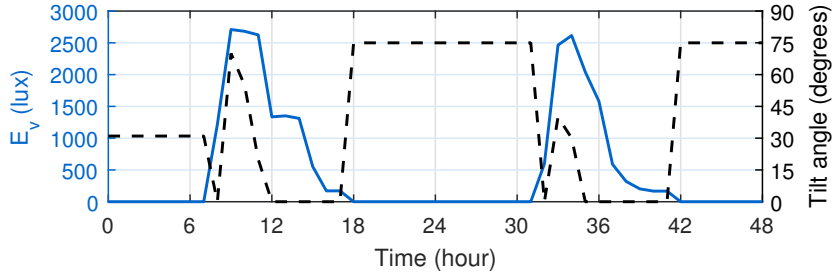

(b) Vertical eye illuminance control

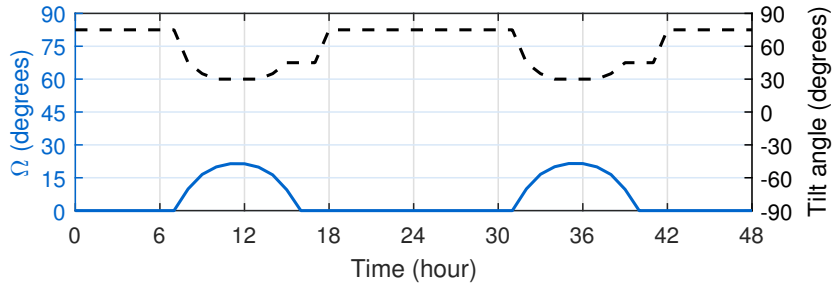

(c) Cut-off angle control

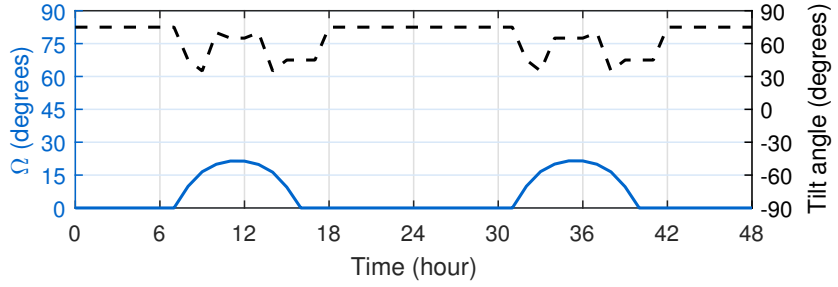

(d) Blocking control

Figure 4.10. Position of the CFS during January, 1st and 2nd at Montreal and south façade orientation for each scenario.

allows have lower absolute angle of louvers than in the first case, while at the middle of day second reflection is possible, furthermore, louvers are perpendicular of profile angle.

Figures 4.11 and 4.12 show the box plot with the position of louvers for each scenario. On each box, the central mark indicates the median, and the bottom and top edges of the box indicate the 25th and 75th percentiles, respectively. The whiskers extend to the most extreme data points not considered outliers, and the outliers are plotted individually using the "+" symbol. It should be noted that strategy S1 have louvers over 45 $^\circ$ generally, strategy S2 have louvers opened 95% of the time approximately and rarely change the position, strategy S3 tends to have the louvers with negative inclination, but with positions more distributed in respect of other strategies, and, strategy S4 on average, have the blinds open, but the distribution tends to positive inclinations. These results are directly related to lighting consumption, as seen in Figures 4.13a and 4.13b below.

Figures 4.13a and 4.13b show measured energy consumption for lighting, heating and cooling in kWh/year for each city and south/north and west façade orientations respectively. In respect of energy consumption, the results are expected, with high cooling consumption because it is a curtain wall (U-value of 2.70 $Wm^{-1}K^{-1}$), and cooling is much higher in Miami (tropical climate), even the double than the other cities, between 915 kWh/year and 1040 kWh/year compared with around of 400 kWh/year for Montreal, Santiago and Boulder. Boulder and Santiago have a similar behaviour with lower heating consumption (between 0 kWh/year and 158 kWh/year) because have a semi-arid climate in both cases with high solar irradiance in the most of the year. Montreal have the most higher heating consumption (between 304 kWh/year and 627 kWh/year) because have a strong winter, nevertheless, correspond to 30% of total energy consumption approximately because the office has high internal gains.

In the case of south/north façade orientation, the four cities have different behaviour in total energy consumption, where the best strategy is strategy S2 for Montreal and Boulder, and S1 and S2 for Santiago of Chile, with total energy consumption between 668

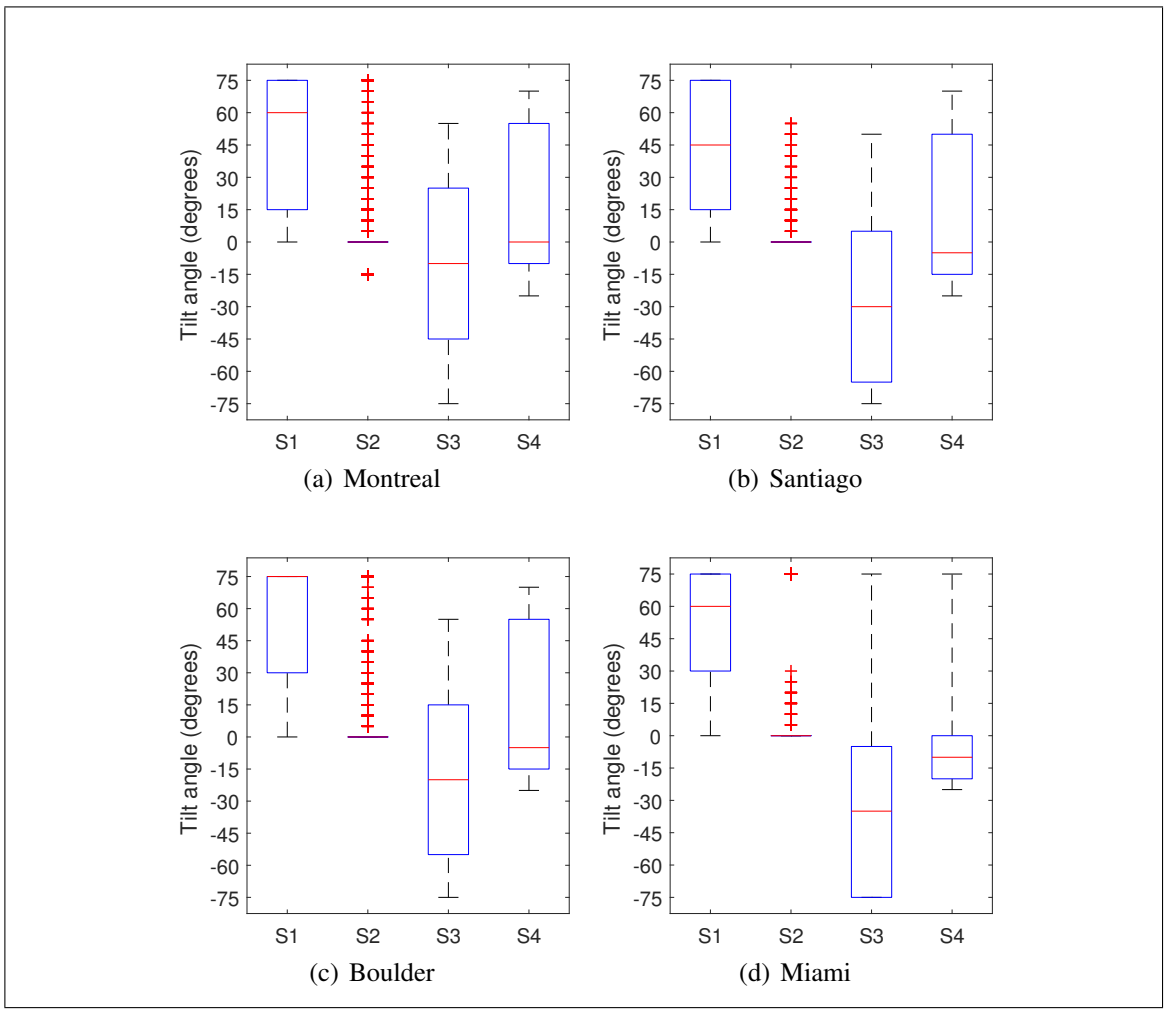

Figure 4.11. Boxplot with position of the CFS for each scenario, south/north façade orientation.

kWh/year and 951 kWh/year and 10% to 23% of energy savings in respect of worst strategy in each case. In the case of S2, the louvers are open 95% of time, furthermore, daylighting is maximized and cooling is minimized in respect of the other strategies, resulting in a lower lighting consumption. Finally, in Miami the best strategy corresponds to S4 blocking control where daylighting is maximized.

In the case of west façade orientation, the behaviour of total energy consumption in Montreal, Santiago and Boulder is the same in respect of total energy consumption, where the best strategy is S2, with total energy consumption between 695 kWh/year and 1152

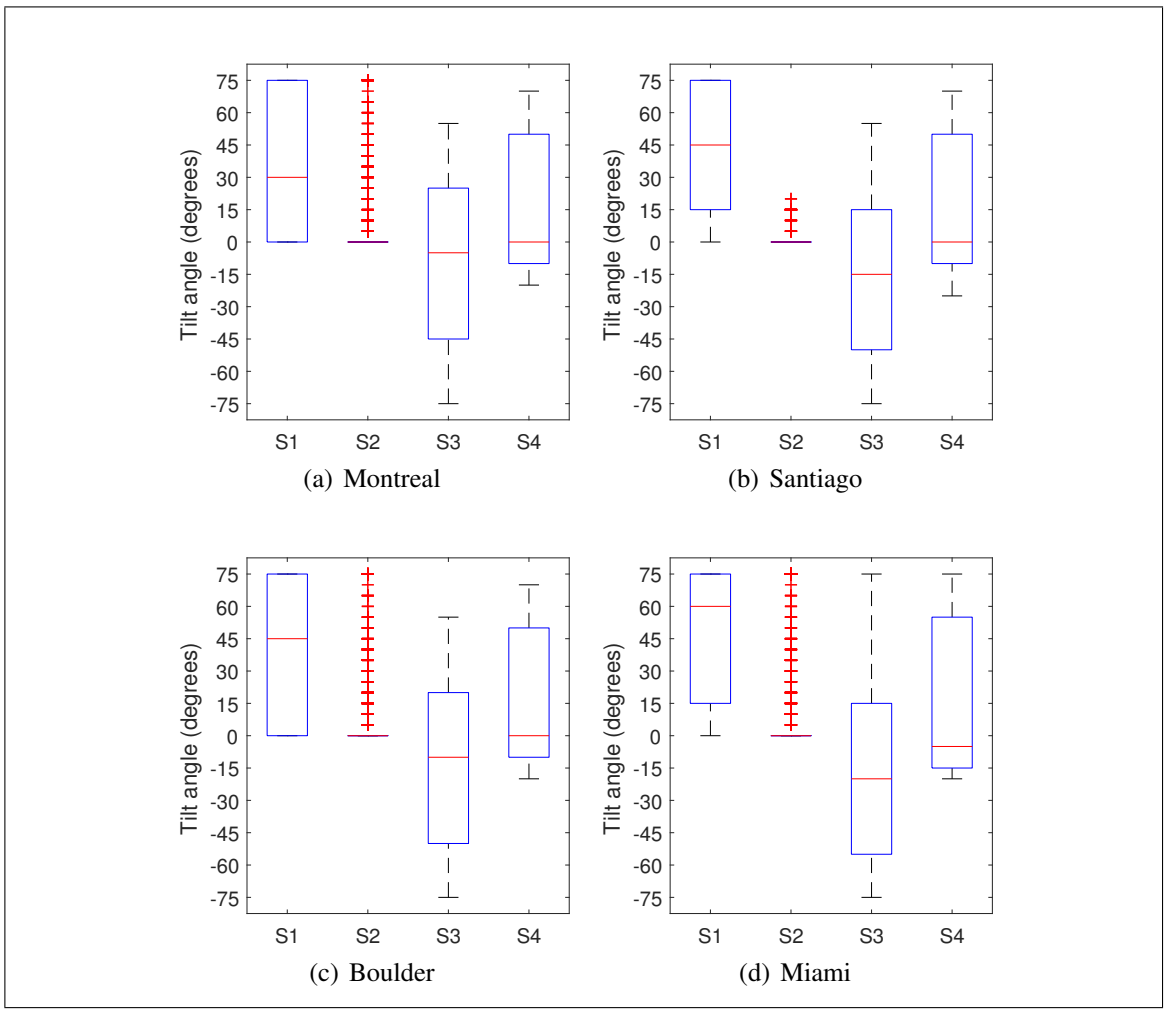

Figure 4.12. Boxplot with position of the CFS for each scenario, west façade orientation.

kWh/year. In case of Miami, the better strategy is S1, contrary to the south façade orientation, with 1326 kWh/year and the higher lighting consumption 222 kWh/year.

In summary, the best strategy for Montreal, Santiago of Chile and Boulder in terms of energy consumption is S2, and for Miami is S4 for south façade orientation and S1 for west façade orientation.

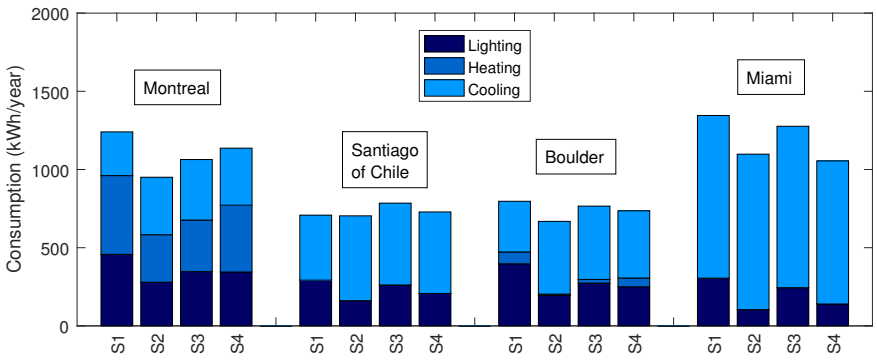

(a) South/north façade orientation.

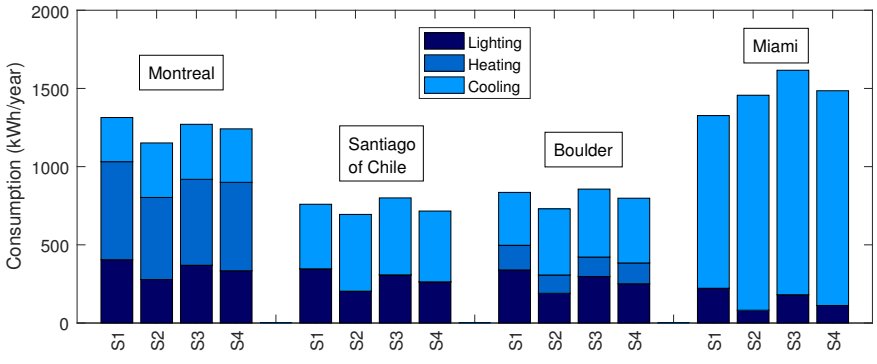

(b) West façade orientation.

Figure 4.13. Measured energy consumption for lighting, heating and cooling (kWh/year) for each scenario.

In Tables 4.6 and 4.7 show the daylight performance indicators for each city and south/north and west façade orientations respectively. Are two daylight performance indicators, for workplane illuminance level are $\text{sDA}_{300/50\%} > 75\%$ and $\text{ASE}_{2000/400h} < 20\%$, and for visual discomfort of the observer use the DGPs.

Table 4.6. Daylight performance indicators for each scenario, south/north orientation.

City	Cases	Workplane illumance		Glare indices		
		$\text{sDA}_{300/50\%}$ (%)	$\text{ASE}_{2000/400h}$ (%)	$L_{DGPs}^{95\%}$	$M_{DGPs}^{5\%}$	Class
Montreal	S1	53.8	16.2	0.26	0.32	A
	S2	85.2	33.0	0.35	0.36	A
	S3	57.0	31.3	0.35	0.43	C
	S4	58.0	27.3	0.31	0.36	A
Santiago	S1	55.3	13.4	0.24	0.27	A
	S2	88.4	28.8	0.32	0.34	A
	S3	54.0	29.1	0.32	0.37	A
	S4	53.2	21.0	0.30	0.32	A
Boulder	S1	52.1	22.0	0.28	0.34	A
	S2	100.0	38.6	0.35	0.36	A
	S3	59.0	37.4	0.37	0.45	C
	S4	53.2	29.8	0.32	0.36	A
Miami	S1	60.4	13.3	0.23	0.25	A
	S2	100.0	28.6	0.30	0.33	A
	S3	62.8	30.7	0.31	0.34	A
	S4	59.0	27.7	0.30	0.32	A

Table 4.7. Daylight performance indicators for each scenario, west orientation.

City	Cases	Workplane illumance		Glare indices		
		$sDA_{300/50\%}$ (%)	$ASE_{2000/400h}$ (%)	$L_{DGPs}^{95\%}$	$M_{DGPs}^{5\%}$	Class
Montreal	S1	58.7	13.0	0.29	0.33	A
	S2	86.8	26.0	0.35	0.36	A
	S3	50.1	27.4	0.34	0.40	B
	S4	53.0	18.6	0.32	0.36	A
Santiago	S1	51.3	13.3	0.26	0.27	A
	S2	93.3	30.1	0.31	0.33	A
	S3	51.0	28.3	0.31	0.32	A
	S4	58.2	19.8	0.30	0.31	A
Boulder	S1	51.4	13.8	0.30	0.34	A
	S2	89.6	26.3	0.35	0.36	A
	S3	51.1	25.8	0.34	0.41	B
	S4	57.0	18.1	0.31	0.36	A
Miami	S1	50.4	19.7	0.28	0.32	A
	S2	89.1	26.2	0.30	0.34	A
	S3	51.2	28.0	0.25	0.33	A
	S4	53.0	20.0	0.26	0.30	A

In case of south/north orientation $sDA_{300/50\%}$ meets with the minimum according to IES in all cases, $ASE_{2000/400h}$ only meets S1 in Montreal, Santiago and Miami, and DGPs meets in all cases with class A, except in Montreal S3 and Boulder S3 where is class C. In case of west façade orientation $sDA_{300/50\%}$ meets with the minimum according to IES in all cases, $ASE_{2000/400h}$ meets for all cities with strategies S1 and S4, and DGPs meets

in all cases with class A, except in Montreal S3 and Boulder S3 where is class B. IES it is a very demanding standard to evaluate visual discomfort in comparison with DGPs, but how the objective is evaluate both indicators the best option for south/north orientation is S1 for all cities (considering that Boulder S1 with $\text{ASE}_{2000/400h} = 22\%$ is near the limit), and for west orientation is S1 for all cities.

Comparing both results, energy consumption and visual comfort, in all cities with south/north façade orientation the best option is S1 and only in Santiago of Chile have the minimum energy consumption. For west façade orientation, in Montreal, Santiago of Chile and Boulder the best strategy is S4 and in Miami is S1; only in the last case have the minimum energy consumption. It should be noted that glare indices shows in all cases that the glare is imperceptible.

4.5. Conclusions

This paper aims to determine the performance of an external CFS (movable undulated horizontal slats or louvers) in four cities (Santiago of Chile, Montreal, Boulder and Miami) in an office space for two façade orientations (south and west for Montreal, Boulder and Miami, and north and west for Santiago of Chile). Four control strategies are evaluated, each one based on incident irradiance level, vertical eye illuminance, cut-off angle and blocking control. In this study *mkSchedule* was used. This is a flexible and time-efficient tool that allows to run integrated thermal and lighting simulations using Radiance and EnergyPlus with different control strategies.

In each case, for evaluating visual comfort, parameters as DGPs, $\text{sDA}_{300,50\%}$ and $\text{ASE}_{2000,400h}$ were considered. Energy performance of the building space, was assessed in terms of energy consumption for lighting, heating and cooling. The main conclusions that can be drawn from this study are:

- Outdoor movable CFS can significantly control daylighting. In terms of visual and thermal comfort, these can generate a positive or a negative occupants' effect. Results show that when a CFS is are not properly designed overheating and/or visual discomfort may occur, where the minimum energy consumption, implies a great visual discomfort.
- *mkSchedule* is an effective tool to be used in early stages of building design for determine the best control strategy of a certain CFS based on visual comfort parameters and energy performance.
- In terms of energy consumption and visual comfort, the most effective control strategy is S1 (incident irradiance level) for all cases with south/north façade orientation, and for west façade orientation in all cases the best strategy is S4 (blocking control), except in Miami, where S1 is the best strategy. Energy savings are about 10%. Furthermore, a correct study of performance of CFS for different control strategies can be an important variable in the design stage to reduce energy consumption.

For analyzing control strategies, further studies are recommended in order to evaluate other strategies and their respective combinations, and optimize the geometry of movable CFS using control strategies to obtain a balanced performance in terms of office energy consumption and occupant's visual comfort.

5. OPTIMIZATION OF A FIXED OUTDOOR COMPLEX FENESTRATION SYSTEM FOR ACHIEVING VISUAL COMFORT AND ENERGY PERFORMANCE CRITERIA

5.1. Abstract

Office buildings are highly affected by solar heat gains through fenestrations. Nowadays, highly glazed façades are commonly in modern architecture. External shading devices allow controlling the solar heat gains which might contribute to improve the building performance in terms of energy efficiency and visual comfort. This paper aims to proposed a methodology to optimize the geometry of a fixed CFS in Montreal (Canada) and Santiago (Chile). The CFS are horizontal, curved, opaque and perforated louvers in the exterior of an office space with a curtain wall and dimming luminaires. The optimization parameters are the percentage of perforations, slats' spacing and the tilt angle of louvers. The optimization process was developed using GenOpt, a tool specialized in building's optimization, using a hybrid of a meta-heuristic algorithm and a pattern search algorithm. GenOpt was integrated with *mkSchedule* and EnergyPlus for lighting and energy simulation respectively. The objective function is in terms of visual comfort and building energy consumption. Visual comfort is assessed based on spatial daylight autonomy (sDA) and annual sunlight exposure (ASE) according to Illuminating Engineering Society (IES) standard, while building energy consumption is calculated for heating, cooling and lighting. The optimized solutions were found with louver slope of 25 °, 15% of perforation and 100 mm spacing for Montreal and louver slope of 50 °, 15% of perforation and 120 mm spacing for Santiago of Chile. The optimized solutions maximize the daylight availability and energy efficiency, and the optimization methodology saves about 97% of computational time in early design stages.

5.2. Introduction

Office buildings are highly affected by solar heat gains through fenestrations. Nowadays, highly glazed façades are a common element used in modern architecture. External shading devices allow lowering these solar heat gains (SHG) which might significantly influence the building performance in terms of improving energy efficiency and visual comfort. It is a common architectural practice to incorporate exterior shading devices to control SHG. There is a large variety of exterior shading devices such as louvers (fixed and movable), venetian blinds, and perforated screens. However, most of these devices correspond to a non-specularly transmitting layer, thus they are defined as complex fenestration systems (CFS). Therefore, CFS have a fundamental role in the energy performance of office buildings, in terms of energy consumption and lighting. These can have a positive or negative effect in visual and thermal comfort of occupants, because if are not well designed can produce overheating and/or glare, for this, it is necessary modelling and optimization in the design stage of building (Nielsen et al., 2011; Kirimtat et al., 2016).

Herein "Building optimization" refers to a method that uses algorithms to find the optimal combination of simulation parameters for architectural design. The goal of the optimization process is to find the optimum for the lowest total energy cost and meets the criteria of visual comfort using a much shorter simulation time that the approach of comparing each possible combination of parameters. Discrete parameters are typically used for façade design problems because continuous parameters are almost non-existent in façade design. Examples of discrete parameters are window dimension, construction material, insulation thickness, glazing types (SHGC, U-value), etc. Continuous parameters methods do not use fixed numbers for the parameter setting for building shape or dimensions such as window-to-wall ratio, building orientation, or compactness. Optimization methods using discrete parameters are more suitable to solve building façade design problems (Shan, 2014). The major obstacles in solving building optimization problems by simulation based methods involve the complex natures of building simulation outputs,

the expensive computational cost, the scale of the problems, multi-objective design problems, and uncertainty of many factors during the optimization, including design variables, environmental variables, model and constraint uncertainty among others (Nguyen et al., 2014). Successful optimization requires a nuanced understanding of the relationships between model parametrization, optimization algorithm, and performance metrics (McNeil & Lee, 2012).

EnergyPlus and TRNSYS are the mostly-used building simulation programs in optimization studies, and the mostly used optimization engines seems to be GenOpt and Matlab optimization toolboxes (Nguyen et al., 2014). There are several optimization algorithms such as: genetic algorithms (GA), particle swarm optimization (PSO), Hooke-Jeeves algorithms (HJ), simplex algorithms, coordinate search algorithms, hybrid algorithms, among others. The stochastic population-based algorithms (GAs, PSO, hybrid algorithms, evolutionary algorithms) have been the most frequently used methods in building performance optimization (Nguyen et al., 2014). Wetter and Wright (2003) compared the performance of a HJ algorithm and a GA in optimizing building energy consumption. Their results indicated that the GA outperformed the HJ algorithm and the latter have been attracted in a local minimum. Wetter and Wright (2004) found that the GA consistently got close to the best minimum and the Hybrid algorithm PSO-HJ achieved the overall best cost reductions. Kämpf et al. (2010) compared the performance of two metaheuristics algorithms, Covariance Matrix Adaptation Evolution Strategy Algorithm (CMA-ES/HDE) and PSO-HJ algorithm. They found that CMA-ES/HDE performed better than the PSO-HJ in solving the benchmark functions with 10 dimensions or less. However, if the number of dimensions is larger than 10, the PSO-HJ performed better.

Nowadays, there are many architects, engineers and scientist working on optimization of buildings components (Blanco et al., 2016). Tsangrassoulis et al. (2006) used a GA to design a slat-type shading system with one design parameter (angle of each slat segment). They demonstrated how GAs can be applied to the design of a shading system. McNeil and Lee (2012) developed an optimization process using GenOpt combined with

Radiance simulation capabilities to search for optimal shapes of microprisms for a specific CFS model. The optimization process considered glare and lighting energy in the objective function to maximize lighting energy savings and minimize glare, tolerate 0.5% increase in glare frequency for a 1% decrease in fractional lighting energy use. Particle swarm algorithms was used. Has developed a film geometry with superior performance to what is commercially available. Rapone and Saro (2012) studied a typical curtain wall façade of an office building in order to find the configuration of selected parameters (percentage of glazed surface, depth of the louvers and spacing of the louvers) that minimizes the total carbon emissions arising from building operation in four climates and the four cardinal orientations. They do not consider visual comfort evaluation. Simulation were based on PSO algorithm (using GenOpt) coupled to a dynamic energy simulation engine (Energy-Plus). Shan (2014) propose a methodology to find the optimal solutions for the total energy demand using a GA. The variables to optimize are the dimension of window grid and the depth of shading system. He used TRNSYS for energy simulations and DAYSIM for calculating loads due to artificial lights and turn off lights if exceed 500 lux, but he do not considered visual comfort metrics to evaluate daylight performance of the shading system. Manzan (2014) used a genetic optimization to design an optimal fixed shading device. The shading device is a flat panel positioned parallel to the window and inclined by its horizontal axis. He carried out this study using ESP-r for energy simulation and DAYSIM for calculating loads due to artificial lights, and ModeFRONTER with NSGA-II algorithm for optimization. The optimization is performed modifying four parameters (shading device height, width, angle and distance from the wall) and the objective function is in terms of total energy consumption. The optimized result was compared with unshaded window and results show energy savings up to 19% and 30% for Trieste and Rome (Italy), respectively. González and Fiorito (2015) developed a simplified method to overcome daylight and energy performance using DIVA, a plug-in for Rhinoceros/Grasshopper software, and Galapagos through GAs. The optimization process was carried out parametrically controlling the shadings' geometries (shading depth, angle on horizontal plane and shading number)

and they have two objective functions in terms of total energy consumption and CO_2 emissions. The optimized result was compared with conventional design techniques showing energy savings between 9.3% and 35.8% and CO_2 emissions reductions between 11.4% and 47.7%. He evaluates the daylight performance for the optimized solution, but they do not considered the visual comfort evaluation inside the optimization process. Futrell et al. (2015) used a hybrid GPS Hooke Jeeves/PSO algorithm in combination with the Epsilon Constraint Method to find Pareto efficient solutions to the daylighting and thermal optimization problem of a classroom design with only one exterior shade (without CFS). They used two objective functions, one for lighting and the other for energy consumption. They conclude that these two objectives are not strongly conflicting. Blanco et al. (2016) studied double skin enclosure built with metal perforated sheet panels. This device controls the light and SHG changing opening areas or perforations depending on location and orientation of façade. They applied a simple optimization methodology to determinate the perforations ratio for different climatic areas in Spain, but does not considered daylight performance.

The most of the studies about optimization of CFS's geometry considerer only the energy consumption in the objective function. In two cases the objective function has the both metrics (energy consumption and visual comfort), (McNeil & Lee, 2012) and (Futrell2015). The first only considerer the lighting consumption and the second methodology are appropriate but do not have CFS. It is needed a methodology that integrate energy consumption (heating, cooling and lighting) and visual comfort to optimize the geometry of CFS in the early design stage of the office buildings to save computational time, and maximize the daylight availability and energy efficiency.

This paper aims to proposed a methodology to optimize the geometry of a fixed CFS in Montreal (Canada) and Santiago (Chile). Montreal has a semi-continental climate, with a warm, humid summer and a very cold winter. Santiago is a semiarid climate characterized by high temperatures and solar irradiance for around 8 months of the year, even in winter

periods. The studies CFS correspond to horizontal, curved, opaque and perforated louvers in the exterior of an office space with curtain wall and dimming luminaires.

5.3. Methodology

The methodology to optimize the CFS's geometry consist in apply some algorithm through an optimization software/engine to a cost function that considerer energy consumption and visual comfort of occupants evaluated through an integrated lighting and energy software to perform simulations. For this study, the optimization engine used is GenOpt (Generic Optimization Program by Lawrence Berkeley National Laboratory) (Wetter, 2001), an optimization software for the minimization cost function that is evaluated by an external simulation software, and its implementation of a hybrid Generalized Pattern Search (GPS) implementing HJ and PSO (PSO-HJ), that reducing significantly the number of cost evaluations called by the algorithm. The tool for integrating the thermal and lighting analysis that it has been used is *mkSchedule* (Vera et al., 2016; Molina, 2014), a tool that integrates EnergyPlus and Radiance to facilitate the combined thermal and lighting analysis of building using control algorithms of CFS and luminaires.

5.3.1. Office space building

The office has been located in Montreal (Canada) and Santiago (Chile), correspond to a 4.0 m x 6.5 m x 2.8 m space. Two sets of dimming luminaires were installed, and two control sensors were located in the space to control each of them: one in the first half of the space and the other one is centered in the second half of it (see Figure 5.1). One façade is a curtain wall oriented to south in case of Montreal and north in case of Santiago. The opaque surfaces are considered adiabatic.

The office is shown in Figure 5.1, and the simulation layout shown in detail in Table 5.1.

The building was designed in SketchUp, and then exported using Groundhog®, an extension for SketchUp that allows exporting the models to Radiance in an appropriated format for multiphase analysis. In this case the Three-phase method (McNeil, 2013; Sexena et al., 2010) is used through *mkSchedule*. This implies exporting the building itself separately from the shading devices, which will allow assessing the bidirectional properties of the latter and change these without changing the building.

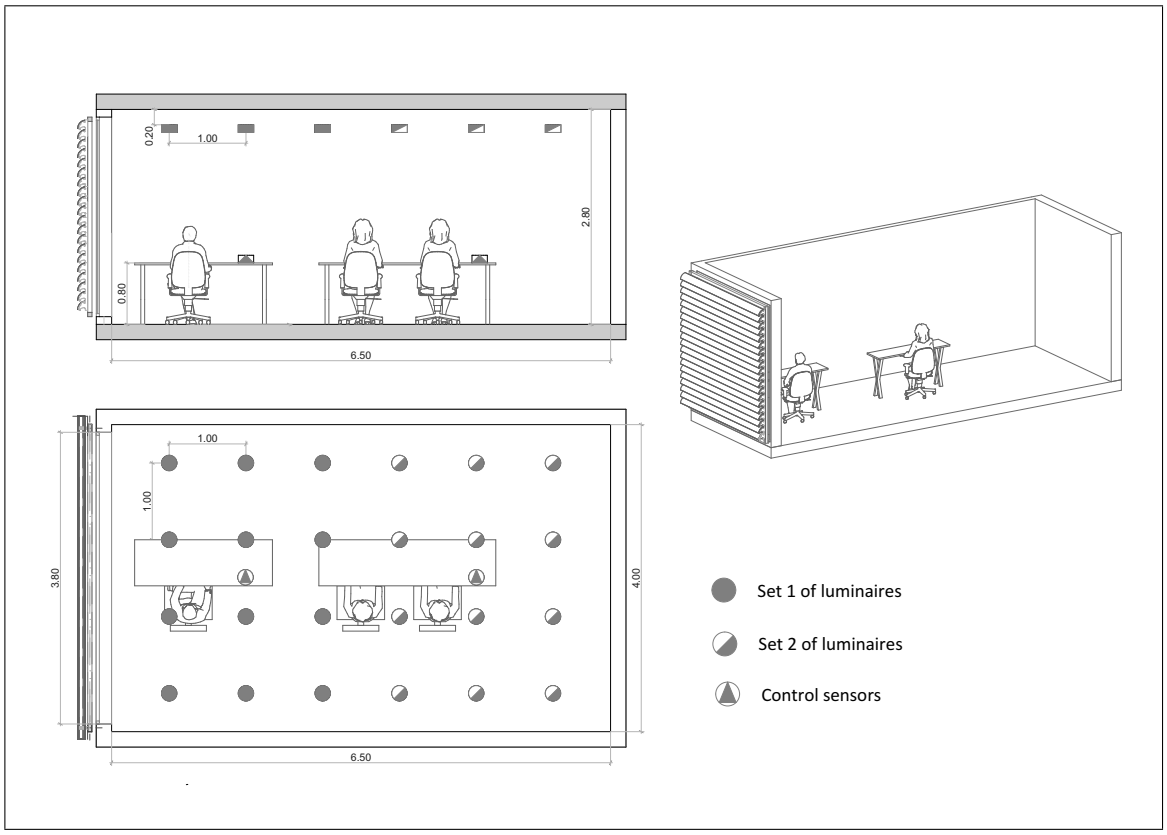

Figure 5.1. Model of the office space with louvers and interior dimensions (m), plain view and side view.

Table 5.1. Simulation layout.

Parameter	Details	
Cities	Santiago (Chile)	S33.38 °, W70.78 °
	Montreal (Canada)	N45.47 °, W73.75 °
Façade orientation	South (Montreal) and north (Santiago)	
Office Space	Size	4.0m(w) x 6.5m(l) x 2.8m(h)
	WWR	0.88
Opaque surfaces	Adiabatic	
Window	Size	3.8(w) x 2.6(h)
(Double clear glass)	T_{vis}	0.83
	SHGC	0.83
	U-factor	2.70 $Wm^{-1}K^{-1}$
Surface reflectances	Floor	20%
	Ceiling	70%
	Wall	50%
HVAC System	Electric heat pump (EHP)	COP 3.0
	Heating thermostat setpoint	20 °C
	Cooling thermostat setopoint	24 °C
Ventilation + infiltration	0.7 ACH (Gowri et al., 2009)	
Internal gains	People	6.7 W/m^2
	People radiant fraction	0.3
	Lighting	13.85 W/m^2
	Light radiant fraction	0.3
	Electric equipment	15 W/m^2
Lighting level setting	Workplane at 0.8 m	500 lux
Schedules	Occupancy, lights,	08:00 - 18:00 hrs. (weekdays)
	equipment & HVAC	

5.3.2. Complex fenestration system

CFS corresponds to a set of horizontal, opaque, curved and perforated louvers (commercial product named Celoscreen of HunterDouglas Company Chile). The main characteristics of this CFS are presented in Figure 5.2. The CFS was designed in SketchUp, and exported to Radiance's *genBSDF* with Groundhog® for assessing the BSDFs of complex fenestration systems. The materials of shading devices correspond to a reflective metal (95% solar and visible reflectance) with 0% specularity. The BSDFs were obtained in Klems full form, which corresponds to a matrix form for performing the annual simulations. After generating the BSDF for each CFS, they were imported to WINDOW 7.3 (LBNL, 2014) to be lately exported into an EnergyPlus readable format.

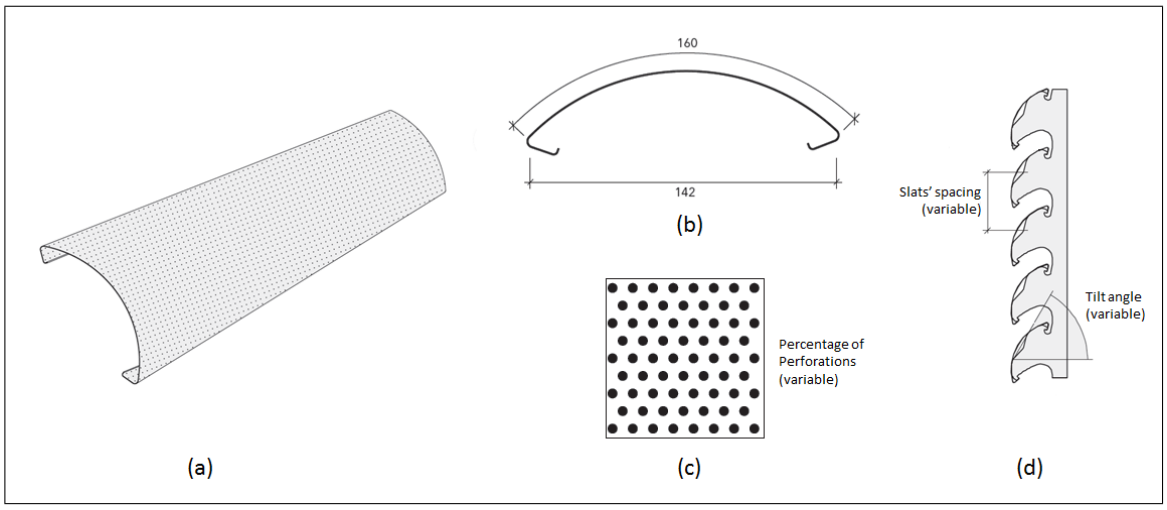

Figure 5.2. Perforated undulated louvers. (a) 3D view of louver. (b) Louver dimensions (mm). (c) Perforation pattern. (d) Installed louver. Adapted from (HunterDouglas, 2013).

Based on the literature review, percentage of perforations, slats slope and spacing are parameters that influence the SHG and lighting transmission. In the case of the selected optimization, these parameters were considered for optimization of CFS. Specific values are included in Table 5.2.

Table 5.2. Optimization parameters. Range and steps.

	Minimum	Maximum	Step
Perforations	10%	50%	5%
Slats' spacing	100 mm	250 mm	10 mm
Tilt angle	15 °	75 °	5 °

A total of 1872 combinations of the optimization parameters are possible. BSDF data base was developed with the 1872 combinations.

To compare results of the optimized CFS or optimized solution (OS), it has been selected the double clear glazing (DCG), where the control of solar heat gains and indoor illuminance levels is simply managed by the transmittance of the glass (in this case fixed throughout all the year).

5.3.3. Performance indicators

The optimization is based on the energy consumption of building and visual comfort of occupants. Following, the performance indicators of both parameters are explained:

- Spatial daylight autonomy (sDA): sDA is a metric describing annual sufficiency of ambient daylight levels in interior environments. It is defined as the percentage of an analysis area that meets a minimum daylight illuminance level for a specified fraction of the operating hours per year (IES, 2013). For this aim, $\text{sDA}_{300/50\%}$ >50% has been considered as the acceptable daylighting level.
- Annual sunlight exposure (ASE): ASE describes the potential for visual discomfort in interior work environments. It is defined as the percentage of an analysis area that exceeds a specified direct sunlight illuminance level more than a specified number of hours per year (IES, 2013). For this aim, $\text{ASE}_{2000/400h}$ <20% has been considered as the visual discomfort parameter.

- Heating energy consumption: this indicator accounts for the total energy consumption on a yearly base the heat pump and is measured in kWh/year.
- Cooling energy consumption: this indicator accounts for the total energy consumption on a yearly base the electric cooling and is measured in kWh/year.
- Lighting energy consumption: this indicator accounts for the total energy consumption on a yearly base the electric lighting and is measured in kWh/year.
- Total Energy Consumption: sum of the site energy consumed for heating, cooling and artificial lighting.
- Total Energy Savings: this indicator compares the total energy consumption of the optimized solution in respect of the double clear glazing on a yearly base.

5.3.4. Optimization problem

Generally, the optimization problem is continuous in building and HVAC design (Wetter & Wright, 2003), and it has the following form

$$\min_{x \in \mathbf{X}} f(x) \tag{5.1}$$

where $x \in \mathbf{X}$ is the vector of design parameters, $f : \mathbb{R}^n \longrightarrow \mathbb{R}$ is a continuously differentiable cost function, and $\mathbf{X}$ is the constraint set, defined as

$$\mathbf{X} \triangleq \left\{ x \in \mathbb{R}^n | l^i \leq x^i \leq u^i, i \in \{1, \ldots, n\} \right\} \tag{5.2}$$

with $\infty \leq l^i < u^i \leq \infty, \forall i \in \{1, \ldots, n\}$.

In this study, not all the CFS allow meeting the visual comfort, for example $\mathrm{ASE}_{2000/400h}$ reaches over 50% in some cases. For this reason, it is needed to apply a constraint that allow obtain an optimized solution that meets the visual comfort criteria. GenOpt can not include constraints directly, but the penalty functions are defined in GenOpt's User Manual (Wetter, 2011) as a possible solution to include constraints. A penalty function add a positive term to the cost function if a constraint is violated.

For this reason, the objective function ($f(x) = OF$) includes both parameters (energy consumption and visual comfort). Visual comfort was included as two penalty functions called ASE_M and sDA_M allowing to reach results that meet both metrics, minimum energy consumption and meeting the visual comfort. The objective function is defined in Equation (5.3).

$$OF = E_T \cdot ASE_M \cdot sDA_M \tag{5.3}$$

where E_T is the total energy consumption in kWh/year and ASE_M and sDA_M are defined following in equations (5.4) and (5.5) respectively.

$$ASE_M = \begin{cases} 1 & \text{if ASE}_{2000/400h} < 0.2 \\ \left(\text{ASE}_{2000/400h} + 0.8\right)^4 & \text{otherwise.} \end{cases} \tag{5.4}$$

$$sDA_M = \begin{cases} 1 & \text{if sDA}_{300/50\%} > 0.5 \\ \left(1.5 - \text{sDA}_{300/50\%}\right)^4 & \text{otherwise.} \end{cases} \tag{5.5}$$

where, $\text{ASE}_{2000/400h}$ and $\text{sDA}_{300/50\%}$ are in fraction form.

sDA_M and ASE_M functions shows graphically in Figures 5.3a and 5.3b respectively.

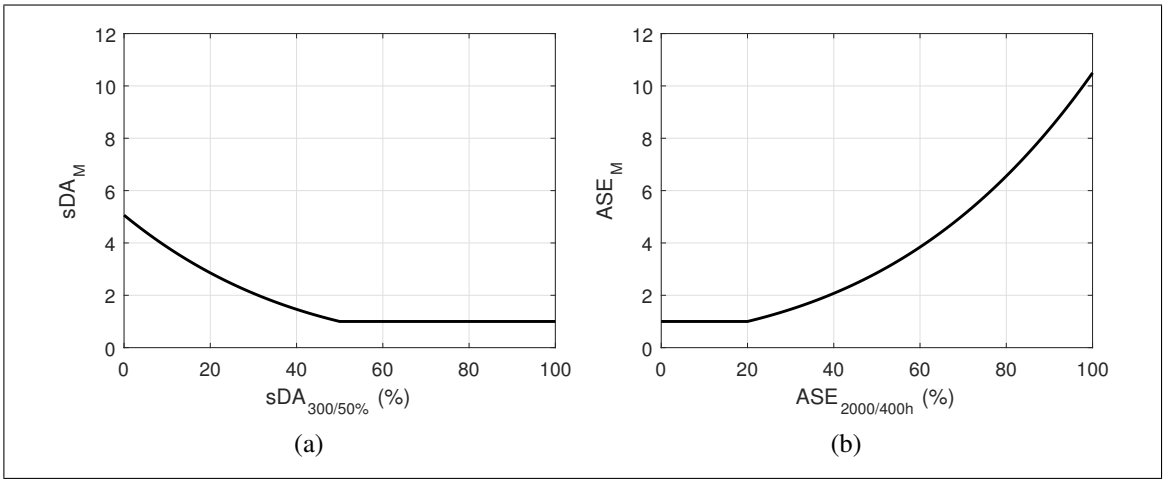

Figure 5.3. Penalty functions. (a) sDA_M, and (b) ASE_M.

5.3.5. Optimization algorithm

In this study, GenOpt's hybrid meta-heuristic algorithm (Particle Swarm Optimization or PSO using a constriction coefficient) and pattern search algorithm (Hooke Jeeves or HJ), referred to as GPSPSOCCHJ, was used to solve the minimization problem of Equation (5.1) to (5.5).

The hybrid global optimization algorithm, implemented in GenOpt, starts by doing a PSO on a mesh for a user-specified number of generations $n_G \in \mathbb{N}$, as described below. Afterwards, it initializes the HJ GPS algorithm to find the particle with the lowest cost function value (Wetter, 2011). Thus, the hybrid algorithm combines the global features of the PSO algorithm with the provable convergence properties of the GPS algorithm.

The PSO algorithm is a population based algorithm that was developed out of the evolutionary computational theory and social behavior theory (Poli, Kennedy, & Blackwell, 2007; Eberhart & Shi, 2001; Shi & Eberhart, 1998). Following, its describes the fundamentals of the PSO algorithm:

- PSO algorithms exploit a set of potential solutions to the optimization problem. Each potential solution is called a *particle*, and the set of potential solutions in each iteration step is called a *population*. The number of *particles* of the *population* is controlled by the *number of particles* parameter.
- For each particle, the best solution found by its neighborhood (neighborhood best) and save the best solution of all of neighborhoods visited (personal best). The number of neighborhoods particles are controlled by the *neighborhood topology* parameter and *neighborhood size* parameter.
- At each iteration, it changes the acceleration magnitude of the particle in the direction of its current neighborhood best solution, proportional to its distance from the neighborhood best solution. This acceleration is controlled by *social acceleration* parameter and a random scalar between 0 and 1 that is dynamically generated. Also, it changes the acceleration magnitude of the particle in the

direction of its personal best solution through the *cognitive acceleration* parameter.

- A constriction coefficient is used to limit the velocity of particles so that they more efficiently converge to an optimum point. At each iteration, scales the acceleration of a particle in each direction by a scalar controlled by the *constriction gain* parameter. A scalar less than one is then applied to the overall velocity of the particle.

The constriction coefficient parameter is important because unconstrained velocity of particles has been demonstrated to be problematic; particles tend to accelerate back and forth about optimal solutions and convergence is not reached (Futrell et al., 2015). The update equation for each *particle* x_i of the *population*, in each *generation* k, is given by:

$$x_i(k+1) = x_i(k) + \chi(\kappa, \varphi) \cdot \{\nu_i(k) + c_1\rho_1(k) \cdot [p_{l,i}(k) - x_i(k)] + c_2\rho_2(k) \cdot [p_{g,i}(k) - x_i(k)]\} \tag{5.6}$$

where c_1 and c_2 are the *cognitive acceleration* and *social acceleration*, $p_{l,i}(k)$ is the position that produced the *personal best* for particle i in all previous generations, $p_{g,i}(k)$ is the position of the overall best particle in all previous generations, and $\rho(k) \sim U(0,1)$. $\chi(\kappa, \varphi)$ is the constriction coefficient, which controls the convergence speed of the algorithm by determining how much of the design space has to be explored. In Table 5.3 can be seen the values of the PSO algorithm's parameters.

A more detailed description of the specific algorithm used can be found in the GenOpt User Manual (Wetter, 2011).

Table 5.3. Parameters of the Particle Swarm Optimization algortihm.

Parameter	Value
Neighborhood topology	Von Neumann
Number of particles	10
Number of generations	10
Cognitive acceleration	2.8
Social acceleration	1.3
Maximum velocity gain	0.5
Constriction gain	0.5

The HJ algorithm based on GPS algorithms, consist of a sequence of *exploratory moves* about a base point which, if successful, are followed by *pattern moves* (Hooke & Jeeves, 1961; Smith, 1969; Bell & Pike, 1966). Following explain the procedure of this algorithm.

- The HJ algorithm starts with a base point in the design space and make *exploratory moves*, from which it searches in their neighborhood with a predefined step size. If any move is a success (i.e. results in a reduced cost function value), the solution with the best performance is identified.
- A *pattern moves* identify the best search direction.
- The base point is moved along the line between it and the best performing solution determined through the *pattern move*.
- The process of evaluating solutions is repeated at the new base point location. When a better solution than the previous base point can not be found, the step size is reduced controlled by *mesh size divider*, *initial mesh size exponent*, *mesh size exponent increment* and *number of step reductions* parameters, allowing for the search to continue within the region of the design space.

- After the maximum *number of step reductions* have been made and the cost function can not be reduced, the algorithm finish.

Table 5.4 shows the values of HJ algorithm's parameters.

Table 5.4. Parameters of the GPS Hooke-Jeeves algortihm.

Parameter	Value
Mesh size divider	2
Initial mesh size exponent	0
Mesh size exponent increment	1
Number of step reductions	2

5.3.6. Optimization process

The workflow for searching the optimized solution is shown in Figure 5.4. It consists of the following steps:

(i) GenOpt accepted as input the parameters to be optimized, along their ranges and initial values.

(ii) GenOpt generate *mkSchedule* script with CFS corresponding and dimming luminaires control.

(iii) GenOpt executed a script that coordinated the execution of Radiance and EnergyPlus.

(iv) Radiance was executed firstly and output hourly illuminance values that were used to calculate sDA and ASE.

(v) Annual simulation of EnergyPlus was executed that output thermal and lighting load data which was converted into kWh/year values for design.

(vi) With the simulations complete, GenOpt then accepted the thermal and daylighting performance scores as input and used them to determine the region of the design space to search next, and begins again in step (ii).

(vii) This process was continued until GenOpt reached its stopping or convergence criteria (*number of step reductions* have been made and a the cost function can not be reduced).

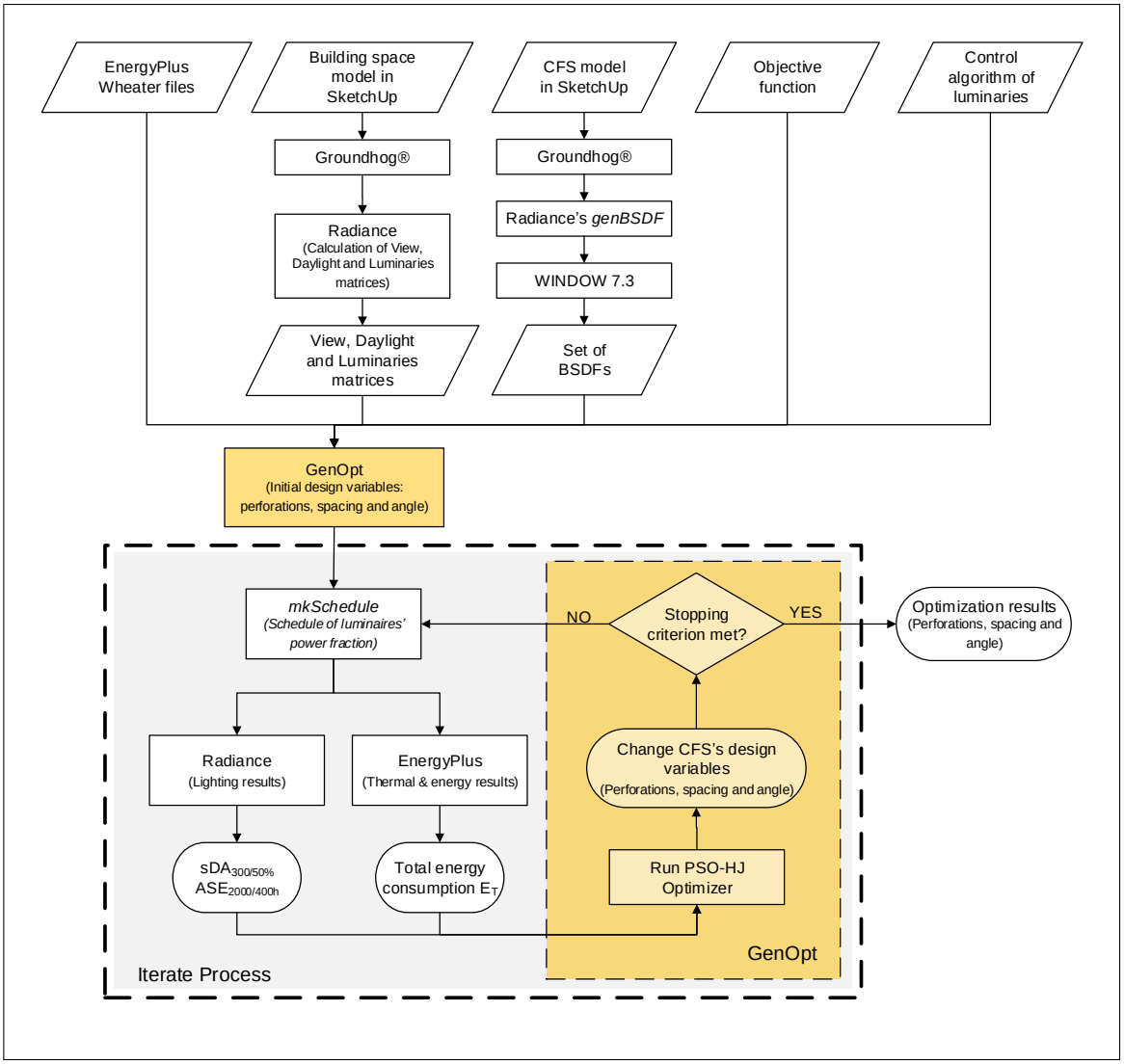

Figure 5.4. Workflow using *mkSchedule* and GenOpt solver.

5.4. Results and analysis

5.4.1. Optimization results

An optimization process was performed to determine the optimum design of a CFS with complex geometry in a building space in Montreal and Santiago of Chile. Shadings corresponds to a set of horizontal, opaque, curved and perforated louvers, and the parameters selected to vary are percentage of perforations, slats' spacing and tilt angle. The optimized solution was found to be a slope of 25 °, 15% of perforation and 100 mm spacing for Montreal and a slope of 50 °, 15% of perforation and 120 mm spacing for Santiago of Chile. Figure 5.5 shows the configuration of the CFS for each city. The optimized system is able to block solar radiation with an incident angle higher than 16 ° in Montreal and 5 ° in Santiago of Chile.

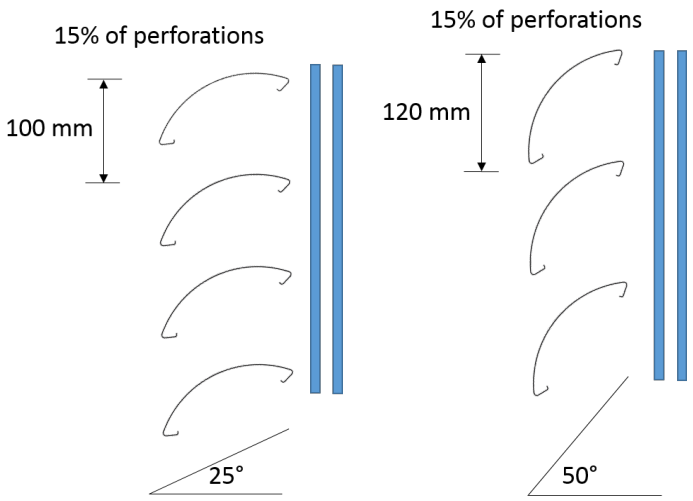

(a) Montreal (b) Santiago of Chile

Figure 5.5. Optimized solution for each city.

With the use of this optimization process, the optimized solution was found with 38 simulations for Montreal and 50 simulations for Santiago of Chile, instead of running 1872 simulations that correspond to the total possible combinations for the design of the

CFS. Therefore, the optimization process saves about 97% of computational time in the early stages of design.

5.4.2. Energy and lighting results

Table 5.5 and Figure 5.6 summarize results obtained during the simulation process and compare them in terms of energy consumption.

Table 5.5. Energy consumption for each scenario: double clear glazing (DCG) and optimized solution (OS).

City	Case	Energy consumption (kWh/year)				Energy savings	
		Heating	Cooling	Lighting	Total	(kWh/year)	(%)
Montreal	DCG	165	941	133	1239	0	0
	OS	281	426	478	1185	54	4.4
Santiago	DCG	0	1217	53	1270	0	0
	OS	0	467	415	882	388	30.6

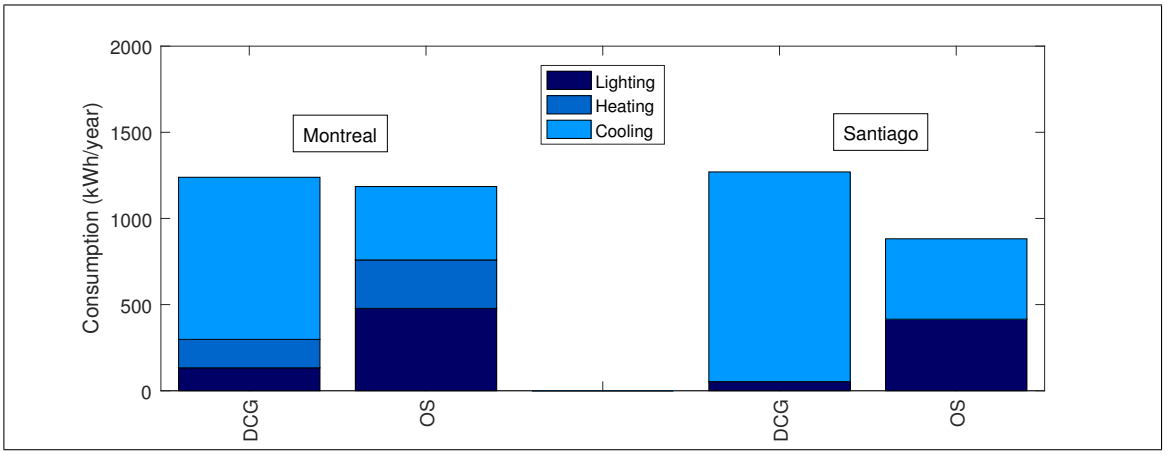

Figure 5.6. Measured energy consumption for lighting, heating and cooling (kWh/year) for each scenario.

Results of visual comfort, $sDA_{300/50\%}$ and $ASE_{2000/400h}$ for the double clear glazing and optimized solution are presented in Table 5.6 for Montreal and Santiago of Chile. Additionally, illuminance level at workplane is presented as temporal maps in Lightsolve format. It should be noted that, in both cities the high values for $sDA_{300/50\%}$ and $ASE_{2000/400h}$ show that a discomfort for occupants, therefore, is not possible use this configuration as solution. On the other hand, the optimized solution meets the both criteria of visual comfort for the two cities, maximizing daylighting and preventing visual discomfort.

5.4.3. Results validation

Computing the cost function through GenOpt involves solving a system of partial and ordinary differential equations that are coupled to algebraic equations. In general, one can not obtain an exact solution, but one can obtain an approximate numerical solution (Wetter, 2011).

A parametric simulation were run with the 1872 BSDFs to obtain the exact solution for each city and validate the proposed methodology. Table 5.7 shows the value of the three variables (percentage of perforations, slats' spacing and tilt angle) for the optimized solution and exact solution. Table 5.8 shows the results of total energy consumption and visual comfort metrics for both cities.

The proposed methodology present similar results in respect of the exact solution. For Montreal, the difference is 0.94% and for Santiago of Chile is 1.62% in terms of total energy consumption. Additionally, the proposed methodology achieve that the optimized solution meets the visual comfort criteria.

Table 5.6. Temporal maps of annual illuminance in lightsolve format for Montreal, values within 300 lux - 2000 lux.

City	CFS	Illuminance Level	$sDA_{300/50\%}$ / $ASE_{2000/400h}$
Montreal	DCG	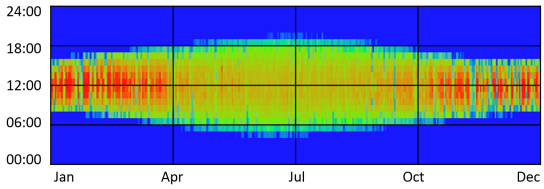	100% / 82%
	OS	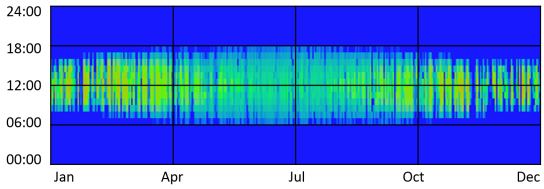	54% / 20%
Santiago	DCG	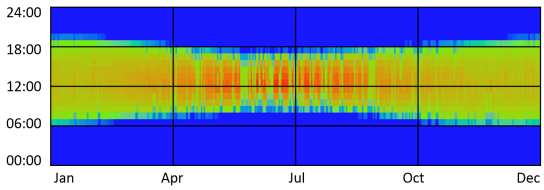	100% / 69%
	OS	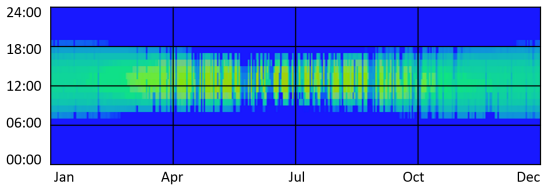	60% / 19%
Legend			

Table 5.7. Variables for exact solution (ES) and optimized solution (OS).

City	Case	% of perforations	Slats' spacing (mm)	Tilt angle
Montreal	OS	15%	100 mm	25 °
	ES	10%	100 mm	20 °
Santiago	OS	15%	120 mm	50 °
	ES	10%	130 mm	55 °

Table 5.8. Comparison between exact solution (ES) and optimized solution (OS) performance of visual comfort and energy consumption.

City	Case	Energy consumption		Visual comfort	
		Total (kWh/year)	Difference	$sDA_{300/50\%}$	$ASE_{2000,400h}$
Montreal	OS	1185	0.94%	54%	20%
	ES	1173	-	54%	17%
Santiago	OS	882	1.62%	60%	19%
	ES	867	-	60%	16%

5.5. Conclusions

This paper aims to optimize the geometry of a fixed CFS in two cities, Montreal (Canada) and Santiago (Chile). The CFS are horizontal, curved, opaque and perforated louvers in the exterior of an office space with curtain wall and dimming luminaires. The optimization parameters are percentage of perforations, slats' spacing and slope angle. The optimization process was developed using *mkSchedule* and GenOpt's hybrid meta-heuristic algorithm (PSO using a constriction coefficient) and pattern search algorithm

(HJ). Building performance was evaluated in terms of visual comfort and energy consumption. Also, the optimized solution achieved a 4.4% of energy savings compared to double clear glazing for Montreal, and, a 30.6% of energy savings for Santiago of Chile.

The main conclusions that can be drawn from this study are:

- The methodology of combination of parametric design of CFS with hybrid metaheuristic algorithm and pattern search algorithm to determine the CFS's geometry, allow to determine solutions to buildings performance in terms of energy consumption and visual comfort.
- Optimized solutions maximize the daylight availability and energy efficiency, validated through a parametric analysis.
- The optimization methodology saves about 97% of computational time, an important variable in the early design stage of the office buildings.

Future work can expand set of optimization criteria, combining energy-related indicator with other visual comfort metrics, such glare discomfort problems, include movable external shading devices, and calculate parametrically the BSDF during optimization progress without the need to use WINDOW software to generate a BSDF's database. Finally, it is needed apply sensitivity analysis to determine the effect of each variable on the optimization problem.

REFERENCES

Andersen, M., & de Boer, J. (2006). Goniophotometry and assessment of bidirectional photometric properties of complex fenestration systems. *Energy and Buildings*, *38*(7), 836–848. doi: 10.1016/j.enbuild.2006.03.009

Appelfeld, D., McNeil, A., & Svendsen, S. (2012). An hourly based performance comparison of an integrated micro-structural perforated shading screen with standard shading systems. *Energy and Buildings*, *50*, 166–176. doi: 10.1016/j.enbuild.2012.03.038

ASHRAE. (2013). *ASHRAE Handbook - Fundamentals* (R. American Society of Heating & A. conditioning Engineers, Eds.).

Bastien, D., & Athienitis, A. K. (2012). A control algorithm for optimal energy performance of a solarium/greenhouse with combined interior and exterior motorized shading. *Energy Procedia*, *30*, 995–1005. doi: 10.1016/j.egypro.2012.11.112

Basurto, C., Kämpf, J. H., & Scartezzini, J.-l. (2015). Annual Performance Assessment of Complex Fenestration Systems in Sunny Climates Using Advanced Computer Simulations. , *2*, 32–43. doi: 10.15627/jd.2015.6

Bell, M., & Pike, M. (1966). Remark on algorithm 178 [e4] direct search. *Communications of the ACM*, *9*, 684-685. doi: 10.1145/365813.365825

Bellia, L., Marino, C., Minichiello, F., & Pedace, A. (2014). An Overview on Solar Shading Systems for Buildings. *Energy Procedia*, *62*, 309–317. doi: 10.1016/j.egypro.2014.12.392

Blanco, J. M., Arriaga, P., Rojí, E., & Cuadrado, J. (2014). Investigating the thermal behavior of double-skin perforated sheet façades: Part A: Model characterization and validation procedure. *Building and Environment*, *82*, 50–62. doi: 10.1016/j.buildenv.2014.08.007

Blanco, J. M., Buruaga, A., Rojí, E., Cuadrado, J., & Pelaz, B. (2016). Energy assessment and optimization of perforated metal sheet double skin façades through

Design Builder; A case study in Spain. *Energy & Buildings*, *111*, 326–336. doi: 10.1016/j.enbuild.2015.11.053

Bourgeois, D., Reinhart, C. F., & Ward, G. (2008). Standard daylight coefficient model for dynamic daylighting simulations. *Building Research & Information*, *36*(1), 68–82. doi: 10.1080/09613210701446325

Breesch, H., & Janssens, a. (2010). Performance evaluation of passive cooling in office buildings based on uncertainty and sensitivity analysis. *Solar Energy*, *84*(8), 1453–1467. doi: 10.1016/j.solener.2010.05.008

Bueno, B., Wienold, J., Katsifaraki, A., & Kuhn, T. E. (2015). Fener: A Radiance-based modelling approach to assess the thermal and daylighting performance of complex fenestration systems in office spaces. *Energy and Buildings*, *94*, 10–20. doi: 10.1016/j.enbuild.2015.02.038

Building automation and perceived control: A field study on motorized exterior blinds in dutch offices. (2014). *Building and Environment*, *79*, 66 - 77. doi: 10.1016/j.buildenv.2014.04.023

Bustamante, W., Vera, S., & Prieto, A. (2014). Solar and Lighting Transmission through Complex Fenestration Systems of Office Buildings in a Warm and Dry Climate of Chile. *Sustainability*, *6*(5), 2786–2801. doi: 10.3390/su6052786

Chan, Y., & Tzempelikos, A. (2013). Efficient venetian blind control strategies considering daylight utilization and glare protection. *Solar Energy*, *98*, 241–254. doi: 10.1016/j.solener.2013.10.005

Chan, Y., & Tzempelikos, A. (2015). Daylighting and energy analysis of multi-sectional facades. In *6th International Building Physics Conference, IBPC 2015 Daylighting*.

Chauvel, P., Collins, J., Dogniaux, R., & Longmore, J. (1982). Glare from windows: current views of the problem. *Lighting Research & Technology*, *14*, 31–46. doi: 10.1177/096032718201400103

Correia da Silva, P., Leal, V., & Andersen, M. (2013). Occupants interaction with electric lighting and shading systems in real single-occupied offices: Results from a monitoring campaign. *Building and Environment*, *64*, 152–168. doi:

10.1016/j.buildenv.2013.03.015

Daylighting Pattern Guide. (n.d.). Retrieved March 06, 2016, from http://patternguide.advancedbuildings.net/

De Michele, G., Oberegger, U., & Baglivo, L. (2015). Coupling dynamic energy and daylighting simulations for complex fenestration systems. In *Building Simulation Applications BSA 2015.*

Duffie, J., & Beckman, W. (1996). *Solar engineering of thermal processes* (3rd ed.). John Wiley & Sons.

Eberhart, R., & Shi, Y. (2001). Particle swarm optimization: developments, applications and resources. In *Proceedings of the Congress on Evolutionary Computation* (Vol. 1, p. 81-86). doi: 10.1109/CEC.2001.934374

Energyplus. (n.d.). Retrieved March 06, 2016, from https://energyplus.net/

Futrell, B. J., Ozelkan, E. C., & Brentrup, D. (2015). Bi-objective Optimization of Building Enclosure Design for Thermal and Lighting Performance. *Building and Environment*, *92*, 591–602. doi: 10.1016/j.buildenv.2015.03.039

Goia, F., Haase, M., & Perino, M. (2013). Optimizing the configuration of a façade module for office buildings by means of integrated thermal and lighting simulations in a total energy perspective. *Applied Energy*, *108*, 515–527. doi: 10.1016/j.apenergy.2013.02.063

González, J., & Fiorito, F. (2015). Daylight Design of Office Buildings: Optimisation of External Solar Shadings by Using Combined Simulation Methods. *Buildings*, *5*, 560–580. doi: 10.3390/buildings5020560

Gowri, K., Winiarski, D., & Jarnagin, R. (2009). *Infiltration Modeling Guidelines Commercial Building Energy Analysis.*

Guglielmetti, R., Macumber, D., & Long, N. (2011). OpenStudio: An Open Source Integrated Analysis Platform. In *12th International Conference of International Building Performance Simulation Association* (pp. 1–9). Sydney, Australia.

Hooke, R., & Jeeves, T. (1961). "direct search" solution of numerical and statistical problems. *Journal of the ACM*, *8*, 212-229. doi: 10.1145/321062.321069

Hopkinson, R. (1972). Glare from daylighting in buildings. *Applied Ergonomics*, *3*, 206–215. doi: 10.1016/0003-6870(72)90102-0

Hopkinson, R., & Collins, J. (1963). The prediction and avoidance of glare in interior lighting. *Ergonomics*, *6*, 379–383. doi: 10.1080/00140136308930712

HunterDouglas. (2013). *Ficha Técnica Celoscreen.* Retrieved from `http://www.hunterdouglas.cl/ap/uploads/cl/productos/productos_archivo_descarga_102.pdf`

IES. (2013). *Approved Method: IES Spatial Daylight Autonomy (sDA) and Annual Sunlight Exposure (ASE).*

Janak, M. (2007). Coupling building energy and lighting simulation. In *5th International Conference of International Building Performance Simulation Association.* Prague, Czech Republic. Retrieved from `http://www.ibpsa.org/%5Cproceedings%5CBS1997%5CBS97_P036.pdf`

Kämpf, J., Wetter, M., & Robinson, D. (2010). A comparison of global optimisation algorithms with standard benchmark functions and real-world applications using energyplus. *Journal of Building Performance Simulation*, *3*, 103-120. doi: 10.1080/19401490903494597

Kirimtat, A., Koyunbaba, B. K., Chatzikonstantinou, I., & Sariyildiz, S. (2016). Review of simulation modeling for shading devices in buildings. *Renewable and Sustainable Energy Reviews*, *53*, 23–49. doi: 10.1016/j.rser.2015.08.020

Konis, K. (2013). Evaluating daylighting effectiveness and occupant visual comfort in a side-lit open-plan office building in San Francisco, California. *Building and Environment*, *59*, 662–677.

Konstantoglou, M., Jonsson, J., & Lee, E. (2009). Simulating Complex Window Systems using BSDF data. In *26th Conference on Passive and Low Energy Architecture.* Retrieved from `http://gaia.lbl.gov/btech/papers/4416.pdf`

Konstantoglou, M., & Tsangrassoulis, A. (2016). Dynamic operation of daylighting and shading systems: A literature review. *Renewable and Sustainable Energy Reviews*, *60*, 268–283. doi: 10.1016/j.rser.2015.12.246

Konstantzos, I., Tzempelikos, A., & Chan, Y.-C. (2015). Experimental and simulation analysis of daylight glare probability in offices with dynamic window shades. *Building and Environment*, *87*, 244–254. doi: 10.1016/j.buildenv.2015.02.007

Kuhn, T. E. (2006). Solar control: A general evaluation method for facades with venetian blinds or other solar control systems. *Energy and Buildings*, *38*(6), 648–660. doi: 10.1016/j.enbuild.2005.10.002

Lam, T. C., Ge, H., & Fazio, P. (2015). Impact of Curtain Wall Configurations on Building Energy Performance in the Perimeter Zone for a Cold Climate. *Energy Procedia*, *78*, 352–357. doi: 10.1016/j.egypro.2015.11.665

Laouadi, A., & Parekh, A. (2007). Optical models of complex fenestration systems. *Lighting Research and Technology*, *39*(2), 123–145. doi: 10.1177/1365782806072671

LBNL. (2014). *WINDOW 7.3*.

Li, D. H. W., & Lam, J. C. (2000). Solar heat gain factors and the implications to building designs in subtropical regions. *Energy and Buildings*, *32*(1), 47–55.

Liu, M., Wittchen, K. B., & Heiselberg, P. K. (2015). Control strategies for intelligent glazed façade and their influence on energy and comfort performance of office buildings in Denmark. *Applied Energy*, *145*, 43–51. doi: 10.1016/j.apenergy.2015.02.003

Mainini, A. G., Poli, T., Zinzi, M., & Speroni, A. (2014). Spectral Light Transmission Measure of Metal Screens for Glass Façades and Assessment of their Shading Potential. *Energy Procedia*, *48*, 1292–1301. doi: 10.1016/j.egypro.2014.02.146

Manzan, M. (2014). Genetic optimization of external fixed shading devices. *Energy & Buildings*, *72*, 431–440. doi: 10.1016/j.enbuild.2014.01.007

Mardaljevic, J., Andersen, M., Roy, N., & Christoffersen, J. (2012). Daylighting metrics: Is there a relation between useful daylight illuminance and daylight glare probability. In *Building Simulation and Optimization Conference BSO12*.

Mardaljevic, J., Heschong, L., & Lee, E. (2009). Daylight metrics and energy savings. *Lighting Research and Technology*, *41*, 261–283. doi: 10.1177/1477153509339703

McCluney, R. (2002). *Suggested methodologies for determining the SHGC of complex fenestration systems for NFRC Ratings.*

McNeil, A. (2013). *The Three-Phase Method for Simulating Complex Fenestration with Radiance.* Retrieved from http://radiance-online.org/learning/tutorials/Tutorial-ThreePhaseMethod.pdf

McNeil, A. (2015a). Daylight simulation of complex fenestration systems. Presented at the Simposio Internacional Arquitectura e Ingeniería de Envolventes de Edificios, Santiago, Chile.

McNeil, A. (2015b). *genBSDF Toturial.* Retrieved from http://www.radiance-online.org/learning/tutorials/Tutorial-genBSDF_v1.0.1.pdf

McNeil, A., Jonsson, C. J., Appelfeld, D., Ward, G., & Lee, E. S. (2013). A validation of a ray-tracing tool used to generate bi-directional scattering distribution functions for complex fenestration systems. *Solar Energy*, *98*, 404–414. doi: 10.1016/j.solener.2013.09.032

McNeil, A., & Lee, E. (2013). A validation of the Radiance three-phase simulation method for modelling annual daylight performance of optically complex fenestration systems. *Journal of Building Performance Simulation*, *6*(1), 24–37. doi: 10.1080/19401493.2012.671852

McNeil, A., & Lee, E. S. (2012). Using radiance and genopt to design static daylight redirection systems [DOE/ CEC PIER Technical Report].

MinEnergía. (2013). *Balance nacional de energía 2012.* Retrieved from http://www.energia.gob.cl/sites/default/files/bne_2013_1.xlsx (Available from: Division of Energy Prospective and Policy)

Molina, G. (2014). *Integrated thermal and lighting analysis of spaces with controled complex fenestration systems and artificial lighting during the design stage* (Unpublished master's thesis). Pontificia Universidad Católica de Chile, Escuela de Ingeniería.

Molina, G., Bustamante, W., Rao, J., Fazio, P., & Vera, S. (2015). Evaluation of radiance's genBSDF capability to assess solar bidirectional properties of complex fenestration systems. *Journal of Building Performance Simulation*, *8*(4), 216-225. doi: 10.1080/19401493.2014.912355

Molina, G., Vera, S., & Bustamante, W. (2014). *Groundhog - lighting analysis within sketchup.* Retrieved from `http://igd-labs.github.io/Groundhog/`

Molina, G., Vera, S., & W., B. (2014). A tool for integrated thermal and lighting analysis of spaces with controlled Complex Fenestration Systems and artificial lighting. In *eSim2014 Removing barriers to application of Building Performance Simulation in design practice.* (Ottawa, Canada, May 7-10)

Neufert, E. (2012). *Architect's data* (4th ed.). Blackwell Publishers.

Nguyen, A.-T., Reiter, S., & Rigo, P. (2014). A review on simulation-based optimization methods applied to building performance analysis. *Applied Energy*, *113*, 1043–1058. doi: 10.1016/j.apenergy.2013.08.061

Nielsen, M. V., Svendsen, S., & Jensen, L. B. (2011). Quantifying the potential of automated dynamic solar shading in office buildings through integrated simulations of energy and daylight. *Solar Energy*, *85*(5), 757–768. doi: 10.1016/j.solener.2011.01.010

Ochoa, C. E., Aries, M. B. C., & Hensen, J. L. M. (2012). Journal of Building Performance Simulation State of the art in lighting simulation for building science : a literature review. *Journal of Building Performance Simulation*, *5*(4), 209–233. doi: 10.1080/19401493.2011.558211

Ochoa, C. E., Aries, M. B. C., van Loenen, E. J., & Hensen, J. L. M. (2012). Considerations on design optimization criteria for windows providing low energy consumption and high visual comfort. *Applied Energy*, *95*, 238–245. doi: 10.1016/j.apenergy.2012.02.042

Perez, R., Ineichen, P., Seals, R., Michalsky, J., & Stewart, R. (1990). Modeling daylight availability and irradiance components from direct and global irradiance. *Solar Energy*, *44*(5), 271–289. Retrieved from `http://www.sciencedirect.com/`

science/article/pii/0038092X9090055H

Perez, R., Seals, R., & Michalsky, J. (1993). All-weather model for sky luminance distribution - Preliminary configuration and validation. *Solar Energy*, *50*(3), 271–289.

Petersen, S., & Svendsen, S. (2010). Method and simulation program informed decisions in the early stages of building design. *Energy & Buildings*, *42*(7), 1113–1119. doi: 10.1016/j.enbuild.2010.02.002

Poli, R., Kennedy, J., & Blackwell, T. (2007). Particle swarm optimization. *Swarm Intelligence*, *1*, 33-57. doi: 10.1007/s11721-007-0002-0

Rapone, G., & Saro, O. (2012). Optimisation of curtain wall façades for office buildings by means of PSO algorithm. *Energy & Buildings*, *45*, 189–196. doi: 10.1016/j.enbuild.2011.11.003

Reilly, S., & Hawthorne, W. (1998). The impact of windows on residential energy use. *ASHRAE Transactions*, *104*(791).

Reinhart, C., & Mardaljevic, Z., Rogers. (2006). Dynamic daylight performance metrics for sustainable building design. *LEUKOS: The Journal of the Illuminating Engineering Society of North America*, *3*, 1–25. doi: 10.1582/LEUKOS.2006.03.01.001

Reinhart, C. F. (2013). *Daysim.* Retrieved March 06, 2016, from http://daysim.ning.com/

Rubin, M., Jonsson, J., Kohler, C., & Klems, J. (2007). Bidirectional Optical Properties of Slat Shading: Comparison Between Raytracing and Radiosity Methods.

Saxena, M., Ward, G., Perry, T., Heschong, L., & Higa, R. (2010). Dynamic Radiance Predicting Annual Daylighting with Variable Fenestration Optics Using BSDFs. In *Fourth National Conference of IBPSA-USA* (pp. 402–409).

Serra, V., Zanghirella, F., & Perino, M. (2010). Experimental evaluation of a climate façade : Energy efficiency and thermal comfort performance. , *42*, 50–62. doi: 10.1016/j.enbuild.2009.07.010

Sexena, M., Ward, G., Perry, T., Heschong, L., & Higa, R. (2010, August). Dynamic Radiance-Predinting annual daylighting with variable fenestration optic using BSDFs. In *Fourth National Conference of IBPSA-USA*.

Shan, R. (2014). Optimization for Heating, Cooling and Lighting Load in Building Façade Design. *Energy Procedia*, *57*, 1716–1725. doi: 10.1016/j.egypro.2014.10.142

Shen, E., Hu, J., & Patel, M. (2014). Energy and visual comfort analysis of lighting and daylight control strategies. *Building and Environment*, *78*, 155–170. doi: 10.1016/j.buildenv.2014.04.028

Shen, H., & Tzempelikos, A. (2012). Daylighting and energy analysis of private offices with automated interior roller shades. *Solar Energy*, *86*(2), 681–704. doi: 10.1016/j.solener.2011.11.016

Shi, Y., & Eberhart, R. (1998). A modified particle swarm optimizer. In *Proceedings of the Congress on Evolutionary Computation* (p. 69-73). doi: 10.1109/ICEC.1998.699146

Smith, L. (1969). Remark on algorithm 178 [e4]: direct search. *Communications of the ACM*, *12*, 638. doi: 10.1145/363269.363624

Stazi, F., Marinelli, S., Perna, C. D., & Munafo, P. (2014). Comparison on solar shadings : Monitoring of the thermo-physical behaviour , assessment of the energy saving , thermal comfort , natural lighting and environmental impact. *Solar Energy*, *105*, 512–528. doi: 10.1016/j.solener.2014.04.005

Tregenza, P. R., & Waters, I. M. (1983). Daylight coefficients. *Lighting Research and Technology*, *15*(2), 65–71. doi: 10.1177/096032718301500201

Trnsys. (n.d.). Retrieved March 06, 2016, from `http://www.trnsys.com/`

Tsangrassoulis, A., Bourdakis, V., Geros, V., & Santamouris, M. (2006). A genetic algorithm solution to the design of slat-type shading system. *Renewable Energy*, *31*, 2321–2328. doi: 10.1016/j.renene.2005.09.031

Tzempelikos, A. (2012). Development and Implementation of Lighting and Shading Control Algorithms in an Airport Building. *Journal of Architectural Engineering*(18), 242–250. doi: 10.1061/(ASCE)AE.1943-5568.0000062.

Tzempelikos, A., & Athienitis, A. K. (2007). The impact of shading design and control on building cooling and lighting demand. *Solar Energy*, *81*(3), 369–382. doi: 10.1016/j.solener.2006.06.015

Tzempelikos, A., & Shen, H. (2013). Comparative control strategies for roller shades with respect to daylighting and energy performance. *Building and Environment*, *67*, 179–192. doi: 10.1016/j.buildenv.2013.05.016

UNEP. (2009). Buildings and Climate Change: Summary for Decision-Makers. *United Nations Environment Programme, Sustainable Buildings and Climate Change*. Retrieved from `http://www.unep.org/sbci/pdfs/SBCI-BCCSummary.pdf`

Van Den Wymelenberg, K., & Inanici, M. (2014). A Critical Investigation of Common Lighting Design Metrics for Predicting Human Visual Comfort in Offices with Daylight. *LEUKOS: The Journal of the Illuminating Engineering Society of North America*, *10*, 145–164. doi: 10.1080/15502724.2014.881720

Vera, S., Bustamante, W., Molina, G., & Uribe, D. (2016). A flexible and time-efficient schedule-based communication tool for integrated lighting and thermal simulations of spaces with controlled artificial lighting and complex fenestration systems. *Journal of Building Performance Simulation*, *9*(4), 382-396. doi: 10.1080/19401493.2015.1062556

Wagner, A., Gossauer, E., Moosmann, C., Gropp, T., & Leonhart, R. (2007). Thermal comfort and workplace occupant satisfaction Results of field studies in German low energy office buildings. *Energy and Buildings*, *39*, 758–769. doi: 10.1016/j.enbuild.2007.02.013

Ward, G. J. (1994). The RADIANCE Lighting Simulation and Rendering System. In *Computer Graphics Proceedings, Annual Conference Series, 1994.*

Wetter, M. (2001). GenOpt ® – A Generic Optimization Program. In *7th IBPSA's Building Simulation Conference, Rio de Janeiro* (pp. 601–608).

Wetter, M. (2011). *Genopt, generic optimization program, version 3.1.0, lawrence berkeley national laboratory.* Retrieved from `https://simulationresearch.lbl.gov/GO/download/manual-3-1-0.pdf`

Wetter, M., & Wright, J. (2003). Comparison of a generalized pattern search and genectic algorithm optimization method. In *8th Conference of International Building Performance Simulation Association.*

Wetter, M., & Wright, J. A. (2004, 08/2004). A comparison of deterministic and probabilistic optimization algorithms for nonsmooth simulation-based optimization. *Building and Environment*, *39*, 989-999. doi: 10.1016/j.buildenv.2004.01.022

Wienold, J. (2007). Dynamic simulation of blind controls strategies for visual comfort and energy balance analysis. In *10th International Building Performance Simulation Association Conference, Beijing* (pp. 1197–1204).

Wienold, J. (2009). Dynamic Daylight Glare Evaluation. In *Eleventh International IBPSA Conference.*

Wienold, J., & Christoffersen, J. (2006). Evaluation methods and development of a new glare prediction model for daylight environments with the use of CCD cameras. *Energy and Buildings*, *38*(7), 743–757. doi: 10.1016/j.enbuild.2006.03.017

Wienold, J., Frontini, F., Herkel, S., & Mende, S. (2011). Climate based simulation of different shading device systems for comfort and energy demand. In *12th Conference of International Building Performance Simulation Association, Sydney.*

Winkelmann, F. C. (2001). Modeling windows in EnergyPlus. *Building Simulation*, 457–464.

Yi, H., Srinivasan, R. S., & Braham, W. W. (2015). An integrated energyemergy approach to building form optimization: Use of energyplus, emergy analysis and taguchi-regression method. *Building and Environment*, *84*, 89 - 104. doi: 10.1016/j.buildenv.2014.10.013

Yun, G., Yoon, K. C., & Kim, K. S. (2014). The influence of shading control strategies on the visual comfort and energy demand of office buildings. *Energy and Buildings*, *84*, 70–85. doi: 10.1016/j.enbuild.2014.07.040

APPENDIX

A. METHODOLOGY FOR THERMAL AND LIGHTING ANALYSIS

The procedure carried out within *mkSchedule* can see in Figure A.1.

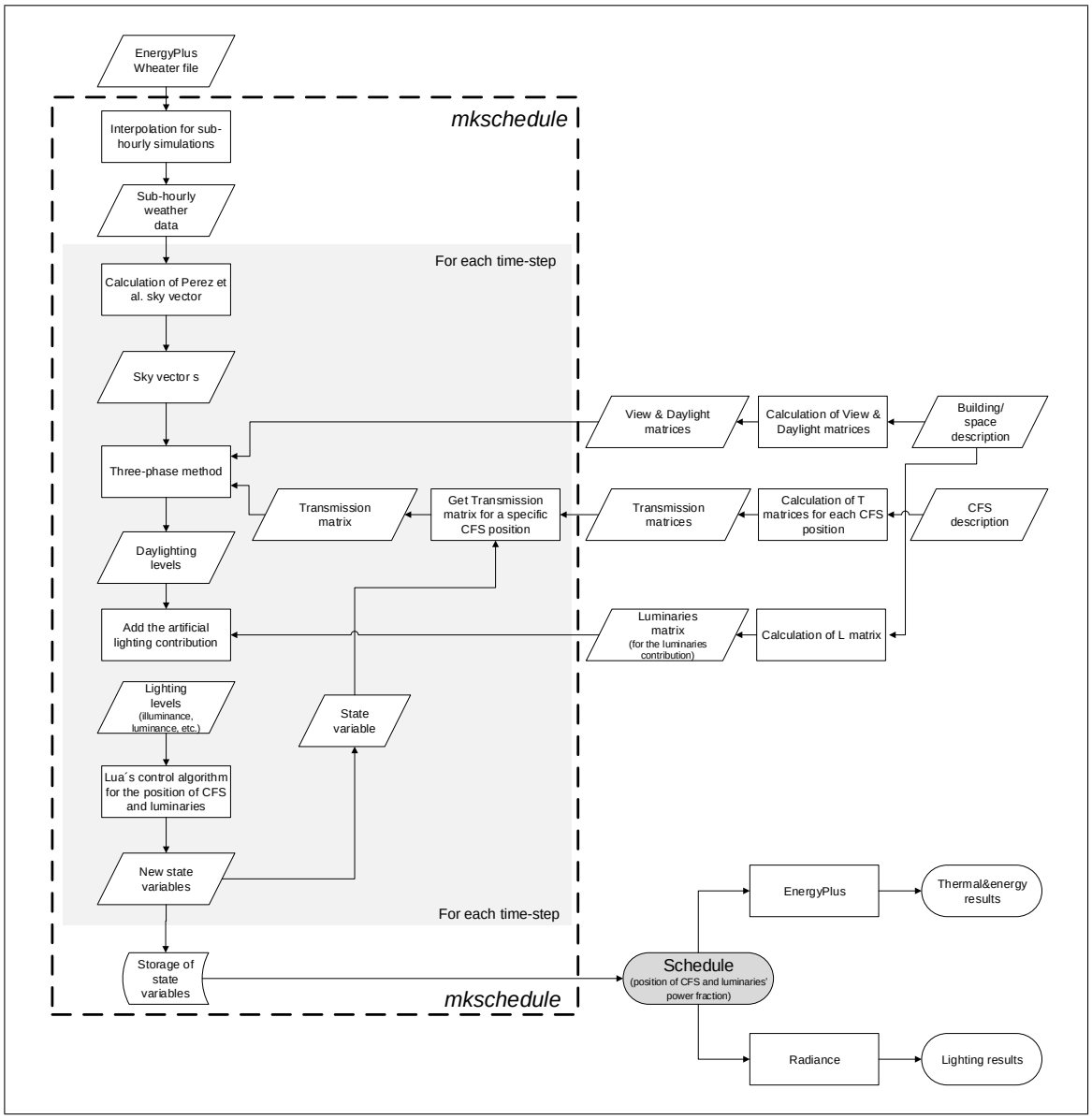

Figure A.1. Flow chart of the proposed methodology for integrating lighting and thermal/energy simulations (Vera et al., 2016).

B. PERL SCRIPTS USED FOR MAKING THE LIGHTING AND THE ENERGY-PLUS SIMULATION IN CHAPTER 3

Script Perl: Matrices for Simulation

```
#!/usr/local/bin/perl

 use POSIX ();
 use POSIX qw(setsid);
 use POSIX qw(:errno_h :fcntl_h);

use Time::HiRes qw( usleep ualarm gettimeofday tv_interval nanosleep
                      clock_gettime clock_getres clock_nanosleep clock
                      stat  );

my $start_time=[Time::HiRes::gettimeofday()];
$time="time_matrix";
open (TXT, ">␣$time.txt");

#################
#### Inputs #####
#################

# Office dimensions
$width=4; #X axis
$length=6.5; #Y axis
$height=2.8; #Z axis

# Window dimensions
$ledge=0.2; #Ledge, or Sprandel in Curtain Walls
$wall_offset=0.2; #the window will be ($width-2*$wall_offset) wide
$ceiling_offset=0.2; #same deal, but with the ceiling. The window will
    be $height-$ledge-$ceiling_offset high

# Sensors distribution
$sensor_spacing=0.5;
$sensor_height=0.8;

# Orientation
# can be between 0 and 360 with step of 45.
@orientation=(0,90,180,270); # 0 positions the window facing South, 90
    facing East.
# 0   Window in facing South
# 45  Window in facing South-East
# 90  Window in facing East
# 135 Window in facing North-East
# 180 Window in facing North
# 225 Window in facing North-West
```

```
# 270 Window in facing West
# 315 Window in facing South-West

# Luminaires
$luminaire_power=30; # Power of each luminaire (W)
$luminaire_file="lum.rad"; # Luminaire. Assuming .rad file
$luminaire_spacing=1.2;
$lum_ceiling_offset=0.2; # Ceiling offset of luminaire

# Control Sensors
@control_sens1=(0.5,0.25,0.8); # Control sensor of set 1 of luminaires Position
@control_sens2=(0.5,0.75,0.8); # Control sensor of set 2 of luminaires Postition
@control_sens3=(0.5,0.15384615,1.15); # Vertical Eye Illuminance Sensor Position

# Processing information
$cores=8; #for multicore processing (rcontrib, rtrace and rfluxmtx runs)
$bins=4; #number of bins of Reinhart's sky subdivition.

# Wall, Ceiling and Floor Reflectance
$rho_wall=0.5;
$rho_ceiling=0.7;
$rho_floor=0.2;

# Make directories
`mkdir -p scenes`;
`mkdir -p scenes/rad`;
`mkdir -p scenes/idf`;
`mkdir -p Workplanes`;
`mkdir -p DMX`;
`mkdir -p VMX`;
`mkdir -p LMX`;
`mkdir -p Schedules`;
`mkdir -p Results `;
`mkdir -p Results/Lighting`;
`mkdir -p Results/Andersen`;
`mkdir -p Results/EPlus`;
`mkdir -p Results/SG`;
`mkdir -p Scripts`;

# Office information
$volume=$heigth*$width*$length;
$floor_area=$length*$width;
$window_area=($width-2*$wall_offset)*($height-$ceiling_offset-$ledge);
$wwr=$window_area/($height*$width);
print "\n\tWindow-to-Wall␣Ratio:\t\t\t\t$wwr\n";
print TXT "\n\tWindow-to-Wall␣Ratio:\t\t\t\t$wwr\n";

```

```
89 # Array of luminaires
90 $lum_x=int($width/$luminaire_spacing); #this will create an array of
       luminaires. lum_x in the X axis and lum_y in the Y axis
91 $lum_y=int(0.5*$length/$luminaire_spacing);
92 $n_luminaires=$lum_x*$lum_y;
93 $lighting_power=$n_luminaires*$luminaire_power;
94 $light_over_area=2*$lighting_power/$floor_area;
95
96 print "\tLuminaire␣power:\t\t\t\t$light_over_area␣W/m2\n";
97 print TXT "\tLuminaire␣power:\t\t\t\t$light_over_area␣W/m2\n";
98
99 $rest_x=($width-($lum_x-1)*$luminaire_spacing)/2;
100 $rest_y=(0.5*$length-($lum_y-1)*$luminaire_spacing)/2;
101 $luminaire_height=$height-$lum_ceiling_offset;
102
103 foreach $orientation (@orientation){
104
105   # Scene file 1
106   $scene_file1="Scene1-$orientation";
107   $z7=$height-$ceiling_offset;
108   $x8=$width-$wall_offset;
109   $z8=$z7;
110   $x9=$x8;
111
112   open (SCENE, ">>temp_rad");
113
114   print SCENE "void␣plastic␣wall\n0\n0\n5\t$rho_wall\t$rho_wall\
          t$rho_wall\t0\t0␣\n\n";
115   print SCENE "void␣plastic␣floor\n0\n0\n5\t$rho_floor\t$rho_floor\
          t$rho_floor\t0\t0␣\n\n";
116   print SCENE "void␣plastic␣ceiling\n0\n0\n5\t$rho_ceiling\
          t$rho_ceiling\t$rho_ceiling\t0\t0␣\n\n";
117   print SCENE "wall␣polygon␣muro_trasero\n0\n0\n12\n\t0\t$length\t0\n\
          t$width\t$length\t0\n\t$width\t$length\t$height\n\t0\t$length\
          t$height\n\n";
118   print SCENE "wall␣polygon␣muro_derecho\n0\n0\n12\n\t$width\t0\t0\n\
          t$width\t$length\t0\n\t$width\t$length\t$height\n\t$width\t0\
          t$height\n\n";
119   print SCENE "wall␣polygon␣muro_izquierdo\n0\n0\n12\n\t0\t0\t0\n\t0\
          t$length\t0\n\t0\t$length\t$height\n\t0\t0\t$height\n\n";
120   print SCENE "ceiling␣polygon␣techo_geom\n0\n0\n12\n\t0\t0\t$height\n\
          t$width\t0\t$height\n\t$width\t$length\t$height\n\t0\t$length\
          t$height\n\n";
121   print SCENE "floor␣polygon␣piso_geom\n0\n0\n12\n\t0\t0\t0\n\t$width\
          t0\t0\n\t$width\t$length\t0\n\t0\t$length\t0\n\n";
122   print SCENE "wall␣polygon␣muro_ventana
123 ␣␣0
124 ␣␣0
125 ␣␣30
126 ␣␣␣␣0␣0␣0
127 ␣␣␣␣$width␣␣0␣0
```

```
␣␣␣␣$width␣␣0␣$height
␣␣␣␣0␣0␣$height
␣␣␣␣0␣0␣0
␣␣␣␣$wall_offset␣␣0␣$ledge
␣␣␣␣$wall_offset␣␣0␣$z7
␣␣␣␣$x8␣0␣$z8
␣␣␣␣$x9␣0␣$ledge
␣␣␣␣$wall_offset␣␣0␣$ledge
␣␣";

  close (SCENE);
  `xform -t $rest_x $rest_y $luminaire_height -a $lum_x -t
     $luminaire_spacing 0 0 -a $lum_y -t 0 $luminaire_spacing 0
     $luminaire_file >> temp_rad`;
  open (SCENEFILE, ">␣scenes/rad/$scene_file1.rad");
  close (SCENEFILE);
  `xform -rz $orientation temp_rad >> scenes/rad/$scene_file1.rad`;
  `rm -f temp_rad`;

  # Scene file 2
  $scene_file2="Scene2-$orientation";
  $z7=$height-$ceiling_offset;
  $x8=$width-$wall_offset;
  $z8=$z7;
  $x9=$x8;

  open (SCENE, ">>temp_rad");

  print SCENE "void␣plastic␣wall\n0\n0\n5\t$rho_wall\t$rho_wall\
     t$rho_wall\t0\t0␣\n\n";
  print SCENE "void␣plastic␣floor\n0\n0\n5\t$rho_floor\t$rho_floor\
     t$rho_floor\t0\t0␣\n\n";
  print SCENE "void␣plastic␣ceiling\n0\n0\n5\t$rho_ceiling\
     t$rho_ceiling\t$rho_ceiling\t0\t0␣\n\n";
  print SCENE "wall␣polygon␣muro_trasero\n0\n0\n12\n\t0\t$length\t0\n\
     t$width\t$length\t0\n\t$width\t$length\t$height\n\t0\t$length\
     t$height\n\n";
  print SCENE "wall␣polygon␣muro_derecho\n0\n0\n12\n\t$width\t0\t0\n\
     t$width\t$length\t0\n\t$width\t$length\t$height\n\t$width\t0\
     t$height\n\n";
  print SCENE "wall␣polygon␣muro_izquierdo\n0\n0\n12\n\t0\t0\t0\n\t0\
     t$length\t0\n\t0\t$length\t$height\n\t0\t0\t$height\n\n";
  print SCENE "ceiling␣polygon␣techo_geom\n0\n0\n12\n\t0\t0\t$height\n\
     t$width\t0\t$height\n\t$width\t$length\t$height\n\t0\t$length\
     t$height\n\n";
  print SCENE "floor␣polygon␣piso_geom\n0\n0\n12\n\t0\t0\t0\n\t$width\
     t0\t0\n\t$width\t$length\t0\n\t0\t$length\t0\n\n";
  print SCENE "wall␣polygon␣muro_ventana
␣␣0
␣␣0
␣␣30
```

```
␣␣␣␣0␣0␣0
␣␣␣␣$width␣␣0␣0
␣␣␣␣$width␣␣0␣$height
␣␣␣␣0␣0␣$height
␣␣␣␣0␣0␣0
␣␣␣␣$wall_offset␣␣0␣$ledge
␣␣␣␣$wall_offset␣␣0␣$z7
␣␣␣␣$x8␣0␣$z8
␣␣␣␣$x9␣0␣$ledge
␣␣␣␣$wall_offset␣␣0␣$ledge
␣␣";

  close (SCENE);
  $rest_y=$rest_y+0.5*$length;
  `xform -t $rest_x $rest_y $luminaire_height -a $lum_x -t
     $luminaire_spacing 0 0 -a $lum_y -t 0 $luminaire_spacing 0
     $luminaire_file >> temp_rad`;
  open (SCENEFILE, ">␣scenes/rad/$scene_file2.rad");
  close (SCENEFILE);
  `xform -rz $orientation temp_rad >> scenes/rad/$scene_file2.rad`;
  `rm -f temp_rad`;

  my $t=Time::HiRes::tv_interval($start_time);
  print "\n\tWrite␣Radiance␣model␣$orientation␣degrees\t\t\t$t\n";
  print TXT "\n\tWrite␣Radiance␣model␣$orientation␣degrees\t\t\t$t\n";


  # Window file
  $win_file="window";
  open (WIN_SCENE, ">␣win_rad");
  print WIN_SCENE "#\@rfluxmtx␣h=kf␣u=Z␣\nvoid␣glass␣black\n0\n0\n3\t0\
     t0\t0\n\n␣\nblack\tpolygon\twindow\n0\n0\n12\t$wall_offset\t0\
     t$ledge\n\t$wall_offset\t0\t$z7\n\t$x8\t0\t$z7\n\t$x8\t0\t$ledge\n
     ";
  close (WIN_SCENE);
  `xform -rz $orientation win_rad > scenes/rad/$win_file.rad`;
  `rm -f win_rad`;
  my $t=Time::HiRes::tv_interval($start_time);
  print "␣Write␣window␣file\t\t\t\t$t\n";


  # Write Control Sensors
  $control_sens="Workplanes/control-$orientation.pts";

  open (SENS, ">".$control_sens);

  # Control sensor of set 1 of luminaires
  @tmp_array=@control_sens1;
  while ($#tmp_array >= 0) {
    $x=@tmp_array[0];
    $y=@tmp_array[1];
```

```
212     $z=@tmp_array[2];
213
214     $a=$x*$width*cos($orientation*3.141592654/180)-$y*$length*sin(
            $orientation*3.141592654/180);
215     $b=$x*$width*sin($orientation*3.141592654/180)+$y*$length*cos(
            $orientation*3.141592654/180);
216
217     print SENS "$a␣$b␣$z␣0␣0␣1\n";
218     shift @tmp_array;
219     shift @tmp_array;
220     shift @tmp_array;
221   }
222
223   # Control sensor of set 2 of luminaires
224   @tmp_array=@control_sens2;
225   while ($#tmp_array >= 0) {
226     $x=@tmp_array[0];
227     $y=@tmp_array[1];
228     $z=@tmp_array[2];
229
230     $a=$x*$width*cos($orientation*3.141592654/180)-$y*$length*sin(
            $orientation*3.141592654/180);
231     $b=$x*$width*sin($orientation*3.141592654/180)+$y*$length*cos(
            $orientation*3.141592654/180);
232
233     print SENS "$a␣$b␣$z␣0␣0␣1\n";
234     shift @tmp_array;
235     shift @tmp_array;
236     shift @tmp_array;
237   }
238
239   # Vertical Eye Illuminance Sensor to window
240   @tmp_array=@control_sens3;
241   while ($#tmp_array >= 0) {
242     $x=@tmp_array[0];
243     $y=@tmp_array[1];
244     $z=@tmp_array[2];
245
246     $a=$x*$width*cos($orientation*3.141592654/180)-$y*$length*sin(
            $orientation*3.141592654/180);
247     $b=$x*$width*sin($orientation*3.141592654/180)+$y*$length*cos(
            $orientation*3.141592654/180);
248
249     if ($orientation == 0) {print SENS "$a␣$b␣$z␣0␣-1␣0\n";}
250     elsif ($orientation == 45) {print SENS "$a␣$b␣$z␣1␣-1␣0\n";}
251     elsif ($orientation == 90) {print SENS "$a␣$b␣$z␣1␣0␣0\n";}
252     elsif ($orientation == 135) {print SENS "$a␣$b␣$z␣1␣1␣0\n";}
253     elsif ($orientation == 180) {print SENS "$a␣$b␣$z␣0␣1␣0\n";}
254     elsif ($orientation == 225) {print SENS "$a␣$b␣$z␣-1␣1␣0\n";}
255     elsif ($orientation == 270) {print SENS "$a␣$b␣$z␣-1␣0␣0\n";}
256     elsif ($orientation == 315) {print SENS "$a␣$b␣$z␣-1␣-1␣0\n";}
```

```
257     shift @tmp_array;
258     shift @tmp_array;
259     shift @tmp_array;
260   }
261
262   # Vertical Eye Illuminance Sensor to lateral wall
263   @tmp_array=@control_sens3;
264   while ($#tmp_array >= 0) {
265     $x=@tmp_array[0];
266     $y=@tmp_array[1];
267     $z=@tmp_array[2];
268
269     $a=$x*$width*cos($orientation*3.141592654/180)-$y*$length*sin(
          $orientation*3.141592654/180);
270     $b=$x*$width*sin($orientation*3.141592654/180)+$y*$length*cos(
          $orientation*3.141592654/180);
271
272     if ($orientation == 0) {print SENS "$a␣$b␣$z␣1␣0␣0\n";}
273     elsif ($orientation == 45) {print SENS "$a␣$b␣$z␣1␣1␣0\n";}
274     elsif ($orientation == 90) {print SENS "$a␣$b␣$z␣0␣1␣0\n";}
275     elsif ($orientation == 135) {print SENS "$a␣$b␣$z␣-1␣1␣0\n";}
276     elsif ($orientation == 180) {print SENS "$a␣$b␣$z␣-1␣0␣0\n";}
277     elsif ($orientation == 225) {print SENS "$a␣$b␣$z␣-1␣-1␣0\n";}
278     elsif ($orientation == 270) {print SENS "$a␣$b␣$z␣0␣-1␣0\n";}
279     elsif ($orientation == 315) {print SENS "$a␣$b␣$z␣1␣-1␣0\n";}
280     shift @tmp_array;
281     shift @tmp_array;
282     shift @tmp_array;
283   }
284
285   # Vertical Eye Illuminance Sensor to back wall
286   @tmp_array=@control_sens3;
287   while ($#tmp_array >= 0) {
288     $x=@tmp_array[0];
289     $y=@tmp_array[1];
290     $z=@tmp_array[2];
291
292     $a=$x*$width*cos($orientation*3.141592654/180)-$y*$length*sin(
          $orientation*3.141592654/180);
293     $b=$x*$width*sin($orientation*3.141592654/180)+$y*$length*cos(
          $orientation*3.141592654/180);
294
295     if ($orientation == 0) {print SENS "$a␣$b␣$z␣0␣1␣0\n";}
296     elsif ($orientation == 45) {print SENS "$a␣$b␣$z␣-1␣1␣0\n";}
297     elsif ($orientation == 90) {print SENS "$a␣$b␣$z␣-1␣0␣0\n";}
298     elsif ($orientation == 135) {print SENS "$a␣$b␣$z␣-1␣-1␣0\n";}
299     elsif ($orientation == 180) {print SENS "$a␣$b␣$z␣0␣-1␣0\n";}
300     elsif ($orientation == 225) {print SENS "$a␣$b␣$z␣1␣-1␣0\n";}
301     elsif ($orientation == 270) {print SENS "$a␣$b␣$z␣1␣0␣0\n";}
302     elsif ($orientation == 315) {print SENS "$a␣$b␣$z␣1␣1␣0\n";}
303     shift @tmp_array;
```

```
304     shift @tmp_array;
305     shift @tmp_array;
306   }
307
308   close(SENS);
309
310   my $t=Time::HiRes::tv_interval($start_time);
311   print "␣Write␣control␣sensors␣\t\t\t$t\n";
312   print TXT "␣Write␣control␣sensors␣\t\t\t$t\n";
313
314   # Write Workplne Sensors
315   $sens_x=int($width/$sensor_spacing);
316   $sens_y=int($length/$sensor_spacing);
317
318   $rest_x=($width-($sens_x-1)*$sensor_spacing)/2;
319   $rest_y=($length-($sens_y-1)*$sensor_spacing)/2;
320
321
322   $wp="Workplanes/WP_$length-$width-$orientation.pts";
323   if (not -e $wp) {
324     open (SENS, ">>".$wp);
325
326     for ($i=$rest_x; $i<$width; $i+=$sensor_spacing){
327       for ($j=$rest_y; $j<$length; $j+=$sensor_spacing){
328         $a=$i*cos($orientation*3.141592654/180)-$j*sin($orientation
              *3.141592654/180);
329         $b=$i*sin($orientation*3.141592654/180)+$j*cos($orientation
              *3.141592654/180);
330         print SENS "$a␣$b␣$sensor_height␣0␣0␣1\n";
331       }
332     }
333
334     close SENS;
335   }
336   my $t=Time::HiRes::tv_interval($start_time);
337   print "␣Write␣Workplane␣sensors␣\t\t\t$t\n";
338   print TXT "␣Write␣Workplane␣sensors␣\t\t\t$t\n";
339
340   ############################
341   #### Luminaire Matrix #####
342   ############################
343
344   # Se asume que no hay otras fuentes de luz.
345
346   $lum_wp1="LMX/LUM_WP-$orientation-1.lmx";
347   `oconv scenes/rad/$scene_file1.rad scenes/rad/$win_file.rad > octree
        `;
348   `cat $wp | rtrace -n $cores -I -af af -ab 6 -ad 2048 -aa 0.2 octree >
        $lum_wp1`;
349   `rm octree af`;
350
```

```
351 my $t=Time::HiRes::tv_interval($start_time);
352 print "␣Luminarie␣1␣contribution␣to␣workplane␣\t$t\n";
353 print TXT "␣Luminarie␣1␣contribution␣to␣workplane␣\t$t\n";
354
355 $lum_wp2="LMX/LUM_WP-$orientation-2.lmx";
356 `oconv scenes/rad/$scene_file2.rad scenes/rad/$win_file.rad > octree
      `;
357 `cat $wp | rtrace -n $cores -I -af af -ab 6 -ad 2048 -aa 0.2 octree >
      $lum_wp2`;
358 `rm octree af`;
359
360 my $t=Time::HiRes::tv_interval($start_time);
361 print "␣Luminarie␣2␣contribution␣to␣workplane␣\t$t\n";
362 print TXT "␣Luminarie␣2␣contribution␣to␣workplane␣\t$t\n";
363
364 $lum_c1="LMX/LUM_Control-$orientation-1.lmx";
365 $control_sens="Workplanes/control-$orientation.pts";
366 `oconv scenes/rad/$scene_file1.rad scenes/rad/$win_file.rad > octree
      `;
367 `cat $control_sens | rtrace -n $cores -I -af af -ab 6 -ad 2048 -aa
      0.2 octree > $lum_c1`;
368 `rm octree af`;
369
370 my $t=Time::HiRes::tv_interval($start_time);
371 print "␣Luminarie␣1␣contribution␣to␣control␣sensors␣$t\n";
372 print TXT "␣Luminarie␣1␣contribution␣to␣control␣sensors␣$t\n";
373
374 $lum_c2="LMX/LUM_Control-$orientation-2.lmx";
375 $control_sens="Workplanes/control-$orientation.pts";
376 `oconv scenes/rad/$scene_file2.rad scenes/rad/$win_file.rad > octree
      `;
377 `cat $control_sens | rtrace -n $cores -I -af af -ab 6 -ad 2048 -aa
      0.2 octree > $lum_c2`;
378 `rm octree af`;
379
380 my $t=Time::HiRes::tv_interval($start_time);
381 print "␣Luminarie␣2␣contribution␣to␣control␣sensors␣$t\n";
382 print TXT "␣Luminarie␣2␣contribution␣to␣control␣sensors␣$t\n";
383
384 ##########################
385 #### Daylight Matrix #####
386 ##########################
387
388 $dmx_file="DMX/D_Scene-$orientation.dmx";
389 $or_x=sin($orientation*3.141592654/180);
390 $or_y=-cos($orientation*3.141592654/180);
391 $or_z=0;
392
```

```
393   `echo "#\@rfluxmtx␣h=u␣u=Y\nvoid␣glow␣ground_glow\n0\n0\n4␣1␣1␣1␣0\n\
         nground_glow␣source␣ground\n0\n0\n4␣0␣0␣-1␣180\n\n#\@rfluxmtx␣h=
         r$bins␣u=Y\n\nvoid␣glow␣skymat\n0\n0\n4␣1␣1␣1␣0\n\nskymat␣source␣
         sky\n0\n0\n4␣0␣0␣1␣␣180\n\n" > white_sky`;
394   `rfluxmtx scenes/rad/$win_file.rad white_sky > $dmx_file`;
395   `rm -f white_sky octree`;
396   my $t=Time::HiRes::tv_interval($start_time);
397   print "␣Calculate␣Daylight␣matrix␣\t\t$t\n";
398   print TXT "␣Calculate␣Daylight␣matrix␣\t\t$t\n";
399
400   ######################
401   #### View Matrix #####
402   ######################
403
404   $vmx_file_WP="VMX/WP_Scene-$orientation.vmx";
405   $or_x=-$or_x;
406   $or_y=-$or_y;
407
408   `echo "void␣glow␣winmat\n0\n0\n4␣1␣1␣1␣0\n\n␣void␣glass␣black_glass\
         n0\n0\n3␣0␣0␣0\n\n" > winfile`;
409   `xform -m winmat scenes/rad/$win_file.rad >> winfile`;
410   `rfluxmtx -I+ -n $cores -ab 9 -ad 16384 -lw 6.1e-5 <$wp - winfile
         scenes/rad/$scene_file1.rad > $vmx_file_WP`;
411   `rm -f winmat winfile octree af`;
412
413   my $t=Time::HiRes::tv_interval($start_time);
414   print "␣Calculate␣View␣matrix␣over␣workplane␣␣\t$t\n";
415   print TXT "␣Calculate␣View␣matrix␣over␣workplane␣␣\t$t\n";
416
417   $vmx_file_C="VMX/C_Scene-$orientation.vmx";
418   $control_sens="Workplanes/control-$orientation.pts";
419   `echo "void␣glow␣winmat\n0\n0\n4␣1␣1␣1␣0\n\n␣void␣glass␣black_glass\
         n0\n0\n3␣0␣0␣0\n\n" > winfile`;
420   `xform -m winmat scenes/rad/$win_file.rad >> winfile`;
421   `rfluxmtx -I+ -n $cores -ab 9 -ad 16384 -lw 6.1e-5 <$control_sens -
         winfile scenes/rad/$scene_file1.rad > $vmx_file_C`;
422   `rm -f winmat winfile octree af`;
423
424   my $t=Time::HiRes::tv_interval($start_time);
425   print "␣Calculate␣View␣matrix␣over␣control␣sensors␣␣$t\n";
426   print TXT "␣Calculate␣View␣matrix␣over␣control␣sensors␣␣$t\n";
427
428 }
429
430 close(TXT);
```

Lum.rad File

```
1 ## Lum.rad
```

```
2 void light bright
3 0
4 0
5 3 256.966647 244.312202 134.770912
6
7 bright sphere bulb
8 0
9 0
10 4 0 0 0 0.03
```

Script Perl: Simulation

```
1 #!/usr/local/bin/perl
2
3  use POSIX ();
4  use POSIX qw(setsid);
5  use POSIX qw(:errno_h :fcntl_h);
6
7 use Time::HiRes qw( usleep ualarm gettimeofday tv_interval nanosleep
8                      clock_gettime clock_getres clock_nanosleep clock
9                      stat  );
10
11 my $start_time=[Time::HiRes::gettimeofday()];
12 $time="time_simulation";
13 open (TXT, ">␣$time.txt");
14
15
16 ############ Simulation Parameters
17
18 # Office dimensions
19 $width=4; #X axis
20 $length=6.5; #Y axis
21 $height=2.8; #Z axis
22 $volume=$heigth*$width*$length;
23 $floor_area=$length*$width;
24
25 # Window dimensions
26 $ledge=0.1; #Ledge, or Sprandel in Curtain Walls
27 $wall_offset=0.1; #the window will be ($width-2*$wall_offset) wide
28 $ceiling_offset=0.1; #same deal, but with the ceiling. The window will
       be $height-$ledge-$ceiling_offset high
29 $z7=$height-$ceiling_offset;
30 $x8=$width-$wall_offset;
31 $z8=$z7;
32 $x9=$x8;
33 $window_area=($width-2*$wall_offset)*($height-$ceiling_offset-$ledge);
34 $wwr=$window_area/($height*$width);
35
36 # Sensors distribution
```

```
$sensor_spacing=0.5;
$sensor_height=0.8;
$sens_x=int($width/$sensor_spacing);
$sens_y=int($length/$sensor_spacing);

# Orientation
# can be between 0 and 360 with step of 45.
@orientations=(0,180); # 0 positions the window facing South, 90 facing East.
# 0   Window in facing South
# 45  Window in facing South-East
# 90  Window in facing East
# 135 Window in facing North-East
# 180 Window in facing North
# 225 Window in facing North-West
# 270 Window in facing West
# 315 Window in facing South-West

# Processing information
$cores=8; #for multicore processing (rcontrib, rtrace and rfluxmtx runs)
$bins=4; #number of bins of Reinhart's sky subdivition.

# Weather file
@epw_files=("CAN_PQ_Montreal.Intl.AP.716270_CWEC","CHL_Santiago.855740_IWEC"); #City
#"CHL_Santiago.855740_IWEC"

$n_positions=4; #number of positions of the shading system

# Reflectancia de los muros, piso y cielo
$rho_wall=0.5;
$rho_ceiling=0.7;
$rho_floor=0.2;

# Material: Hormigón
$terminacion_hormigon="Smooth";
$espesor_hormigon=0.15;
$conductividad_hormigon=1.66;
$densidad_hormigon=2500;
$calor_especifico_hormigon=750;

# Material Aislante: EPS
$terminacion_aislante="Smooth";
$resistividad_aislante=2;

# Luminaires
$luminaire_power=30; #power of each luminaire (W)
$luminaire_spacing=1.2;
$lum_ceiling_offset=0.2; # Ceiling offset of luminaire
$luminaire_file="lum.rad"; # Luminaire. Assuming .rad file
```

```
85
86 # Array of luminaires
87 $lum_x=int($width/$luminaire_spacing); #this will create an array of
       luminaires. lum_x in the X axis and lum_y in the Y axis
88 $lum_y=int(0.5*$length/$luminaire_spacing);
89 $n_luminaires=$lum_x*$lum_y;
90 $lighting_power=$n_luminaires*$luminaire_power;
91 $light_over_area=$lighting_power/$floor_area;
92
93 $rest_x=($width-($lum_x-1)*$luminaire_spacing)/2;
94 $rest_y=(0.5*$length-($lum_y-1)*$luminaire_spacing)/2;
95 $luminaire_height=$height-$lum_ceiling_offset;
96
97 # Number of people in the office
98 $area_per_person=12; #12 m2 per person
99 $People_gains=6.7; #W/m2
100
101 #Equipment Gains
102 $Equipment_gains=15; #W/m2
103
104 #Infiltration Changes
105 $infiltration_changes=0.7; #air changes per hour
106
107 # Comfort temperature
108 $T_min=20; #thermostat setpoints.
109 $T_max=24;
110
111 #Control Files
112 @controls=(1,2,3,4);
113
114 #### Simulation
115
116 $scene_file="Scene";
117 $x=$sens_y*$sens_x;
118
119 foreach $epw_file (@epw_files){
120   foreach $control (@controls){
121     foreach $orientation (@orientations){
122
123       ###################################
124       #### mkSchedule & uSchedule #####
125       ###################################
126
127       $weather="EPW/$epw_file.epw";
128       $n_epw=8760;
129
130       $schedule="Schedules/schedule-$epw_file-$orientation-$control.txt
              ";
131       $control_script="Scripts/script$control.lua";
132       $lum_c1="LMX/LUM_Control-$orientation-1.lmx";
133       $lum_c2="LMX/LUM_Control-$orientation-2.lmx";
```

```
134         $lum_wp1="LMX/LUM_WP-$orientation-1.lmx";
135         $lum_wp2="LMX/LUM_WP-$orientation-2.lmx";
136         $vmx_file_C="VMX/C_$scene_file-$orientation.vmx";
137         $vmx_file_WP="VMX/WP_$scene_file-$orientation.vmx";
138         $dmx_file="DMX/D_$scene_file-$orientation.dmx";
139         `cat $lum_c1 > LMX-control-1.lmx`;
140         `cat $lum_c2 > LMX-control-2.lmx`;
141         `cat $lum_wp1 > LMX-workplane-1.lmx`;
142         `cat $lum_wp2 > LMX-workplane-2.lmx`;
143         `cat $vmx_file_C > WindowSet_1-control.vmx`;
144         `cat $vmx_file_WP > WindowSet_1-WP.vmx`;
145         `cat $dmx_file > WindowSet_1.dmx`;
146         `~/Escritorio/05-Optimizacin/mkSchedule -o AAA -f $weather -m
               $bins -w 1 -x 5 -l 2 -L LMX-control-%d.lmx -V WindowSet_%d-
               control.vmx -D WindowSet_%d.dmx -T $n_positions BSDF/CFS%d.xml
                -u $control_script > $schedule`;
147         my $t=Time::HiRes::tv_interval($start_time);
148         print "\trun mkSchedule $epw_file-$orientation-$control    $t\n";
149         print TXT "\trun mkSchedule $epw_file-$orientation-$control $t\n"
               ;
150
151         $light_file="Results/Lighting/results-$epw_file-$orientation-
               $control.txt";
152         `~/Escritorio/05-Optimizacin/uSchedule -n $n_epw -u $schedule -
               V WindowSet_%d-WP.vmx -L LMX-workplane-%d.lmx -x $x -m $bins >
                $light_file`;
153         my $t=Time::HiRes::tv_interval($start_time);
154         print "\trun uSchedule $epw_file-$orientation-$control     $t\n";
155         print TXT "\trun uSchedule $epw_file-$orientation-$control  $t\n"
               ;
156
157         `rm LMX-control-1.lmx LMX-control-2.lmx LMX-workplane-1.lmx LMX-
               workplane-2.lmx WindowSet_1-control.vmx WindowSet_1-WP.vmx
               WindowSet_1.dmx`;
158
159         ############################
160         #### EPlus Simulation #####
161         ############################
162
163         $ePlus_file="EPlus_input-$epw_file-$orientation-$control";
164
165         open (IDF, "> $ePlus_file.idf");
166
```

```
      print IDF "!length:␣$length\n!width:␣$width\n!height:␣$height\n!
          ledge:␣$ledge\n!Margen␣muro:␣$wall_offset\n!Margen␣techo:␣
          $ceiling_offset\n!Ref.␣piso:␣$rho_floor\n!Ref.␣techo:␣
          $rho_ceiling\n!Ref.␣muros:␣$rho_wall\n!Orientacion:␣
          $orientation\n!Terminacion␣hormigon:␣$terminacion_hormigon\n!
          Terminacion␣aislante:␣$terminacion_aislante-$espesor_hormigon\
          n!Conductividad␣hormigon:␣$conductividad_hormigon\n!Densidad␣
          hormigon:␣$densidad_hormigon\n!Calor␣especifico␣hormigon:␣
          $calor_especifico_hormigon\n!Conductividad␣aislante:␣
          $resistividad_aislante\n\n\n";

print IDF "
!-␣␣␣==========␣␣ALL␣OBJECTS␣IN␣CLASS:␣BUILDING␣==========

Building,
␣␣␣␣Case,␣␣␣␣␣␣␣␣␣␣␣␣␣␣␣␣␣␣␣!-␣Name
␣␣␣␣$orientation,␣␣␣␣␣␣␣␣␣!-␣North␣Axis␣{deg}
␣␣␣␣City,␣␣␣␣␣␣␣␣␣␣␣␣␣␣␣␣␣!-␣Terrain
␣␣␣␣,␣␣␣␣␣␣␣␣␣␣␣␣␣␣␣␣␣␣␣␣!-␣Loads␣Convergence␣Tolerance␣Value
␣␣␣␣,␣␣␣␣␣␣␣␣␣␣␣␣␣␣␣␣␣␣␣␣!-␣Temperature␣Convergence␣Tolerance␣
    Value␣{deltaC}
␣␣␣␣FullInteriorAndExteriorWithReflections,␣␣!-␣Solar␣Distribution
␣␣␣␣25,␣␣␣␣␣␣␣␣␣␣␣␣␣␣␣␣␣␣!-␣Maximum␣Number␣of␣Warmup␣Days
␣␣␣␣6;␣␣␣␣␣␣␣␣␣␣␣␣␣␣␣␣␣␣␣!-␣Minimum␣Number␣of␣Warmup␣Days


!-␣␣␣==========␣␣ALL␣OBJECTS␣IN␣CLASS:␣SCHEDULE:FILE␣==========

ScheduleTypeLimits,
␣␣␣␣Int,␣␣␣␣␣␣!-␣Name
␣␣␣␣0.0,␣␣␣␣␣␣!-␣Lower␣Limit
␣␣␣␣$n_positions,␣␣␣!-␣Upper␣limit
␣␣␣␣discrete,␣␣␣␣␣!-␣Numeric␣Type
␣␣␣␣Dimensionless;

Schedule:File,
␣␣␣␣Win1,␣␣␣␣␣␣␣␣␣␣␣␣␣␣␣␣␣!-␣Name
␣␣␣␣Int,␣␣␣␣␣␣␣␣␣␣␣␣␣␣␣␣␣!-␣Schedule␣Type␣Limits␣Name
␣␣␣␣$schedule,␣␣␣␣␣␣␣␣␣␣␣!-␣File␣Name
␣␣␣␣11,␣␣␣␣␣␣␣␣␣␣␣␣␣␣␣␣␣!-␣Column␣Number
␣␣␣␣11,␣␣␣␣␣␣␣␣␣␣␣␣␣␣␣␣␣!-␣Rows␣to␣Skip␣at␣Top
␣␣␣␣8760,␣␣␣␣␣␣␣␣␣␣␣␣␣␣␣!-␣Number␣of␣Hours␣of␣Data
␣␣␣␣Comma,␣␣␣␣␣␣␣␣␣␣␣␣␣␣!-␣Column␣Separator
␣␣␣␣No;␣␣␣␣␣␣␣␣␣␣␣␣␣␣␣␣␣!-␣Interpolate␣to␣Timestep

Schedule:File,
␣␣␣␣Lum1,␣␣␣␣␣␣␣␣␣␣␣␣␣␣␣␣!-␣Name
␣␣␣␣Fraction,␣␣␣␣␣␣␣␣␣␣␣␣␣!-␣Schedule␣Type␣Limits␣Name
␣␣␣␣$schedule,␣␣␣␣␣␣␣␣␣␣␣!-␣File␣Name
␣␣␣␣12,␣␣␣␣␣␣␣␣␣␣␣␣␣␣␣␣␣!-␣Column␣Number
␣␣␣␣11,␣␣␣␣␣␣␣␣␣␣␣␣␣␣␣␣␣!-␣Rows␣to␣Skip␣at␣Top
```

```
    8760,                    !- Number of Hours of Data
    Comma,                   !- Column Separator
    Yes;

Schedule:File,
    Lum2,                    !- Name
    Fraction,                !- Schedule Type Limits Name
    $schedule,               !- File Name
    13,                      !- Column Number
    11,                      !- Rows to Skip at Top
    8760,                    !- Number of Hours of Data
    Comma,                   !- Column Separator
    Yes;

!-   ===========  ALL OBJECTS IN CLASS: MATERIAL ===========

Material,
    Hormigon,                !- Name
    $terminacion_hormigon,   !- Roughness
    $espesor_hormigon,       !- Thickness {m}
    $conductividad_hormigon, !- Conductivity {W/m-K}
    $densidad_hormigon,      !- Density {kg/m3}
    $calor_especifico_hormigon, !- Specific Heat {J/kg-K}
    0.9,                     !- Thermal Absorptance
    0.6,                     !- Solar Absorptance
    0.6;                     !- Visible Absorptance

Material:NoMass,
    Aislante,                !- Name
    $terminacion_aislante,   !- Roughness
    $resistividad_aislante,  !- R (m2K/W)
    0.9,
    0.7,
    0.7;

!-   ===========  ALL OBJECTS IN CLASS: BUILDINGSURFACE:DETAILED
     ===========

BuildingSurface:Detailed,
    South,                   !- Name
    Wall,                    !- Surface Type
    Construction,            !- Construction Name
    Room,                    !- Zone Name
    Outdoors,                !- Outside Boundary Condition
    ,                        !- Outside Boundary Condition Object
    SunExposed,              !- Sun Exposure
    WindExposed,             !- Wind Exposure
    0.5,                     !- View Factor to Ground
    4,                       !- Number of Vertices
    0,0,0,
    $width,0,0,
```

```
    $width,0,$height,
    0,0,$height;

BuildingSurface:Detailed,
    East,                    !- Name
    Wall,                    !- Surface Type
    Construction,            !- Construction Name
    Room,                    !- Zone Name
    Adiabatic,               !- Outside Boundary Condition
    ,                        !- Outside Boundary Condition Object
    NoSun,                   !- Sun Exposure
    NoWind,                  !- Wind Exposure
    0.5,                     !- View Factor to Ground
    4,                       !- Number of Vertices
    $width,0,0,
    $width,$length,0,
    $width,$length,$height,
    $width,0,$height;

BuildingSurface:Detailed,
    West,                    !- Name
    Wall,                    !- Surface Type
    Construction,            !- Construction Name
    Room,                    !- Zone Name
    Adiabatic,               !- Outside Boundary Condition
    ,                        !- Outside Boundary Condition Object
    NoSun,                   !- Sun Exposure
    NoWind,                  !- Wind Exposure
    0.5,                     !- View Factor to Ground
    4,                       !- Number of Vertices
    0,$length,0,
    0,0,0,
    0,0,$height,
    0,$length,$height;

BuildingSurface:Detailed,
    North,                   !- Name
    Wall,                    !- Surface Type
    Construction,            !- Construction Name
    Room,                    !- Zone Name
    Adiabatic,               !- Outside Boundary Condition
    ,                        !- Outside Boundary Condition Object
    NoSun,                   !- Sun Exposure
    NoWind,                  !- Wind Exposure
    0.5,                     !- View Factor to Ground
    4,                       !- Number of Vertices
    $width,$length,0,
    0,$length,0,
    0,$length,$height,
    $width,$length,$height;

```

```
BuildingSurface:Detailed,
    Floor,                    !- Name
    Floor,                    !- Surface Type
    Construction,             !- Construction Name
    Room,                     !- Zone Name
    Adiabatic,                !- Outside Boundary Condition
    ,                         !- Outside Boundary Condition Object
    NoSun,                    !- Sun Exposure
    NoWind,                   !- Wind Exposure
    0,                        !- View Factor to Ground
    4,                        !- Number of Vertices
    0,0,0,
    0,$length,0,
    $width,$length,0,
    $width,0,0;

BuildingSurface:Detailed,
    Roof,                     !- Name
    Roof,                     !- Surface Type
    Construction,             !- Construction Name
    Room,                     !- Zone Name
    Adiabatic,                !- Outside Boundary Condition
    ,                         !- Outside Boundary Condition Object
    NoSun,                    !- Sun Exposure
    NoWind,                   !- Wind Exposure
    0,                        !- View Factor to Ground
    4,                        !- Number of Vertices
    0,0,$height,
    $width,0,$height,
    $width,$length,$height,
    0,$length,$height;

!- ===========  ALL OBJECTS IN CLASS: FENESTRATIONSURFACE:DETAILED
   ===========

FenestrationSurface:Detailed,
    South-win,      !-Name
    WINDOW,         !- Type
    CFS_Glz_104,    !- Construction Name
    South,          !- Building Surface Name
    ,               !- Outside Boundary Condition
    0.5,            !- View Factor to Ground
    ,               !- Shading Control Name
    ,               !- Frame Divider Name
    1,              !- Multiplier
    4,              !- Number of Vertices
    $wall_offset, 0, $ledge,
    $x8, 0, $ledge,
    $x8, 0, $z7,
    $wall_offset, 0, $z7;

```

```
359
360 !-␣␣␣==========␣␣ALL␣OBJECTS␣IN␣CLASS:␣LIGHTS␣==========
361
362 Lights,
363 ␣␣␣␣Lum1,␣␣␣␣␣␣␣␣␣␣␣␣␣␣␣␣␣␣␣␣␣!-␣Name
364 ␣␣␣␣Room,␣␣␣␣␣␣␣␣␣␣␣␣␣␣␣␣␣␣␣␣␣!-␣Zone␣or␣ZoneList␣Name
365 ␣␣␣␣Lum1,␣␣␣␣␣␣␣␣␣␣␣␣␣␣␣␣␣␣␣␣␣!-␣Schedule␣Name
366 ␣␣␣␣LightingLevel,␣␣␣␣␣␣␣␣␣␣␣!-␣Design␣Level␣Calculation␣Method
367 ␣␣␣␣$lighting_power,␣␣␣␣␣␣␣␣␣!-␣Lighting␣Level␣{W}
368 ␣␣␣␣,␣␣␣␣␣␣␣␣␣␣␣␣␣␣␣␣␣␣␣␣␣␣␣!-␣Watts␣per␣Zone␣Floor␣Area␣{W/m2}
369 ␣␣␣␣,␣␣␣␣␣␣␣␣␣␣␣␣␣␣␣␣␣␣␣␣␣␣␣!-␣Watts␣per␣Person␣{W/person}
370 ␣␣␣␣0,␣␣␣␣␣␣␣␣␣␣␣␣␣␣␣␣␣␣␣␣␣␣!-␣Return␣Air␣Fraction
371 ␣␣␣␣0.3,␣␣␣␣␣␣␣␣␣␣␣␣␣␣␣␣␣␣␣␣␣!-␣Fraction␣Radiant
372 ␣␣␣␣0.7,␣␣␣␣␣␣␣␣␣␣␣␣␣␣␣␣␣␣␣␣␣!-␣Fraction␣Visible
373 ␣␣␣␣0,␣␣␣␣␣␣␣␣␣␣␣␣␣␣␣␣␣␣␣␣␣␣!-␣Fraction␣Replaceable
374 ␣␣␣␣General,␣␣␣␣␣␣␣␣␣␣␣␣␣␣␣␣␣!-␣End-Use␣Subcategory
375 ␣␣␣␣No;␣␣␣␣␣␣␣␣␣␣␣␣␣␣␣␣␣␣␣␣␣!-␣Return␣Air␣Fraction␣Calculated␣from␣
       Plenum␣Temperature
376
377 Lights,
378 ␣␣␣␣Lum2,␣␣␣␣␣␣␣␣␣␣␣␣␣␣␣␣␣␣␣␣␣!-␣Name
379 ␣␣␣␣Room,␣␣␣␣␣␣␣␣␣␣␣␣␣␣␣␣␣␣␣␣␣!-␣Zone␣or␣ZoneList␣Name
380 ␣␣␣␣Lum2,␣␣␣␣␣␣␣␣␣␣␣␣␣␣␣␣␣␣␣␣␣!-␣Schedule␣Name
381 ␣␣␣␣LightingLevel,␣␣␣␣␣␣␣␣␣␣␣!-␣Design␣Level␣Calculation␣Method
382 ␣␣␣␣$lighting_power,␣␣␣␣␣␣␣␣␣!-␣Lighting␣Level␣{W}
383 ␣␣␣␣,␣␣␣␣␣␣␣␣␣␣␣␣␣␣␣␣␣␣␣␣␣␣␣!-␣Watts␣per␣Zone␣Floor␣Area␣{W/m2}
384 ␣␣␣␣,␣␣␣␣␣␣␣␣␣␣␣␣␣␣␣␣␣␣␣␣␣␣␣!-␣Watts␣per␣Person␣{W/person}
385 ␣␣␣␣0,␣␣␣␣␣␣␣␣␣␣␣␣␣␣␣␣␣␣␣␣␣␣!-␣Return␣Air␣Fraction
386 ␣␣␣␣0.3,␣␣␣␣␣␣␣␣␣␣␣␣␣␣␣␣␣␣␣␣␣!-␣Fraction␣Radiant
387 ␣␣␣␣0.7,␣␣␣␣␣␣␣␣␣␣␣␣␣␣␣␣␣␣␣␣␣!-␣Fraction␣Visible
388 ␣␣␣␣0,␣␣␣␣␣␣␣␣␣␣␣␣␣␣␣␣␣␣␣␣␣␣!-␣Fraction␣Replaceable
389 ␣␣␣␣General,␣␣␣␣␣␣␣␣␣␣␣␣␣␣␣␣␣!-␣End-Use␣Subcategory
390 ␣␣␣␣No;␣␣␣␣␣␣␣␣␣␣␣␣␣␣␣␣␣␣␣␣␣!-␣Return␣Air␣Fraction␣Calculated␣from␣
       Plenum␣Temperature
391
392 !-␣␣␣==========␣␣ALL␣OBJECTS␣IN␣CLASS:␣ZONE␣==========
393
394 Zone,
395 ␣␣␣␣Room,␣␣␣␣␣␣␣␣␣␣␣␣␣␣␣␣␣␣␣␣␣!-␣Name
396 ␣␣␣␣0,␣␣␣␣␣␣␣␣␣␣␣␣␣␣␣␣␣␣␣␣␣␣!-␣Direction␣of␣Relative␣North␣{deg}
397 ␣␣␣␣0,␣␣␣␣␣␣␣␣␣␣␣␣␣␣␣␣␣␣␣␣␣␣!-␣X␣Origin␣{m}
398 ␣␣␣␣0,␣␣␣␣␣␣␣␣␣␣␣␣␣␣␣␣␣␣␣␣␣␣!-␣Y␣Origin␣{m}
399 ␣␣␣␣0,␣␣␣␣␣␣␣␣␣␣␣␣␣␣␣␣␣␣␣␣␣␣!-␣Z␣Origin␣{m}
400 ␣␣␣␣1,␣␣␣␣␣␣␣␣␣␣␣␣␣␣␣␣␣␣␣␣␣␣!-␣Type
401 ␣␣␣␣1,␣␣␣␣␣␣␣␣␣␣␣␣␣␣␣␣␣␣␣␣␣␣!-␣Multiplier
402 ␣␣␣␣$height,␣␣␣␣␣␣␣␣␣␣␣␣␣␣␣␣␣!-␣Ceiling␣Height␣{m}
403 ␣␣␣␣$volume,␣␣␣␣␣␣␣␣␣␣␣␣␣␣␣␣␣!-␣Volume␣{m3}
404 ␣␣␣␣$floor_area,␣␣␣␣␣␣␣␣␣␣␣!-␣Floor␣Area␣{m2}
405 ␣␣␣␣,␣␣␣␣␣␣␣␣␣␣␣␣␣␣␣␣␣␣␣␣␣␣␣!-␣Zone␣Inside␣Convection␣Algorithm
406 ␣␣␣␣,␣␣␣␣␣␣␣␣␣␣␣␣␣␣␣␣␣␣␣␣␣␣␣!-␣Zone␣Outside␣Convection␣Algorithm
407 ␣␣␣␣Yes;␣␣␣␣␣␣␣␣␣␣␣␣␣␣␣␣␣␣␣␣!-␣Part␣of␣Total␣Floor␣Area
```

```
 !-   ========== ALL OBJECTS IN CLASS: SCHEDULE:COMPACT ==========

  Schedule:Compact,
    ALWAYS 4,                !- Name
    Any Number,              !- Schedule Type Limits Name
    Through: 12/31,          !- Field 1
    For: AllDays,            !- Field 2
    Until: 24:00,4;          !- Field 3

  Schedule:Compact,
    ALWAYS ON,               !- Name
    Any Number,              !- Schedule Type Limits Name
    Through: 12/31,          !- Field 1
    For: AllDays,            !- Field 2
    Until: 24:00,1;          !- Field 3

  Schedule:Compact,
    ALWAYS OFF,              !- Name
    Any Number,              !- Schedule Type Limits Name
    Through: 12/31,          !- Field 1
    For: AllDays,            !- Field 2
    Until: 24:00,0;          !- Field 3

  Schedule:Compact,
    ALWAYS $T_min,           !- Name
    Any Number,              !- Schedule Type Limits Name
    Through: 12/31,          !- Field 1
    For: AllDays,            !- Field 2
    Until: 24:00,$T_min;     !- Field 3

  Schedule:Compact,
    ALWAYS $T_max,           !- Name
    Any Number,              !- Schedule Type Limits Name
    Through: 12/31,          !- Field 1
    For: AllDays,            !- Field 2
    Until: 24:00,$T_max;     !- Field 3

Schedule:Compact,
    Office Occupancy,        !- Name
    Fraction,                !- Schedule Type Limits Name
    Through: 12/31,          !- Field 1
    For: Weekdays ,          !- Field 2
    Until: 07:00,0.0,        !- Field 3
    Until: 20:00,1.0,        !- Field 4
    Until: 24:00,0.0,        !- Field 5
    For: Saturday ,          !- Field 6
    Until: 08:00,0.0,        !- Field 7
    Until: 12:00,0.0,        !- Field 8
    Until: 24:00,0.0,        !- Field 9
```

```
␣␣␣␣For:␣Sunday␣Holidays␣AllOtherDays,␣!-␣Field␣10
␣␣␣␣Until:␣24:00,0.0;␣␣␣␣␣␣␣␣!-␣Field␣11

␣Schedule:Compact,
␣␣␣␣Activity␣Lvl,␣␣␣␣␣␣␣␣!-␣Name
␣␣␣␣Any␣Number,␣␣␣␣␣␣␣␣␣␣␣␣!-␣Schedule␣Type␣Limits␣Name
␣␣␣␣Through:12/31,␣␣␣␣␣␣␣␣␣␣!-␣Field␣1
␣␣␣␣For:␣AllDays,␣␣␣␣␣␣␣␣␣␣!-␣Field␣2
␣␣␣␣Until:␣24:00,110.7;␣␣␣␣␣␣!-␣Field␣3

␣Schedule:Compact,
␣␣␣␣Office␣OpenOff␣Equip,␣!-␣Name
␣␣␣␣Fraction,␣␣␣␣␣!-␣Schedule␣Type␣Limits␣Name
␣␣␣␣Through:␣12/31,␣␣␣!-␣Field␣1
␣␣␣␣For:␣Weekdays,␣␣␣␣!-␣Field␣2
␣␣␣␣Until:␣07:00,␣0.05,␣␣␣!-␣Field␣3
␣␣␣␣Until:␣20:00,␣1,␣␣␣␣!-␣Field␣4
␣␣␣␣Until:␣24:00,␣0.05,␣␣␣!-␣Field␣5
␣␣␣␣For:␣Weekends␣Holidays,␣␣␣!-␣Field␣6
␣␣␣␣Until:␣24:00,␣0.05,␣␣␣!-␣Field␣7
␣␣␣␣For:␣AllOtherDays,␣␣␣␣!-␣Field␣8
␣␣␣␣Until:␣24:00,␣0;␣␣␣␣!-␣Field␣9

!-␣␣␣==========␣␣ALL␣OBJECTS␣IN␣CLASS:␣DUAL␣SETPOINT␣WITH␣DEADBAND␣
    ==========

ThermostatSetpoint:DualSetpoint,
␣␣␣␣Office␣Thermostat␣Dual␣SP␣Control,␣␣!-␣Name
␣␣␣␣ALWAYS␣$T_min,␣␣␣␣␣␣␣␣␣␣␣␣!-␣Heating␣Setpoint␣Temperature␣
    Schedule␣Name
␣␣␣␣ALWAYS␣$T_max;␣␣␣␣␣␣␣␣␣␣␣␣!-␣Cooling␣Setpoint␣Temperature␣
    Schedule␣Name

!-␣␣␣==========␣␣ALL␣OBJECTS␣IN␣CLASS:␣PEOPLE␣==========

People,
␣␣␣␣Occupants,␣␣␣␣␣␣!-␣Name
␣␣␣␣Room,␣␣␣␣␣␣␣!-␣Zone␣or␣ZoneList␣Name
␣␣␣␣Office␣Occupancy,␣␣␣␣␣␣␣␣!-␣Number␣of␣People␣Schedule␣Name
␣␣␣␣area/person,␣␣␣␣␣␣␣␣␣␣␣␣!-␣Number␣of␣People␣Calculation␣Method
␣␣␣␣,␣␣␣␣␣␣␣␣␣␣␣␣␣␣␣␣␣!-␣Number␣of␣People
␣␣␣␣,␣␣␣␣␣␣␣␣␣␣␣␣␣␣␣␣␣␣␣␣␣!-␣People␣per␣Zone␣Floor␣Area␣{person/m2}
␣␣␣␣$area_per_person,␣␣␣␣␣␣␣␣␣!-␣Zone␣Floor␣Area␣per␣Person␣{m2/
    person}
␣␣␣␣0.3000000,␣␣␣␣␣␣␣␣␣␣␣␣␣!-␣Fraction␣Radiant
␣␣␣␣,␣␣␣␣␣␣␣␣␣␣␣␣␣␣␣␣␣␣␣␣␣!-␣Sensible␣Heat␣Fraction
␣␣␣␣Activity␣Lvl;␣␣␣␣␣␣␣␣!-␣Activity␣Level␣Schedule␣Name

!-␣␣␣==========␣␣ALL␣OBJECTS␣IN␣CLASS:␣ELECTRIC␣EQUIPMENT␣==========

ElectricEquipment,
```

```
␣␣␣␣Room␣Equipment,␣␣␣␣␣!-␣Name
␣␣␣␣Room,␣␣␣␣␣␣␣␣␣␣␣␣␣␣␣!-␣Zone␣Name
␣␣␣␣Office␣OpenOff␣Equip,␣␣␣␣␣␣␣!-␣Equipment␣SCHEDULE␣Name
␣␣␣␣Watts/Area,␣␣␣␣␣␣␣␣␣␣!-␣Design␣Level␣calculation␣method
␣␣␣␣,␣␣␣␣␣␣␣␣␣␣␣␣␣␣␣␣␣␣␣␣␣!-␣Design␣Equipment␣Level␣(W)
␣␣␣␣$Equipment_gains,␣␣␣␣␣␣␣␣␣!-␣Watts␣per␣Zone␣Area␣{watts/m2}
␣␣␣␣,␣␣␣␣␣␣␣␣␣␣␣␣␣␣␣␣␣␣␣␣␣!-␣Watts␣per␣Person␣{watts/person}
␣␣␣␣0,␣␣␣␣␣␣␣␣␣␣␣␣␣␣␣␣␣␣␣␣!-␣Latent␣fraction
␣␣␣␣.2,␣␣␣␣␣␣␣␣␣␣␣␣␣␣␣␣␣␣␣␣!-␣Radiant␣fraction
␣␣␣␣0,␣␣␣␣␣␣␣␣␣␣␣␣␣␣␣␣␣␣␣␣!-␣Fraction␣Lost
␣␣␣␣Computers;␣␣␣␣␣␣␣␣␣␣␣!-␣End-use␣category

!-␣␣␣==========␣␣ALL␣OBJECTS␣IN␣CLASS:␣ZONE␣INFILTRATION␣==========

ZoneInfiltration:DesignFlowRate,
␣␣␣Room␣Infiltration,␣␣!-␣Name
␣␣␣Room,␣␣␣␣␣␣␣␣␣␣␣␣␣␣␣␣␣␣␣!-␣Zone␣Name
␣␣␣ALWAYS␣ON,␣␣␣␣␣␣␣␣␣␣␣␣␣␣␣␣␣␣␣␣␣␣␣␣␣␣␣␣␣␣␣␣␣␣␣␣␣␣␣␣␣␣␣␣␣␣␣!-␣Infiltration␣
    SCHEDULE␣Name
␣␣␣AirChanges/Hour,␣␣␣␣␣␣␣␣␣␣␣␣␣␣␣␣␣␣␣␣␣␣␣␣␣␣␣␣␣!-␣Design␣Volume␣
    Flow␣Rate␣calculation␣method
␣␣␣,␣␣␣␣␣␣␣␣␣␣␣␣␣␣␣␣␣␣␣␣␣␣␣␣␣␣␣␣␣␣␣␣␣␣␣␣␣␣␣␣␣!-␣Design␣Volume␣Flow␣Rate␣(m3/
    s)
␣␣␣,␣␣␣␣␣␣␣␣␣␣␣␣␣␣␣␣␣␣␣␣␣␣␣␣␣␣␣␣␣␣␣␣␣␣␣␣␣␣␣␣␣␣␣␣␣␣␣␣␣␣␣␣␣␣␣!-␣Flow␣per␣Zone␣Floor␣
    Area␣{m3/s/m2}
␣␣␣,␣␣␣␣␣␣␣␣␣␣␣␣␣␣␣␣␣␣␣␣␣␣␣␣␣␣␣␣␣␣␣␣␣␣␣␣␣␣␣␣␣␣␣␣␣␣␣␣␣␣␣␣␣␣␣!-␣Flow␣per␣Exterior␣
    Surface␣Area␣{m3/s/m2}
␣␣␣$infiltration_changes,␣␣␣␣␣␣␣␣␣␣␣␣␣␣␣␣␣␣␣␣␣␣␣␣␣␣␣␣␣␣␣␣␣␣␣␣␣␣␣␣␣␣␣␣␣␣␣␣␣␣␣␣␣␣␣␣␣␣␣!-␣
    Air␣Changes␣Per␣Hour
␣␣␣1,␣␣␣␣␣␣␣␣␣␣␣␣␣␣␣␣␣␣␣␣␣␣␣␣␣␣␣␣␣␣␣␣␣␣␣␣␣␣␣␣␣␣␣␣␣␣␣␣␣␣␣␣␣␣␣!-␣Constant␣Term␣
    Coefficient
␣␣␣0,␣␣␣␣␣␣␣␣␣␣␣␣␣␣␣␣␣␣␣␣␣␣␣␣␣␣␣␣␣␣␣␣␣␣␣␣␣␣␣␣␣␣␣␣␣␣␣␣␣␣␣␣␣␣␣!-␣Temperature␣Term␣
    Coefficient
␣␣␣0,␣␣␣␣␣␣␣␣␣␣␣␣␣␣␣␣␣␣␣␣␣␣␣␣␣␣␣␣␣␣␣␣␣␣␣␣␣␣␣␣␣␣␣␣␣␣␣␣␣␣␣␣␣␣␣!-␣Velocity␣Term␣
    Coefficient
␣␣␣0;␣␣␣␣␣␣␣␣␣␣␣␣␣␣␣␣␣␣␣␣␣␣␣␣␣␣␣␣␣␣␣␣␣␣␣␣␣␣␣␣␣␣␣␣␣␣␣␣␣␣␣␣␣␣␣!-␣Velocity␣Squared␣Term
    ␣Coefficient

!-Generator␣IDFEditor␣1.44
!-Option␣SortedOrder

!-NOTE:␣All␣comments␣with␣'!-'␣are␣ignored␣by␣the␣IDFEditor␣and␣are␣
    generated␣automatically.
!-␣␣␣␣␣Use␣'!'␣comments␣if␣they␣need␣to␣be␣retained␣when␣using␣the␣
    IDFEditor.


!-␣␣␣==========␣␣ALL␣OBJECTS␣IN␣CLASS:␣VERSION␣==========

Version,
␣␣␣␣8.2;␣␣␣␣␣␣␣␣␣␣␣␣␣␣␣␣␣!-␣Version␣Identifier
```

```
545
546
547 !-␣␣␣==========␣␣ALL␣OBJECTS␣IN␣CLASS:␣SIMULATIONCONTROL␣==========
548
549 SimulationControl,
550 ␣␣␣␣Yes,␣␣␣␣␣␣␣␣␣␣␣␣␣␣␣␣␣␣␣␣␣!-␣Do␣Zone␣Sizing␣Calculation
551 ␣␣␣␣Yes,␣␣␣␣␣␣␣␣␣␣␣␣␣␣␣␣␣␣␣␣␣!-␣Do␣System␣Sizing␣Calculation
552 ␣␣␣␣No,␣␣␣␣␣␣␣␣␣␣␣␣␣␣␣␣␣␣␣␣␣!-␣Do␣Plant␣Sizing␣Calculation
553 ␣␣␣␣No,␣␣␣␣␣␣␣␣␣␣␣␣␣␣␣␣␣␣␣␣␣!-␣Run␣Simulation␣for␣Sizing␣Periods
554 ␣␣␣␣Yes;␣␣␣␣␣␣␣␣␣␣␣␣␣␣␣␣␣␣␣␣!-␣Run␣Simulation␣for␣Weather␣File␣Run␣
       Periods
555
556
557 !-␣␣␣==========␣␣ALL␣OBJECTS␣IN␣CLASS:␣SHADOWCALCULATION␣==========
558
559 ShadowCalculation,
560 ␣␣␣␣AverageOverDaysInFrequency,␣␣!-␣Calculation␣Method
561 ␣␣␣␣1,␣␣␣␣␣␣␣␣␣␣␣␣␣␣␣␣␣␣␣␣␣!-␣Calculation␣Frequency
562 ␣␣␣␣15000,␣␣␣␣␣␣␣␣␣␣␣␣␣␣␣␣␣!-␣Maximum␣Figures␣in␣Shadow␣Overlap␣
       Calculations
563 ␣␣␣␣,␣␣␣␣␣␣␣␣␣␣␣␣␣␣␣␣␣␣␣␣␣!-␣Polygon␣Clipping␣Algorithm
564 ␣␣␣␣DetailedSkyDiffuseModeling;␣␣!-␣Sky␣Diffuse␣Modeling␣Algorithm
565
566
567 !-␣␣␣==========␣␣ALL␣OBJECTS␣IN␣CLASS:␣SURFACECONVECTIONALGORITHM:
       INSIDE␣==========
568
569 SurfaceConvectionAlgorithm:Inside,
570 ␣␣␣␣AdaptiveConvectionAlgorithm;␣␣!-␣Algorithm
571
572
573 !-␣␣␣==========␣␣ALL␣OBJECTS␣IN␣CLASS:␣SURFACECONVECTIONALGORITHM:
       OUTSIDE␣==========
574
575 SurfaceConvectionAlgorithm:Outside,
576 ␣␣␣␣MoWiTT;␣␣␣␣␣␣␣␣␣␣␣␣␣␣␣␣␣!-␣Algorithm
577
578
579 !-␣␣␣==========␣␣ALL␣OBJECTS␣IN␣CLASS:␣HEATBALANCEALGORITHM␣
       ==========
580
581 HeatBalanceAlgorithm,
582 ␣␣␣␣ConductionTransferFunction,␣␣!-␣Algorithm
583 ␣␣␣␣200,␣␣␣␣␣␣␣␣␣␣␣␣␣␣␣␣␣␣␣␣␣!-␣Surface␣Temperature␣Upper␣Limit␣{C}
584 ␣␣␣␣0.1,␣␣␣␣␣␣␣␣␣␣␣␣␣␣␣␣␣␣␣␣␣!-␣Minimum␣Surface␣Convection␣Heat␣
       Transfer␣Coefficient␣Value␣{W/m2-K}
585 ␣␣␣␣1000;␣␣␣␣␣␣␣␣␣␣␣␣␣␣␣␣␣␣␣␣␣!-␣Maximum␣Surface␣Convection␣Heat␣
       Transfer␣Coefficient␣Value␣{W/m2-K}
586
587
588 !-␣␣␣==========␣␣ALL␣OBJECTS␣IN␣CLASS:␣TIMESTEP␣==========
```

```
589
590 Timestep,
591 ␣␣␣␣6;␣␣␣␣␣␣␣␣␣␣␣␣␣␣␣␣␣␣␣␣␣␣␣!-␣Number␣of␣Timesteps␣per␣Hour
592
593
594 !-␣␣␣==========␣␣ALL␣OBJECTS␣IN␣CLASS:␣RUNPERIOD␣==========
595
596 RunPeriod,
597 ␣␣␣␣,␣␣␣␣␣␣␣␣␣␣␣␣␣␣␣␣␣␣␣␣␣␣␣!-␣Name
598 ␣␣␣␣1,␣␣␣␣␣␣␣␣␣␣␣␣␣␣␣␣␣␣␣␣␣␣!-␣Begin␣Month
599 ␣␣␣␣1,␣␣␣␣␣␣␣␣␣␣␣␣␣␣␣␣␣␣␣␣␣␣!-␣Begin␣Day␣of␣Month
600 ␣␣␣␣12,␣␣␣␣␣␣␣␣␣␣␣␣␣␣␣␣␣␣␣␣␣!-␣End␣Month
601 ␣␣␣␣31,␣␣␣␣␣␣␣␣␣␣␣␣␣␣␣␣␣␣␣␣␣!-␣End␣Day␣of␣Month
602 ␣␣␣␣UseWeatherFile,␣␣␣␣␣␣␣␣␣␣!-␣Day␣of␣Week␣for␣Start␣Day
603 ␣␣␣␣Yes,␣␣␣␣␣␣␣␣␣␣␣␣␣␣␣␣␣␣␣!-␣Use␣Weather␣File␣Holidays␣and␣Special␣
       Days
604 ␣␣␣␣Yes,␣␣␣␣␣␣␣␣␣␣␣␣␣␣␣␣␣␣␣!-␣Use␣Weather␣File␣Daylight␣Saving␣Period
605 ␣␣␣␣No,␣␣␣␣␣␣␣␣␣␣␣␣␣␣␣␣␣␣␣␣!-␣Apply␣Weekend␣Holiday␣Rule
606 ␣␣␣␣Yes,␣␣␣␣␣␣␣␣␣␣␣␣␣␣␣␣␣␣␣!-␣Use␣Weather␣File␣Rain␣Indicators
607 ␣␣␣␣Yes,␣␣␣␣␣␣␣␣␣␣␣␣␣␣␣␣␣␣␣!-␣Use␣Weather␣File␣Snow␣Indicators
608 ␣␣␣␣1,␣␣␣␣␣␣␣␣␣␣␣␣␣␣␣␣␣␣␣␣␣!-␣Number␣of␣Times␣Runperiod␣to␣be␣
       Repeated
609 ␣␣␣␣Yes;␣␣␣␣␣␣␣␣␣␣␣␣␣␣␣␣␣␣␣!-␣Increment␣Day␣of␣Week␣on␣repeat
610
611
612 !-␣␣␣==========␣␣ALL␣OBJECTS␣IN␣CLASS:␣SCHEDULETYPELIMITS␣==========
613
614 ScheduleTypeLimits,
615 ␣␣␣␣Fraction,␣␣␣␣␣␣␣␣␣␣␣␣␣␣␣!-␣Name
616 ␣␣␣␣0,␣␣␣␣␣␣␣␣␣␣␣␣␣␣␣␣␣␣␣␣␣!-␣Lower␣Limit␣Value
617 ␣␣␣␣1,␣␣␣␣␣␣␣␣␣␣␣␣␣␣␣␣␣␣␣␣␣!-␣Upper␣Limit␣Value
618 ␣␣␣␣Continuous,␣␣␣␣␣␣␣␣␣␣␣␣␣!-␣Numeric␣Type
619 ␣␣␣␣Dimensionless;␣␣␣␣␣␣␣␣␣␣!-␣Unit␣Type
620
621 ScheduleTypeLimits,
622 ␣␣␣␣Any␣Number;␣␣␣␣␣␣␣␣!-␣Name
623
624 !-␣␣␣==========␣␣ALL␣OBJECTS␣IN␣CLASS:␣WINDOWMATERIAL:GLAZING␣
       ==========
625
626 WindowMaterial:Glazing,
627 ␣␣␣␣Glass,␣␣␣␣␣␣␣␣␣␣␣␣␣␣␣␣␣␣!-␣Name
628 ␣␣␣␣BSDF,␣␣␣␣␣␣␣␣␣␣␣␣␣␣␣␣␣␣!-␣Optical␣Data␣Type
629 ␣␣␣␣,␣␣␣␣␣␣␣␣␣␣␣␣␣␣␣␣␣␣␣␣␣!-␣Window␣Glass␣Spectral␣Data␣Set␣Name
630 ␣␣␣␣0.006,␣␣␣␣␣␣␣␣␣␣␣␣␣␣␣␣␣!-␣Thickness␣{m}
631 ␣␣␣␣0.9,␣␣␣␣␣␣␣␣␣␣␣␣␣␣␣␣␣␣!-␣Solar␣Transmittance␣at␣Normal␣Incidence
632 ␣␣␣␣0.1,␣␣␣␣␣␣␣␣␣␣␣␣␣␣␣␣␣␣!-␣Front␣Side␣Solar␣Reflectance␣at␣Normal␣
       Incidence
633 ␣␣␣␣0.1,␣␣␣␣␣␣␣␣␣␣␣␣␣␣␣␣␣␣!-␣Back␣Side␣Solar␣Reflectance␣at␣Normal␣
       Incidence
```

```
    0.9,                    !- Visible Transmittance at Normal
        Incidence
    0.1,                    !- Front Side Visible Reflectance at
        Normal Incidence
    0.1,                    !- Back Side Visible Reflectance at Normal
        Incidence
    0.9,                    !- Infrared Transmittance at Normal
        Incidence
    0.84,                   !- Front Side Infrared Hemispherical
        Emissivity
    0.84,                   !- Back Side Infrared Hemispherical
        Emissivity
    0.9,                    !- Conductivity {W/m-K}
    1,                      !- Dirt Correction Factor for Solar and
        Visible Transmittance
    No,                     !- Solar Diffusing
    72000000000,            !- Young\92s modulus {Pa}
    0.22;                   !- Poisson\92s ratio


!- ===========  ALL OBJECTS IN CLASS: WINDOWMATERIAL:COMPLEXSHADE
    ===========

WindowMaterial:ComplexShade,
    CFS_Glz_104-Layer,      !- Name
    BSDF,                   !- Layer Type
    0.002,                  !- Thickness {m}
    1,                      !- Conductivity {W/m-K}
    ,                       !- IR Transmittance
    0.84,                   !- Front Emissivity
    0.84,                   !- Back Emissivity
    ,                       !- Top Opening Multiplier
    ,                       !- Bottom Opening Multiplier
    ,                       !- Left Side Opening Multiplier
    ,                       !- Right Side Opening Multiplier
    0.05,                   !- Front Opening Multiplier
    0.016,                  !- Slat Width {m}
    0.012,                  !- Slat Spacing {m}
    0.0006,                 !- Slat Thickness {m}
    90,                     !- Slat Angle {deg}
    160;                    !- Slat Conductivity {W/m-K}

WindowMaterial:ComplexShade,
    CFS_Glz_73-Layer,       !- Name
    BSDF,                   !- Layer Type
    0.002,                  !- Thickness {m}
    1,                      !- Conductivity {W/m-K}
    ,                       !- IR Transmittance
    0.84,                   !- Front Emissivity
    0.84,                   !- Back Emissivity
    ,                       !- Top Opening Multiplier
```

```
    ,                           !- Bottom Opening Multiplier
    ,                           !- Left Side Opening Multiplier
    ,                           !- Right Side Opening Multiplier
    0.05,                       !- Front Opening Multiplier
    0.016,                      !- Slat Width {m}
    0.012,                      !- Slat Spacing {m}
    0.0006,                     !- Slat Thickness {m}
    90,                         !- Slat Angle {deg}
    160;                        !- Slat Conductivity {W/m-K}

!- ===========  ALL OBJECTS IN CLASS: CONSTRUCTION ===========

Construction,
    Construction,               !- Name
    Aislante,        !- Outside
    Hormigon;                   !- Inside Layer


!- ===========  ALL OBJECTS IN CLASS: WINDOWTHERMALMODEL:PARAMS
    ===========

WindowThermalModel:Params,
    WindowModel,                !- Name
    ISO15099,                   !- standard
    ISO15099,                   !- Thermal Model
    1,                          !- SDScalar
    NoDeflection,               !- Deflection Model
    13.238,                     !- Vacuum Pressure Limit {Pa}
    25,                         !- Initial temperature {C}
    101325;                     !- Initial pressure {Pa}


!- ===========  ALL OBJECTS IN CLASS: GLOBALGEOMETRYRULES ===========

GlobalGeometryRules,
    UpperLeftCorner,            !- Starting Vertex Position
    Counterclockwise,           !- Vertex Entry Direction
    Relative,                   !- Coordinate System
    Relative,                   !- Daylighting Reference Point Coordinate
    System
    Relative;                   !- Rectangular Surface Coordinate System


!- ===========  ALL OBJECTS IN CLASS: ZONECONTROL:THERMOSTAT
    ===========

ZoneControl:Thermostat,
    RoomThermostat,             !- Name
    Room,                       !- Zone or ZoneList Name
    ALWAYS 4,                   !- Control Type Schedule Name
    ThermostatSetpoint:DualSetpoint,  !- Control 1 Object Type
```

```
    Office Thermostat Dual SP Control;  !- Control 1 Name


!-   ==========  ALL OBJECTS IN CLASS: ENERGYMANAGEMENTSYSTEM:SENSOR
    ==========

EnergyManagementSystem:Sensor,
    win1_sensor,              !- Name
    win1,                     !- Output:Variable or Output:Meter Index
    Key Name
    Schedule Value;           !- Output:Variable or Output:Meter Name


!-   ==========  ALL OBJECTS IN CLASS: ENERGYMANAGEMENTSYSTEM:ACTUATOR
    ==========
EnergyManagementSystem:Actuator,
    win1_actuator,            !- Name
    South-win,                !- Actuated Component Unique Name
    Surface,                  !- Actuated Component Type
    Construction State;       !- Actuated Component Control Type


!-   ==========  ALL OBJECTS IN CLASS: ENERGYMANAGEMENTSYSTEM:
    PROGRAMCALLINGMANAGER ==========

EnergyManagementSystem:ProgramCallingManager,
    Manager0,                 !- Name
    BeginTimestepBeforePredictor,  !- EnergyPlus Model Calling Point
    Control0;                 !- Program Name 1


!-   ==========  ALL OBJECTS IN CLASS: ENERGYMANAGEMENTSYSTEM:PROGRAM
    ==========

EnergyManagementSystem:Program,
    Control0,                 !- Name
    IF win1_sensor<=1.5,      !- Program Line 1
    SET win1_actuator =SouthState1,  !- Program Line 2
    ELSEIF win1_sensor<=2.5,  !- A4
    SET win1_actuator =SouthState2,  !- A5
    ELSEIF win1_sensor<=3.5,  !- A4
    SET win1_actuator =SouthState3,  !- A5
    ELSEIF win1_sensor<=4.5,  !- A4
    SET win1_actuator =SouthState4,  !- A5
    ENDIF;                    !- A12


!-   ==========  ALL OBJECTS IN CLASS: ENERGYMANAGEMENTSYSTEM:
    CONSTRUCTIONINDEXVARIABLE ==========

```

```
EnergyManagementSystem:ConstructionIndexVariable,
␣␣␣␣SouthState1,␣␣␣␣␣␣␣␣␣␣␣␣!-␣Name
␣␣␣␣CFS_Glz_73;␣␣␣␣␣␣␣␣␣␣␣␣!-␣Construction␣Object␣Name

EnergyManagementSystem:ConstructionIndexVariable,
␣␣␣␣SouthState2,␣␣␣␣␣␣␣␣␣␣␣␣!-␣Name
␣␣␣␣CFS_Glz_104;␣␣␣␣␣␣␣␣␣␣␣␣!-␣Construction␣Object␣Name

EnergyManagementSystem:ConstructionIndexVariable,
␣␣␣␣SouthState3,␣␣␣␣␣␣␣␣␣␣␣␣!-␣Name
␣␣␣␣CFS_Glz_105;␣␣␣␣␣␣␣␣␣␣␣␣!-␣Construction␣Object␣Name

EnergyManagementSystem:ConstructionIndexVariable,
␣␣␣␣SouthState4,␣␣␣␣␣␣␣␣␣␣␣␣!-␣Name
␣␣␣␣CFS_Glz_106;␣␣␣␣␣␣␣␣␣␣␣␣!-␣Construction␣Object␣Name



!-␣Start␣detailed␣HVAC␣data␣definition
!-␣Here,␣copy␣and␣paste␣the␣file␣with␣HVAC␣definition...␣it␣is␣very
long


!-␣␣␣==========␣␣ALL␣OBJECTS␣IN␣CLASS:␣OUTPUT:VARIABLE␣==========

Output:Variable,
␣␣␣␣South-win,␣␣␣␣␣␣␣␣␣␣␣␣!-␣Key␣Value
␣␣␣␣Surface␣Outside␣Face␣Incident␣Solar␣Radiation␣Rate␣per␣Area,␣␣!-␣
    Variable␣Name
␣␣␣␣Environment;␣␣␣␣␣␣␣␣␣␣␣␣!-␣Reporting␣Frequency

Output:Variable,
␣␣␣␣*,␣␣␣␣␣␣␣␣␣␣␣␣␣␣␣␣␣␣␣!-␣Key␣Value
␣␣␣␣Surface␣Window␣Transmitted␣Solar␣Radiation␣Rate,␣␣!-␣Variable␣Name
␣␣␣␣Environment;␣␣␣␣␣␣␣␣␣␣␣␣!-␣Reporting␣Frequency

Output:Variable,
␣␣␣␣*,␣␣␣␣␣␣␣␣␣␣␣␣␣␣␣␣␣␣␣!-␣Key␣Value
␣␣␣␣Heating␣Coil␣Electric␣Energy,␣␣!-␣Variable␣Name
␣␣␣␣Environment;␣␣␣␣␣␣␣␣␣␣␣␣!-␣Reporting␣Frequency

Output:Variable,
␣␣␣␣*,␣␣␣␣␣␣␣␣␣␣␣␣␣␣␣␣␣␣␣!-␣Key␣Value
␣␣␣␣Cooling␣Coil␣Electric␣Energy,␣␣!-␣Variable␣Name
␣␣␣␣Environment;␣␣␣␣␣␣␣␣␣␣␣␣!-␣Reporting␣Frequency

Output:Variable,
␣␣␣␣*,␣␣␣␣␣␣␣␣␣␣␣␣␣␣␣␣␣␣␣!-␣Key␣Value
␣␣␣␣Zone␣Lights␣Electric␣Energy,␣␣!-␣Variable␣Name
␣␣␣␣Environment;␣␣␣␣␣␣␣␣␣␣␣␣!-␣Reporting␣Frequency

```

```
Output:Variable,
    Room,          !- Key Value
    Zone Mean Air Temperature,    !- Variable Name
    Environment;               !- Reporting Frequency

\n\n";

close(IDF);

      if ($epw_file eq "CAN_PQ_Montreal.Intl.AP.716270_CWEC") {
        `cat DesignDay_Montreal.idf >> $ePlus_file.idf`;
      }
      if ($epw_file eq "CHL_Santiago.855740_IWEC") {
        `cat DesignDay_Santiago.idf >> $ePlus_file.idf`;
      }

      `cat BSDF/CFS1.idf >> $ePlus_file.idf`;
      `cat BSDF/CFS2.idf >> $ePlus_file.idf`;
      `cat BSDF/CFS3.idf >> $ePlus_file.idf`;
      `cat BSDF/CFS4.idf >> $ePlus_file.idf`;

      $ePlus_result="Results/EPlus/$ePlus_file.csv";

      `runenergyplus $ePlus_file.idf $epw_file.epw`;
      `cp Output/$ePlus_file.csv $ePlus_result`;
      `cp $ePlus_file.idf scenes/idf`;
      `rm $ePlus_file.idf`;
      `rm Output/*`;
      `rmdir Output`;

      my $t=Time::HiRes::tv_interval($start_time);
      print "\trun EnergyPlus $epw_file-$orientation-$control   $t\n";
      print TXT "\trun EnergyPlus $epw_file-$orientation-$control $t\n"
          ;

    }
  }
}

close(TXT);
```

C. CONTROL STRATEGIES USED IN LIGHTING SIMULATION IN CHAPTER 4

```
1  -- Irradiance Algorithm / South facade
2  -- Script used in case study paper 2 Daniel Uribe
3
4  -- win1=1 -- -75 degrees
5  -- win1=2 -- -70 degrees
6  -- win1=3 -- -65 degrees
7  -- win1=4 -- -60 degrees
8  -- win1=5 -- -55 degrees
9  -- win1=6 -- -50 degrees
10 -- win1=7 -- -45 degrees
11 -- win1=8 -- -40 degrees
12 -- win1=9 -- -35 degrees
13 -- win1=10 -- -30 degrees
14 -- win1=11 -- -25 degrees
15 -- win1=12 -- -20 degrees
16 -- win1=13 -- -15 degrees
17 -- win1=14 -- -10 degrees
18 -- win1=15 -- -5 degrees
19 -- win1=16 -- 0 degrees
20 -- win1=17 -- 5 degrees
21 -- win1=18 -- 10 degrees
22 -- win1=19 -- 15 degrees
23 -- win1=20 -- 20 degrees
24 -- win1=21 -- 25 degrees
25 -- win1=22 -- 30 degrees
26 -- win1=23 -- 35 degrees
27 -- win1=24 -- 40 degrees
28 -- win1=25 -- 45 degrees
29 -- win1=26 -- 50 degrees
30 -- win1=27 -- 55 degrees
31 -- win1=28 -- 60 degrees
32 -- win1=29 -- 65 degrees
33 -- win1=30 -- 70 degrees
34 -- win1=31 -- 75 degrees
35 -- win1=32 -- Double clear glazing
36
37 if hour() > 8 and hour() < 18 then
38
39 -- First, calculate exterior irradiance over the window.
40 ext_rad=math.abs(irradiance(0,-1,0)) --irradiance over the south
       facade.
41 max=300 --Parameter to control the blinds.
42
43 if ext_rad > max then
44 win1=31 --75 degrees
45 elseif ext_rad > 5*max/6 then
```

```
win1=28 -- 60 degrees
elseif ext_rad > 4*max/6 then
win1=25 -- 45 degrees
elseif ext_rad > 3*max/6 then
win1=22 -- 30 degrees
elseif ext_rad > 2*max/6 then
win1=19 -- 15 degrees
else
win1=16 -- 0 degrees
end
update() -- update sensor values using the new shading position


-- dim the lights to achieve the correct luminance, recursively
-- night() returns the value of the sensor at night with all the
    luminaires at full power.

set1=night(1)
set2=night(2)

dim=0.05 -- Dim at a 5% resolution
dif=set1-sensor(1)
sign=math.abs(dif)/dif

while (math.abs(dif) > 20 and lum(1)>=0 and lum(1)<=1) do
lum1=lum(1)+sign*dim
update()
dif=set1-sensor(1)
sign=math.abs(dif)/dif
end

dif=set2-sensor(2)
sign=math.abs(dif)/dif

while (math.abs(dif) > 20 and lum(2)>=0 and lum(2)<=1) do
lum2=lum(2)+sign*dim
update()
dif=set2-sensor(2)
sign=math.abs(dif)/dif
end

if lum1>1 then lum1=1 elseif lum1<0 then lum1=0 end
if lum2>1 then lum2=1 elseif lum2<0 then lum2=0 end
update()

else
lum1=0
lum2=0
win1=31 -- close blinds in the night
update()

```

```
end
```

```
-- Vertical Eye Illuminance Algorithm
-- Script used in Case Study Paper 2 Daniel Uribe

if hour() > 8 and hour() < 18 then

win1=16 -- set open blinds
update()
illum=sensor(4) --illuminance at sensor see to the lateral wall.
max=2760 --Control parameter of louvers, maximum illuminance level.

a=0 -- auxiliar variable
b=16 -- CFS position
while (illum>max and a==0) do
if b<31 then
b=b+1
win1=b
update()
illum=sensor(4)
else
win1=31
update()
a=1 -- to close while cicle
end
end


-- dim the lights to achieve the correct luminance, recursively
-- night() returns the value of the sensor at night with all the
   luminaires at full power.

set1=night(1)
set2=night(2)

dim=0.05 -- Dim at a 5% resolution
dif=set1-sensor(1)
sign=math.abs(dif)/dif

while (math.abs(dif) > 20 and lum(1)>=0 and lum(1)<=1) do
lum1=lum(1)+sign*dim
update()
dif=set1-sensor(1)
sign=math.abs(dif)/dif
end

dif=set2-sensor(2)
sign=math.abs(dif)/dif

```

```
47 while (math.abs(dif) > 20 and lum(2)>=0 and lum(2)<=1) do
48 lum2=lum(2)+sign*dim
49 update()
50 dif=set2-sensor(2)
51 sign=math.abs(dif)/dif
52 end
53
54 if lum1>1 then lum1=1 elseif lum1<0 then lum1=0 end
55 if lum2>1 then lum2=1 elseif lum2<0 then lum2=0 end
56 update()
57
58 else
59 lum1=0
60 lum2=0
61 win1=31 -- close blinds in the night
62 update()
63 end
```

```
 1 -- Cut-off angle algorithm / North facade
 2 -- Script used in Case Study Paper 2 Daniel Uribe
 3
 4 if hour() > 8 and hour() < 18 then
 5
 6 -- Solar Profile Angle
 7 azimuth_surf=0 -- North surface azimuth
 8 omega=math.abs(math.atan(math.tan(altitude())/math.cos(azimuth()-
       math.rad(azimuth_surf)))) -- Profile angle
 9 --deg_omega=math.deg(omega)
10 --print(deg_omega)
11
12 -- Cut-Off Angle
13 d=120 -- slat spacing
14 w=142 -- slat width
15 beta_cutoff=math.deg(math.asin(d*math.cos(omega)/w)-omega)
16 -- print(beta_cutoff)
17
18 -- Change Louver Position
19
20 a=0
21
22 if beta_cutoff>=0 then
23
24 a=1
25 while (beta_cutoff>(a-1)*5) do
26 a=a+1
27 end
28 a=a+14
29
30 if a<=31 then
```

```
a=a
else
a=31
end

win1=a
update()


else

a=15
while (beta_cutoff>a*(-5)) do
a=a-1
end

if a<15 then
a=a+1
end

if a==15 then
a=1
elseif a==14 then
a=2
elseif a==13 then
a=3
elseif a==12 then
a=4
elseif a==11 then
a=5
elseif a==10 then
a=6
elseif a==9 then
a=7
elseif a==8 then
a=8
elseif a==7 then
a=9
elseif a==6 then
a=10
elseif a==5 then
a=11
elseif a==4 then
a=12
elseif a==3 then
a=13
elseif a==2 then
a=14
elseif a==1 then
a=15
end
```

```
82
83 win1=a
84 update()
85
86 end
87
88
89 -- dim the lights to achieve the correct luminance, recursively
90 -- night() returns the value of the sensor at night with all the
       luminaires at full power.
91
92 set1=night(1)
93 set2=night(2)
94
95 dim=0.05 -- Dim at a 5% resolution
96 dif=set1-sensor(1)
97 sign=math.abs(dif)/dif
98
99 while (math.abs(dif) > 20 and lum(1)>=0 and lum(1)<=1) do
100 lum1=lum(1)+sign*dim
101 update()
102 dif=set1-sensor(1)
103 sign=math.abs(dif)/dif
104 end
105
106 dif=set2-sensor(2)
107 sign=math.abs(dif)/dif
108
109 while (math.abs(dif) > 20 and lum(2)>=0 and lum(2)<=1) do
110 lum2=lum(2)+sign*dim
111 update()
112 dif=set2-sensor(2)
113 sign=math.abs(dif)/dif
114 end
115
116 if lum1>1 then lum1=1 elseif lum1<0 then lum1=0 end
117 if lum2>1 then lum2=1 elseif lum2<0 then lum2=0 end
118 update()
119
120 else
121 lum1=0
122 lum2=0
123 win1=31 -- close blinds in the night
124 update()
125 end
```

```
1 -- Blocking control algorithm / North facade
2 -- Script used in Case Study Paper 2 Daniel Uribe
3
```

```
4  if hour() > 8 and hour() < 18 then
5
6  -- Solar Profile Angle
7  azimuth_surf=0 -- North surface azimuth
8  omega=math.abs(math.atan(math.tan(altitude())/math.cos(azimuth()-
       math.rad(azimuth_surf)))) -- Profile angle
9  deg_omega=math.deg(omega)
10 --print(deg_omega)
11
12 -- Cut-Off Angle
13 d=120 -- slat spacing
14 w=142 -- slat width
15 beta_cutoff=math.deg(math.asin(d*math.cos(omega)/w)-omega)
16 -- print(beta_cutoff)
17
18 -- Design Angle
19 delta_design=math.rad(48.99) -- depends of observer position
20 beta_design=math.deg((delta_design-omega)/2)
21
22
23 -- Determine if second reflection occurs
24 delta=omega+2*math.rad(beta_cutoff)
25
26 beta=0 --slat angle
27
28 if ((math.cos(math.rad(beta_cutoff))*math.tan(delta))>(1+math.sin(
       math.rad(beta_cutoff)))) then
29
30 beta=90-deg_omega
31
32 -- Change Louver Position
33
34 a=0
35
36 if beta>=0 then
37
38 a=1
39 while (beta>(a-1)*5) do
40 a=a+1
41 end
42 a=a+14
43
44 if a<=31 then
45 a=a
46 else
47 a=31
48 end
49
50 win1=a
51 update()
52
```

```
53
54 else
55
56 a=15
57 while (beta>a*(-5)) do
58 a=a-1
59 end
60
61 if a<15 then
62 a=a+1
63 end
64
65 if a==15 then
66 a=1
67 elseif a==14 then
68 a=2
69 elseif a==13 then
70 a=3
71 elseif a==12 then
72 a=4
73 elseif a==11 then
74 a=5
75 elseif a==10 then
76 a=6
77 elseif a==9 then
78 a=7
79 elseif a==8 then
80 a=8
81 elseif a==7 then
82 a=9
83 elseif a==6 then
84 a=10
85 elseif a==5 then
86 a=11
87 elseif a==4 then
88 a=12
89 elseif a==3 then
90 a=13
91 elseif a==2 then
92 a=14
93 elseif a==1 then
94 a=15
95 end
96
97 win1=a
98 update()
99
100 end
101
102 else
103
```

```
104 -- Determine slat angle for blocking daylight
105
106 if beta_cutoff>beta_design then
107 beta=beta_cutoff
108 else
109 beta=beta_design
110 end
111 -- print(beta)
112
113 -- Change Louver Position
114
115 a=0
116
117 if beta>=0 then
118
119 a=1
120 while (beta>(a-1)*5) do
121 a=a+1
122 end
123 a=a+14
124
125 if a<=31 then
126 a=a
127 else
128 a=31
129 end
130
131 win1=a
132 update()
133
134
135 else
136
137 a=15
138 while (beta>a*(-5)) do
139 a=a-1
140 end
141
142 if a<15 then
143 a=a+1
144 end
145
146 if a==15 then
147 a=1
148 elseif a==14 then
149 a=2
150 elseif a==13 then
151 a=3
152 elseif a==12 then
153 a=4
154 elseif a==11 then
```

```
a=5
elseif a==10 then
a=6
elseif a==9 then
a=7
elseif a==8 then
a=8
elseif a==7 then
a=9
elseif a==6 then
a=10
elseif a==5 then
a=11
elseif a==4 then
a=12
elseif a==3 then
a=13
elseif a==2 then
a=14
elseif a==1 then
a=15
end

win1=a
update()

end

end

-- dim the lights to achieve the correct luminance, recursively
-- night() returns the value of the sensor at night with all the
   luminaires at full power.

set1=night(1)
set2=night(2)

dim=0.05 -- Dim at a 5% resolution
dif=set1-sensor(1)
sign=math.abs(dif)/dif

while (math.abs(dif) > 20 and lum(1)>=0 and lum(1)<=1) do
lum1=lum(1)+sign*dim
update()
dif=set1-sensor(1)
sign=math.abs(dif)/dif
end

dif=set2-sensor(2)
sign=math.abs(dif)/dif

```

```
205 while (math.abs(dif) > 20 and lum(2)>=0 and lum(2)<=1) do
206 lum2=lum(2)+sign*dim
207 update()
208 dif=set2-sensor(2)
209 sign=math.abs(dif)/dif
210 end
211
212 if lum1>1 then lum1=1 elseif lum1<0 then lum1=0 end
213 if lum2>1 then lum2=1 elseif lum2<0 then lum2=0 end
214 update()
215
216 else
217 lum1=0
218 lum2=0
219 win1=31 -- close blinds in the night
220 update()
221 end
```

D. SCRIPTS USED IN OPTIMIZATION OF CHAPTER 5

CFG file

```
/* GenOpt configuration file for
   Simulation Paper 4 Daniel Uribe on Linux
   dnuribe@uc.cl, 2016-03-10
*/

// Error messages of the simulation program.
SimulationError
{
    ErrorMessage = "** ␣␣Fatal␣␣ **";
    ErrorMessage = "** ␣Terminated--Error(s)␣Detected";
}

// Number format for writing the simulation input files.
IO
{
    NumberFormat = Double;
}

/*  Specifying how to start the simulation program.
    In "Command", only those words in %xx% are
    replaced (possibly with empty Strings).
*/
SimulationStart
{
    Command = "perl␣%Simulation.Files.Input.File1%.pl";
    WriteInputFileExtension = false;
}
```

command.txt

```
/* GenOpt command file
   dnuribe@uc.cl, 2016/03/10
*/
Vary{
  Parameter{   // perforations (%)
    Name    = perf;
    Min     =  10;
    Ini     =  10;
    Max     =  50;
    Step    =  20; // 5 10
  }
  Parameter{    // separation (m)
    Name    = sep;
```

```
    Min     =  0.1;
    Ini     =  0.1;
    Max     =  0.25;
    Step    =  0.04; // 0.01 0.02
  }
  Parameter{ // angle (degrees)
    Name    = angle;
    Min     =  15;
    Ini     =  15;
    Max     =  75;
    Step    =  20; // 5 10
  }
}

OptimizationSettings{
  MaxIte = 200;
  MaxEqualResults = 10;
  WriteStepNumber = false;
  UnitsOfExecution = 0;
}

Algorithm{
  Main = GPSPSOCCHJ;
  NeighborhoodTopology = vonNeumann;
  NeighborhoodSize = 5;
  NumberOfParticle = 10;
  NumberOfGeneration = 10;
  Seed = 1;
  CognitiveAcceleration = 2.8;
  SocialAcceleration = 1.3;
  MaxVelocityGainContinuous = 0.5;
  MaxVelocityDiscrete = 4;
  ConstrictionGain = 0.5;
  MeshSizeDivider = 2;
  InitialMeshSizeExponent = 0;
  MeshSizeExponentIncrement = 1;
  NumberOfStepReduction = 2;
}
```

INI file for Montreal

```
/* GenOpt initialization file for Optimization Process Paper 4 Thesis
   Operating system: Linux
   dnuribe@uc.cl, 2016-03-10
*/
Simulation {
  Files {
    Template {
      File1 = simulation_template.pl;
```

```
    }
    Input {
      File1 = simulation.pl;
    }
    Log {
      File1 = Output.err;
    }
    Output {
      File1 = EPlus_input-CAN_PQ_Montreal.Intl.AP.716270_CWEC.eso;
    }
    Configuration {
      File1 = "../../../../cfg/Paper4.cfg";
    }
  }
 //CallParameter { // optional section
 //
 //}
  ObjectiveFunctionLocation
  {

      Name1      = FO;
      Function1  = "multiply(%Es_tot%,␣%ASE_M%,␣%sDA_M%)";

      Name2      = Es_tot;
      Function2  = "add(%Es_heat1%,␣%Es_heat2%,␣%Es_cool%,␣%Es_light%)"
          ;

      Name3      = Es_heat1;
      Function3  = "divide(␣%Q_heat1%,␣3600000)";

      Name4      = Es_heat2;
      Function4  = "divide(␣%Q_heat2%,␣3600000)";

      Name5      = Es_cool;
      Function5  = "divide(␣%Q_cool%,␣3600000)";

      Name6      = Es_light;
      Function6  = "divide(␣%E_lights%,␣3600000)";

      Name7             = Q_heat1;
      Delimiter7        = "376,";
      FirstCharacterAt7 = 1;

      Name8             = Q_heat2;
      Delimiter8        = "390,";
      FirstCharacterAt8 = 1;

      Name9             = Q_cool;
      Delimiter9        = "354,";
      FirstCharacterAt9 = 1;

```

```
      Name10             = E_lights;
      Delimiter10        = "67,";
      FirstCharacterAt10 = 1;

      Name11             = ASE_M;
      Delimiter11        = "ASE_M,";
      FirstCharacterAt11 = 1;

      Name12             = sDA_M;
      Delimiter12        = "sDA_M,";
      FirstCharacterAt12 = 1;

  }
} // end of section Simulation

Optimization {
  Files {
    Command {
      File1 = command.txt;
    }
  }
} // end of configuration file
```